POLITECNICO DI TORINO

Department of ENERGY

Master's Degree in Energy and Nuclear Engineering

Final Thesis Project:

Techno-economic analysis of hydrogen-based Power-to-Power systems and their participation in the Italian ancillary services energy market

December 4th, 2020

Supervisors:

Prof. Santarelli Massimo

Prof. Mazza Andrea

Prof. Ferrero Domenico

Prof. Campanari Stefano

Student:

Curti Gianmarco s264900

Academic Year 2019/2020

Acknowledgements

I would like to express my deep gratitude to my thesis supervisor, Professor Massimo Santarelli, and the STEPS group at Politecnico di Torino. They guided and supported me along the path, contributing to make incredibly fulfilling the conclusion of my academic experience.

Throughout the writing of this dissertation, I have received generous support from Professor Andrea Mazza, whose expertise was invaluable in formulating the research topic and methodology in particular.

A particular thanks goes to Francesco and my colleagues at Engie EPS, they have welcomed me like family and shown me the way for a bright future, as man and engineer.

Finally, my most heartfelt gratitude goes to Beatrice, my family and friends. They are literally my tower of strength, the whole reason why I have never given up, and I never will, with you by my side.

Abstract

Nowadays, the framework of renewable energy sources is highly dynamic and constantly evolving; the urgent need of cutting CO_2 emissions is pushing humankind to find alternatives to the energy paradigm as it was. In order to be effective for our health, this major shift needs a comprehensive and coordinated set of actions, ranging from a more rational use of the already existent forms of energy, passing through the impactful penetration of renewables and alternative energy vectors (e.g. hydrogen-based technologies), to the work on systems' interoperability, in the attempt of taking out their full potential. Another crucial aspect is the worldwide access to energy. Although the disruptive technological advancement in this field, people who live in remote or with challenging access areas still struggle for resources for power their daily activities. Special conditions need *ad hoc* technical configurations, such as Power-to-Power (P2P) energy systems, which have been identified as the pivotal point of the EU-funded REMOTE project. This work aims at demonstrating the technical and economic validity of such systems in other contexts out of remote areas framework. Indeed, they can provide an outstanding degree of flexibility, which made them particularly suitable also for grid-connected applications. Specifically, it has been investigated the participation of P2P systems to the Italian ancillary services energy market, complying with the official regulations released by the Transmission System Operator, with the purpose of improving the security of the electricity grid.

The results show a deep impact of the natural resources availability, as well as of the design choices on the overall system's profitability, which makes them still not ready for the adoption on a massive scale. Nevertheless, all the current technological trends are heading towards a raising cooperation between such systems and the electricity grid, in order to increase its security, to prepare it for the staggering rise in non-dispatchable energy production which await us in the next decades.

List of Contents

List of Figures

List of Tables

Nomenclature	
EGP	Enel Green Power
EPC	Engineering, Procurement and Construction
PEM	Proton Exchange Membrane
STEPS	Synergies of Thermo-chemical and Electro-chemical Power Systems
P2P	Power-to-Power
P2G	Power-to-Gas
G2P	Gas-to-Power
CHP	Combined Heat and Power
ARERA	Autorità di Regolazione per Energia Reti e Ambiente
MSD	Mercato dei Servizi di Dispacciamento
UVAM	Unità Virtuali Abilitate Mista
EV	Electric Vehicle
RES	Renewable Energy Sources
SoC	State of Charge
OEM	Original Equipment Manufacturer

1. Introduction

The need for energy accompanied the human species throughout its evolution. In ancient times, our predecessors had to continuously look for energy sources for power their daily activities, relying on what Nature gifted them. The advent of the Industrial Revolution men introduced new ways to produce and consume energy, making it a controllable asset.

Nonetheless, what enabled humankind to accomplish unthinkable things before then, has brought as legacy the grave depletion and pollution of natural resources. The impact on environment, society and economy from climate change is no more sustainable;

immediate and drastic actions are mandatory if we are willing to get the Planet back on the right track.

The paradigm shift has started, though it is progressing too slowly if compared with the rate of devastation of our ecosystems. Solar, wind, hydro, geothermal energy sources have proven to be plentiful enough for humans to rely on, made competitive with fossil fuels thanks to crucial progresses on Materials Science, Chemistry, Optics and many other disciplines. Still this cannot be enough. The combination of such technologies is the real game-changing step forward that has to be made, since it would allow to exploit the whole asset productivity as well as tailoring it to the wide variety of Planet needs.

Within this framework are inserted the hydrogen-based Power-to-Power (P2P) energy systems. Unlike plants which constitute the state of the art, they are equipped with both short-term and long-term storage, which provide substantial improvements on matching the end-user demand with supply coming from renewables. The REMOTE project has as final objective to assess the overall profitability of such systems, testing them in widely different contexts.

To make this change possible, the global energy infrastructure must be prepared to embrace the broad set of innovative paradigms. As far Italy is concerned, public authority has already taken the first step publishing the Integrated National Energy and Climate Plan for 2030, with the intent of renovating energy policies and procedures also in accordance with EU directives [1]. As part of a more comprehensive plan, one of the main lines of action concerns the development of the Italian energy market in relationship with the need of a more secure electricity grid.

This introductory chapter aims at introducing the general framework of this work, describing the two fundamental projects as starting point of a gainful integration.

1.1. REMOTE project

1.1.1. Context presentation

The project name REMOTE is an acronym which means "Remote area Energy supply with Multiple Options for integrated hydrogen-based TEchnologies". It is a 4-years project (2018 – 2022) with an estimated budget of 6.76 M€, of which 4.99 M€ are granted under the European Union's Horizon 2020 program [2].

The final objective is to demonstrate the technical and economic feasibility of innovative hybrid systems based on different renewable energy sources coupled with hydrogen-based power components, as the case of fuel cells and electrolyzers. The opportunities which can be derived from such systems are tested on four demonstration sites – called DEMO for shortening – which are representative of different sets of requirements. Thus the analysis outcomes would be as much meaningful as possible.

The common factor of the DEMOs is the geographic location: they are all placed in remote areas, where the energy demand either cannot be fulfilled by the public electricity grid or hindrances are present, thus making the supply from the grid even less convenient than to employ their own stand-alone power production system.

The higher level of unpredictability of renewables compared to fossil fuels makes the use of energy storage system essential, given the well-known asynchrony between the energy demand and provision. Adding storage technologies would allow to reach another milestone of the REMOTE project, namely the willing of achieving the full independence from non-renewable sources.

The main stakeholders involved in the project are summarized in Table 1.1 [3].

Role	Stakeholder	Main task
Project coordinator	STEPS group, belonging to the Department of Energy (DENERG) at Politecnico of Torino	Overall management of the project, stakeholders' stewardship for the compliance with project's deadlines, active role on deliverables production.
Academic partner	SINTEF (Norway)	It has made available its highly recognized expertise on hydrogen-related technology. It is following closer activities related to DEMO 4 (Rye/Froan).
Industrial partner	Enel Green Power (Italy)	EGP is the worldwide leader of the clean energy sector. It performs the EPC for DEMO 1 (Ginostra), becoming the end user after plant's completion.
Industrial partner	Engie EPS (Italy)	Player specialized in storage solutions and micro-grids active globally. It manages the EPC phase for DEMO 2 (Agkistro) as well as dealing with the energy storage section of all DEMOs.
Industrial partner	Ballard Europe (Denmark)	It is a developer and manufacturer of PEM fuel cell products.
Industrial partner	PowiDian (France)	It supplies the software responsible for remote monitoring and control.

Table 1.1 REMOTE project: Stakeholders overview

1.1.2. DEMO sites description

Each demonstration site has peculiar features and presents different technical and logistics problems which have to be overcome to accomplish the final target. A brief characterization is reported below [4]:

- DEMO 1 – Ginostra (Italy): small island close to Stromboli volcano, currently powered through diesel generation, which emits 200 Gtons of CO_2 each year [5]. The EGP intent, as owner of the plant, is to install a 170 kW photovoltaic plant [6], which would allow inhabitants to reach 100% of renewable energy production in island-mode.
- DEMO 2 – Agkistro (Greece): it is already present a 0.9 MW hydroelectric plant [6], which will feed an agri-food processing unit which is planned to be built close to the site. In this case, the P2P system would act as backup, avoiding expensive grid interconnection.
- DEMO 3 – Ambornetti (Italy): the mountain location makes feasible the testing of a solar-plus-biomass CHP plant, avoiding any kind of fossil fuel back up thanks to the foreseen hydrogen storage [6]. This would be a pathfinder site, since it avoids invasive works and the whole grid infrastructure, thus preserving the precious environmental heritage of Italian Alps.
- DEMO 4 – Froan/Rye (Norway): the only plant where a grid connection exists, although it consists in an outdated sea cable. It has been assessed that renovation costs of the existent infrastructure overcome those needed for the P2P system. Besides, Froan island has been declared natural reserve [6], thus it would be forbidden to use Diesel generators as backup system for energy supply to the island.

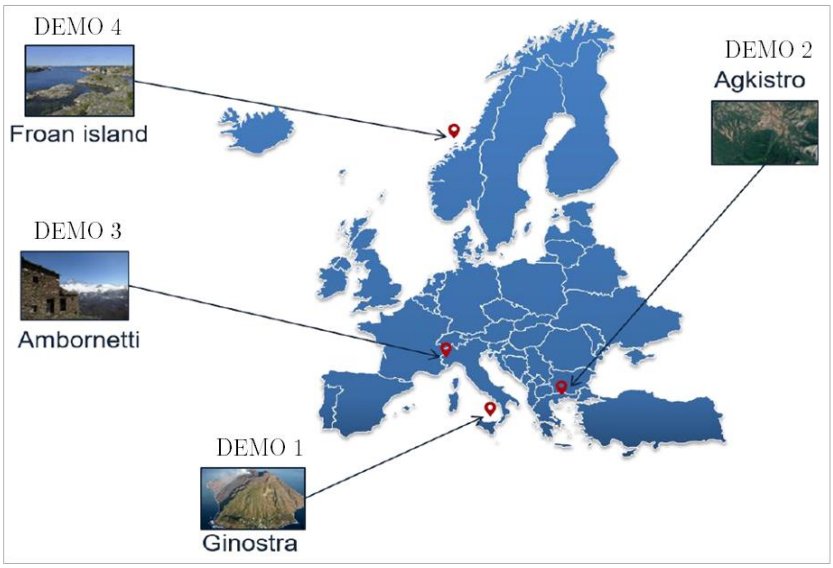

Figure 1.1: Location of DEMO sites [6]

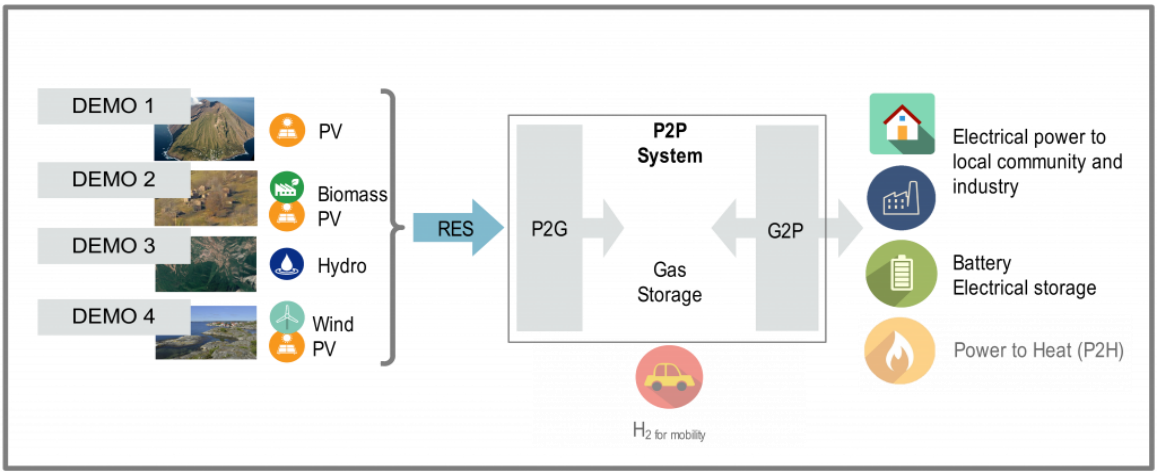

Figure 1.2: General technical configuration of P2P systems

1.1.3. Contribution to the project

Among the four demonstration sites, Froan/Rye (Norway) has been selected in this work for several reasons:

- The state of the advancement of the DEMO site is the highest with respect to the four DEMOs. It has already completed the installation phase with success and it is currently under testing in Rye, thus means that the plant's layout, together with

technical specifications of all components is available to perform the preliminary assessment regarding the proper operation of the system. Therefore, the outcomes of this work are based on authentic load energy profiles and the system is evaluated considering the actual performance curve of the plant components.

- DEMO 4 uses solar and wind renewable sources, two technologies that are widely employed in different locations. This adds a flexibility component to the system, allowing its testing in other contexts as well.
- It is the only site which foresees the connection with public electricity grid, giving the possibility to operate it both in grid-connected and island mode. This aspect is crucial for the purpose of this work, since it could open up a broad range of future-proof opportunities for P2P systems.

The contribution of this work to the project is the development of a flexible tool, in form of MATLAB set of algorithms, which measures the added value derived from P2P systems' interface with public electricity grid. To increase renewables penetration on national energy mix, countries started incentivizing green technologies by offering exceptional remuneration for interventions in the ancillary services market, as it is happening in United Kingdom and Italy [7].

The techno-economic assessment is first made by fixing the size of the components, for the sake of simplicity. Then it has been implemented an optimization procedure with the aim of maximizing the income coming from the market participation and, at the same time, lowering the upfront costs for the system.

1.2. Terna pilot projects

1.2.1. Regulatory framework

In May 2017, the Italian public authority ARERA has released the document *Delibera 300/2017/R/eel* proposing the progressive opening of the ancillary services energy market (MSD) to both production units fed by renewable energy sources and storage systems.

Before the comprehensive employment, the authority has decided, in accordance with the Italian Transmission System Operator Terna, to launch a set of pilot projects. The objective is to gather meaningful insights, finalized to a structural reform of that market, adapting it for the entrance of new flexibility sources (e.g. Vehicle-to-Grid, industrial producers) [8].

Terna plays the role of unique TSO in Italy; its main task is to transport energy at high voltage level along the whole territory. While performing it, Terna must satisfy the need of perfect balance between energy request and production. Most of the energy – produced and thus consumed – is traded in the traditional energy market, regulated by the public authority Gestore dei Mercati Energetici (GME), which selects the energy price by matching the load and supply daily curves. Nonetheless, unexpected events or systems flaws are very frequent, also given the system's scale, therefore the TSO needs an articulated control systems which is able to guarantee high reliability and security of the grid. For this purpose Terna procures the necessary sources to ensure the continuity of the national energy supply in the so called Mercato dei Servizi di Dispacciamento (MSD). This market is organized on six sessions [9] distributed over the day before and partially overlapping the day of delivery. When all sessions are over, Terna assigns dispatch orders for each daily hour, on the basis of the offers received. If something unforeseen happen, there is an additional safety net called Mercato del Bilanciamento (MB), where Terna performs a real-time energy provision to ensure the perfect match between demand and supply.

Before the introduction of pilot projects, MSD participation was allowed just to relevant production units – having more than 10 MW of nominal power. Therefore, until short time,

this function was covered by centralized power plants powered with fossil fuels. With the progressive phase-out of carbon-fed plants, the TSO has planned to qualify new energy sources, as aggregated units, for MSD participation.

1.2.2. Outline of UVAM aggregated units

On the one hand, the participation to MSD of alternative sources would be an important step forward in the path for de-carbonization of Italian energy mix. On the other hand, the TSO has not enough capillarity to reach all the distributed sources spread in the territory, besides most of the cases the single alternative unit has a nominal power which are not compliant with the current regulation – Codice di Rete – that defines the minimum threshold to be marked as relevant unit, mandatory requirement for market participants.

For these reasons, the distributed sources have to be aggregated on functional units called Unità Virtuali Abilitate Miste (UVAM). As virtual unit, it could be formed by one or more devices linked to different Points of Dispatch[1], as long as they belong to the same perimeter aggregation[2]. In addition to this, the unit must be enabled to MSD participation, which means to stay within energy and power thresholds, as well as respecting the requirements in term of dynamic response to Terna's dispatch orders.

The entity can be formed by four different configurations [10]:

[1] The Point of Dispatch is defined by the TSO as the connection point of the system with the national transmission grid. Usually it coincides with the Primary cabin, which contains the transformer.

[2] Be careful to not confuse the perimeter of aggregation, which is a virtual space of aggregation existent only in the framework of UVAM regulation, and the Point of Dispatch, which constitutes the physical point where the power exchanges occur.

I. All not relevant[3] production units, also not belonging to the same Point of Dispatch but under the same perimeter of aggregation.

II. All not-relevant consumption units, also not belonging to the same Point of Dispatch but under the same perimeter of aggregation.

III. A blended configuration of not-relevant production units together with storage systems. In this situation, the regulation imposes limits regarding the minimum energy content which storage systems must ensure in order to be authorized.

IV. The all-inclusive case: a blended configuration described above mixed with one or more consumption units. In right-bottom part of Figure 1.3 is depicted another possible situation, when the net qualified power at the grid interchange is however lower than 10 MVA, although a relevant production unit is present.

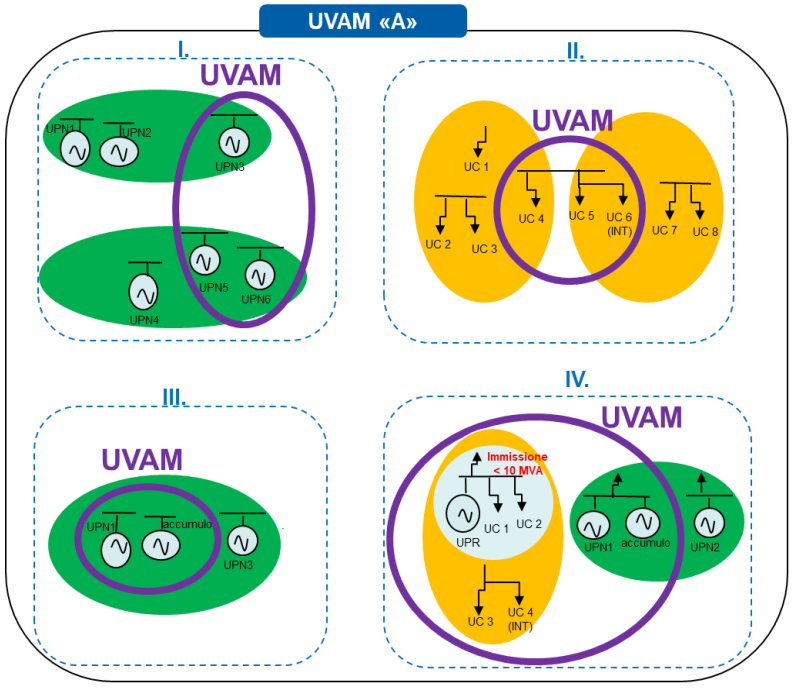

Figure 1.3: UVAM configurations [10]

[3] The regulation defines "relevant" the consumption or production units which ensure a maximum power above the 10 MW threshold. As consequence, "not-relevant" units are those not able to satisfy the requirement.

With the intent to keep clearly separated the business in the energy market with MSD, Terna decided to introduce a new player along the market value chain [10], which is the Balancing Service Provider (BSP). It is identified as third party between the grid operator (Terna), and the Balancing Responsible Party – what in the Italian energy market is called Utente del Dispacciamento [11], who operates in the common energy market. The BSP is the aggregator responsible for the performance provided in the MSD and it deals with the remuneration mechanisms by conveying the revenue streams coming from market operations to the plants' owners, obviously retaining a margin from the earnings.

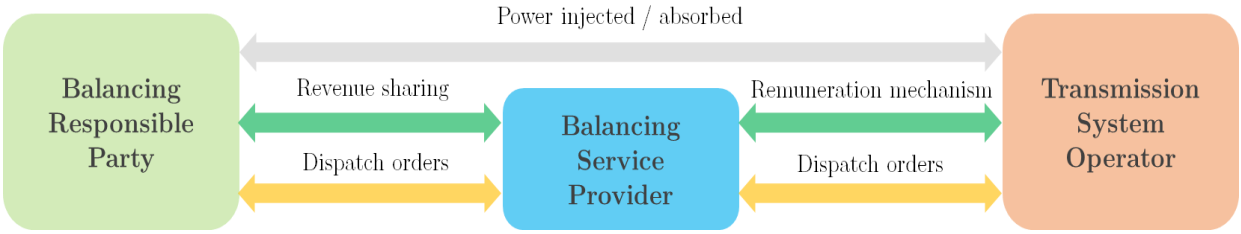

Figure 1.4 MSD market dynamics

1.2.3. Participation of UVAM to MSD: rules and requirements

To obtain the qualification for operating in the ancillary services market, UVAM must comply with a set of requirements imposed by Terna, which are listed in the official regulation [12].

The first threshold regards the minimum power allowed for assets characterization, in the first place this limit was set to set to 1 MW (both upwards and downwards[4]). Nevertheless, on June 3rd, 2020 ARERA published an update on the official regulation which confirmed the extension of the threshold to 200 kW, in order to broaden the participation to a wider

[4] The terms upwards and downwards in this specific case are referred to the ability of a generic power unit to either decrease its withdrawal – for consumption units – or increase its injection – for production units – thus generating a net positive variation of the power value in correspondence with the Point of Dispatch.

pool of distributed energy sources as well as to incentivize the roll-out of Vehicle-to-Grid paradigm [11] [12], where cars batteries can be exploited as valuable stationary assets when the vehicle is parked, at the same generating value for both, the TSO and the EV owners.

The market gathers an array of different services which differ from each other on a time duration basis. They are listed in the Table 1.2 (notice that all the values are valid both for upwards and downwards dispatch orders).

Table 1.2: Time duration of the MSD services

Service	**Starting time for modulation (after receiving the dispatch order)**	**Minimum modulation time**
Congestions resolution	*Within 15 min*	*120 min*
Rotating tertiary reserve	*Within 15 min*	*120*
Substitution tertiary reserve	*Within 120 min*	*480*
Balancing	*Within 15 min*	*120*

It is important to highlight that Terna employs a unique market channel to provide the necessary quantity of energy in order to build the consistent safety margin to operate. Therefore offers are presented following the unified procedure and the TSO is responsible for their management.

Regarding the offers' presentation, the BSP in charge for the UVAM has obliged to present a pre-defined offer[5], which is valid for the aggregate unless further indications. Offers are expressed under the form of a couple *quantity-price*, both upwards and downwards, according the system's availability. The quantity offer cannot be lower than the Qualified

[5] The pre-defined offer must be uploaded on Terna's digital portal by the first day of service delivery. It could be changed by the BSP every day for the following until 10 P.M.

Power[6], instead regarding the economic value of the asset, Terna has set the hourly strike price at 400 $\frac{€}{MWh}$.

Nevertheless, the selling-purchase market prices are highly volatile, depending on time of the day and plants' location. Terna makes use of the energy available in the market to solve unbalances which frequently occurs in the national grid, especially during peak hours, given that in Italy renewable energy production is mostly concentrated on the South whereas consumption follows the opposite scheme, being higher in the North.

More in general, wherever this kind of discrepancy exists, the TSO struggles to manage the congestions. This concept highlights one more time the importance of flexible systems to ensure safety and long-term reliability.

The economic remuneration provided by Terna is adequate to the importance of such services and it is divided as follows:

- *Spot market*: the operator recognises the service payment to the BSP in compliance with the value of energy made available. It is measured in $\frac{€}{MWh}$ and it strictly depends on the ability of following the market's needs, taking action when is actually necessary. On the other hand, if a generic player commits itself to take an action on the market – selling or buying an amount of power within a time slot – and it does not manage to uphold the dispatch order, the regulation foresees a penalty proportional to the mistake made.
- *Futures market*: it refers to a fixed yearly payment which Terna recognises to the BSP to obtain the guarantees for energy delivery, at pre-established conditions. For this kind of remuneration as well the regulator has established a cap price at 30'000 $\frac{€}{MW*year}$.

[6] The Qualified Power is established during the UVAM permitting process, it is possible to modify it under explicit request to the authority, however it cannot fall under the minimum threshold of 200 kW.

The tool developed in this work aims at optimizing the size of system's components taking into account in a detailed manner the remuneration mechanisms. The rationale behind the optimization is represented by the selection of an array of Key Performance Indicators (KPI) which have been considered important to assess the profitability of the system as well its potentiality for further development in the future.

1.2.4. Admission of P2P systems in UVAM

In the just described regulatory framework, P2P systems present several mainstays which made them particularly suitable for the application.

Unlike renewable energy sources in stand-alone configuration, P2P systems are equipped with storage assets, which help to smooth the typical component of unpredictability. Indeed, MSD participation requires a minimum commitment for UVAM in order to award the above-mentioned remuneration, which is difficult to observe during the whole year without an "energy buffer". For this reason, most of the aggregates which are already qualified or in the process of doing it present either a controllable energy source able to cover the load required by the regulator in case of lack of RES production, or a storage system of whatever kind.

In addition to this, the storage system comprised in P2P is perfectly capable to comply with dispatch orders sent by Terna[7] in terms of dynamic response to external signals.

[7] The regulation set clear indications about the time frequency and quality of the power measurement. However, a detailed explanation of this topic would be out of the scope of this work.

2. Technical analysis of the P2P system

2.1. Introduction and design aspects

The purpose of this chapter is the detailed analysis of each component of the technical configuration under study, in order to retrieve the necessary data as input of the model shown in the Chapter . It is depicted in the Figure 2.1.

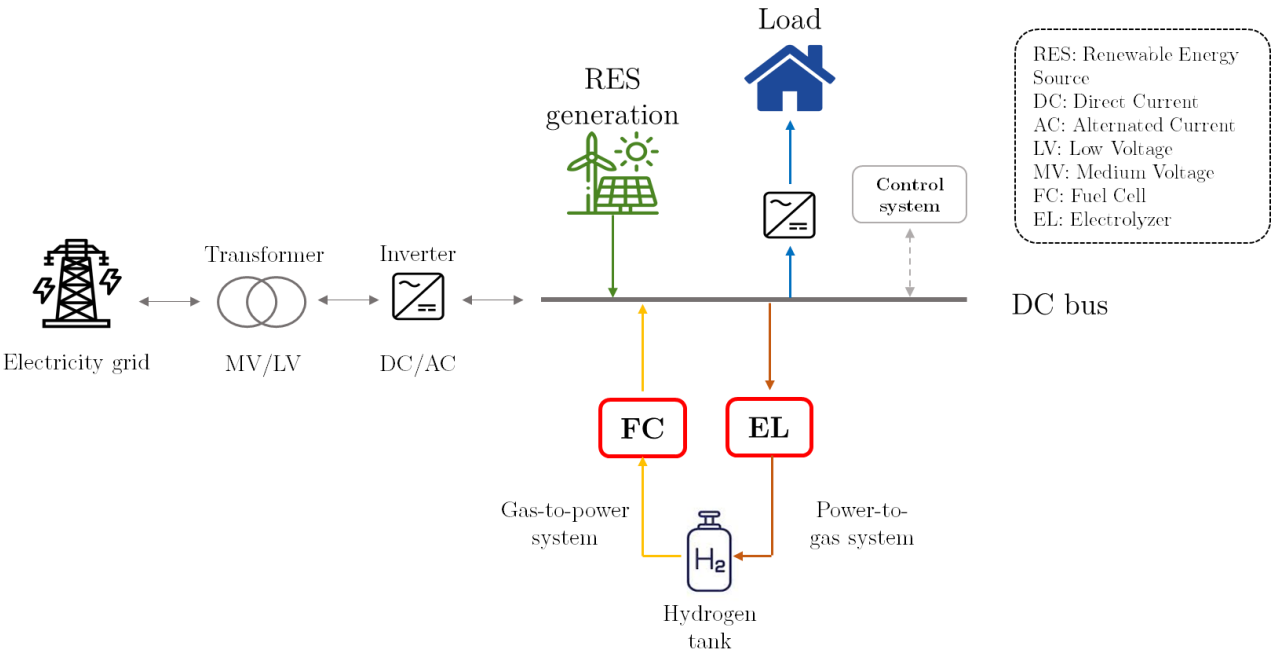

Figure 2.1: State-of-the-art configuration of a P2P system

The fundamental element of the whole system is the DC bus, which is the electrical node at which all the components are connected. Given the complex nature of the aggregate, a control system is needed. It has a twofold aspect:

- Software is used to redirect in a correct manner power fluxes, following pre-defined logic of functioning – the plant controller can set the control system for accomplishing specific needs, as in this case where the system must comply with requirements coming from specific grid regulations.

- Hardware instead is crucial in terms of voltage stabilization at the electric node. Therefore, inductances and filters are needed, especially when the plant is scaled up towards hundreds of MW of peak power.

Once verified the correct functioning of the DC bus and its related control system, the direction of the power flow is determined by the algebraic sum of the singular contributions, in terms of instantaneous active power. A first characterization of system components can be made according to the nature of energy source:

- Energy source: a positive power contribution to the DC bus is coming from the photovoltaic system, the wind turbine, as well as the fuel cell – which takes advantage of the hydrogen contained in the tank. In case energy demand cannot be satisfied by internal components, the electric grid makes available the power needed to maintain the above-mentioned equilibrium. Taking the power value derived from the external sources, it is mandatory to account for losses due to the transformer and the AC/DC conversion through the inverter[8] (Figure 2.1).
- Energy sinks: the primary objective of the system is to satisfy the load profile connected to the DC bus through a commercial inverter. It has the priority over all the other sinks. Where there is energy surplus at the node, this is used either to fill up the hydrogen tank (thanks to the electrolyzer) or is injected into the electricity grid in order to enforce potential dispatch orders in the MSD.

It could be noticed that the system under study lacks a short-term energy option as Battery Energy Storage System (BESS). This choice is well-founded due to four main reasons:

i. For the final purpose of this work, the elaboration of a tool including both short-term and long-term energy storage would be too challenging from the perspective of the control strategy that has to be implemented. In order to have a well-structured

[8] It is worth mentioning that the model developed contains the right efficiency chain for each component of the system.

algorithm, the dynamic assessment of which option to prioritize must be driven by more sophisticated prediction instruments. The decision of taking BESS out made feasible to implement an algorithm having as objective the optimal sizes of the components. Thus, the introduction of another form of storage in the system has been set as one of the future improvements of this work.

ii. Among the criticalities of P2P systems, there is surely the dynamic response to steep changes of level and/or sign of power signals (Figure 2.2), which actually are very frequent given the presence of not fully predictable source as PV and wind. Regarding this aspect, the P2G+G2P system depicted in Figure 2.1 is proven as suitable as battery systems to chase highly fragmented trends[9], as reported in [15] and [16].

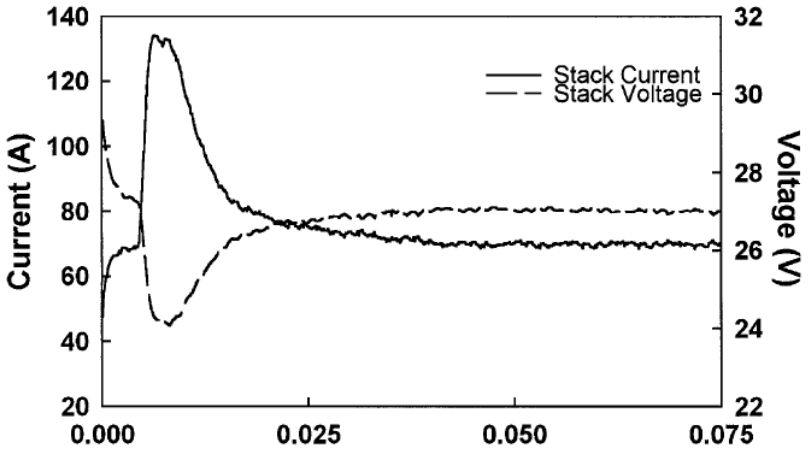

Figure 2.2: Dynamic response of a PEM fuel cell stack [14]

iii. Moreover, the hourly time discretization employed for the model makes the slight oscillatory behaviour, which is typically bounded within the first seconds after the signal delivery, negligible. Nevertheless, the issue of working outside the range of optimal performance could arise. The efficiency curves reported in Figure 2.3 describe a characteristic behaviour of such chemical machines: they are able to guarantee a significant conversion efficiency in a wide range of power, except for very low loads,

[9] This is verified in both direction of the power flow and thus in both the working configurations of the aggregate.

where irreversibilities takes over. The developed model takes into account the differentiated behaviour of the components; its main objective is to pinpoint the optimal sizing of the whole system allowing each element to operate as the best conditions as possible.

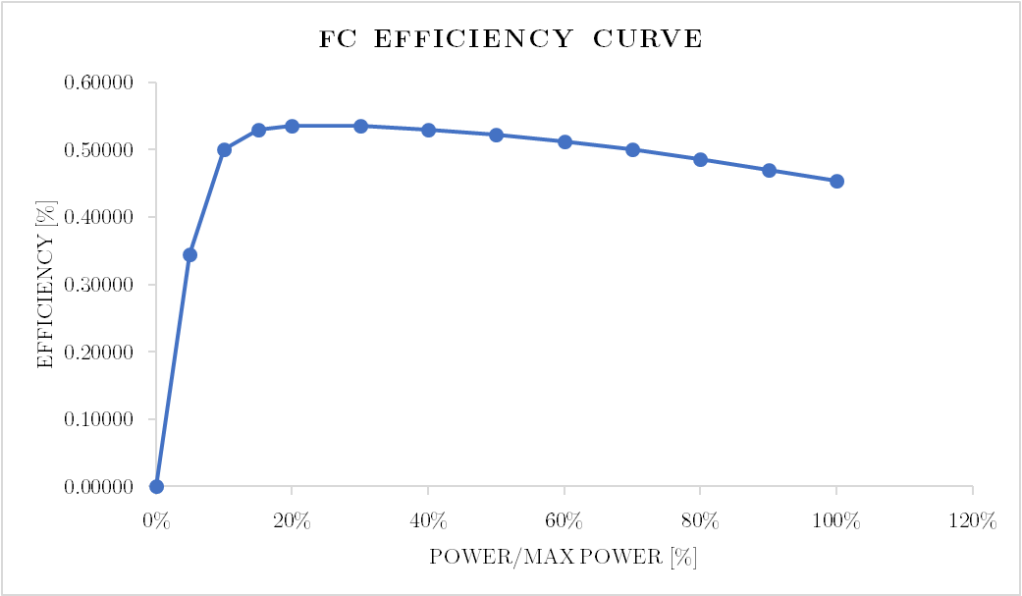

Figure 2.3: Fuel Cell efficiency curve

iv. Finally, employing a dual technology for energy storage rises an economic issue. Once stated the willing of deepening systems including hydrogen-based technologies, there is no room for adding the BESS. Such systems still entail too high upfront cost and need frequent – and expensive – replacement procedures due to the significant rate of degradation related to materials implied. At the moment, the expenditure conventionally expressed in €/kW is too large to justify a combined deployment. However, as it will be further discussed later, the economic projection regarding such components are strongly digressive in a mid/short-time horizon, both for high-pace advancement in Materials Science and targeted policies in the field of sustainable development.

2.2. Load profile

In the framework of the REMOTE project, it has been made the end-user characterization for the DEMO 4 (Rye, Norway); therefore, that information was picked up.

In particular, the load profile represents the annual consumption of a medium-size Norwegian farm [17]: it is surely a reliable input for the developed model since it captures the actual trend in terms of absorbed power at the node. Describing a common situation, such profile can be considered location-independent and thus it has been imported to Italy for the simulation of MSD participation.

The profile has been rescaled on the base of yearly energy consumption, which has been set around *400 MWh* measured at the DC bus – therefore including the inverter efficiency (97%) as well, since appliances of both residential and small commercial applications are almost all powered in AC – while the overall shape was maintained.

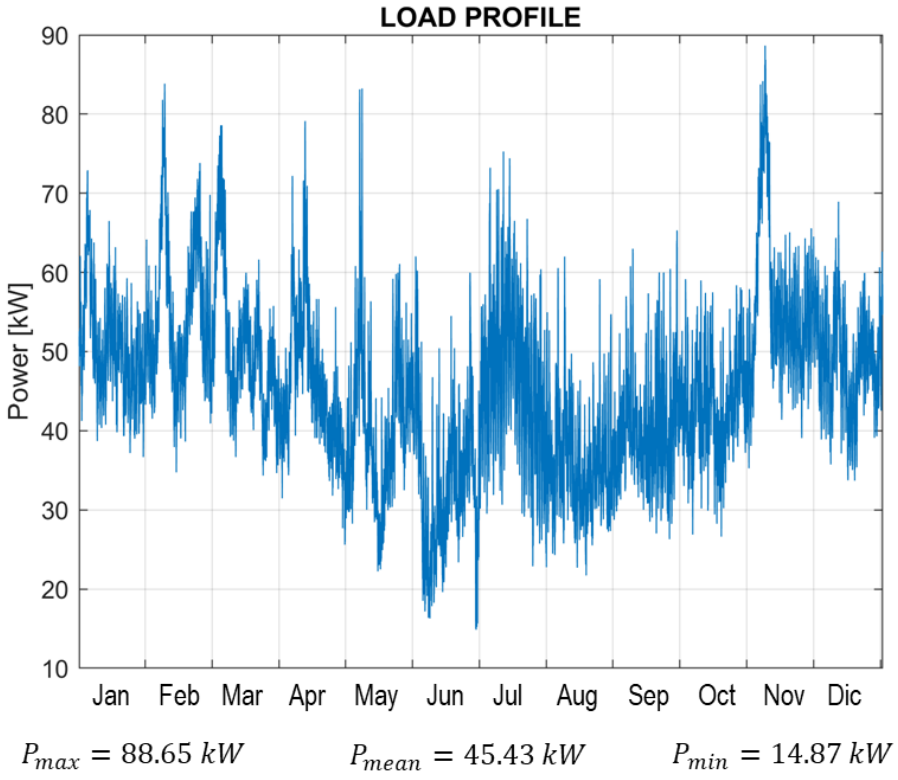

Figure 2.4: Load profile of Rye farm [16]

Therefore the profile depicted in Figure 2.4 has been imported in the central area of Italy, in the surroundings of Gubbio (PG). The precise location is highlighted in red in Figure 2.5 and consists of a countryside area close to Apennine mountain chain and a small industrial area.

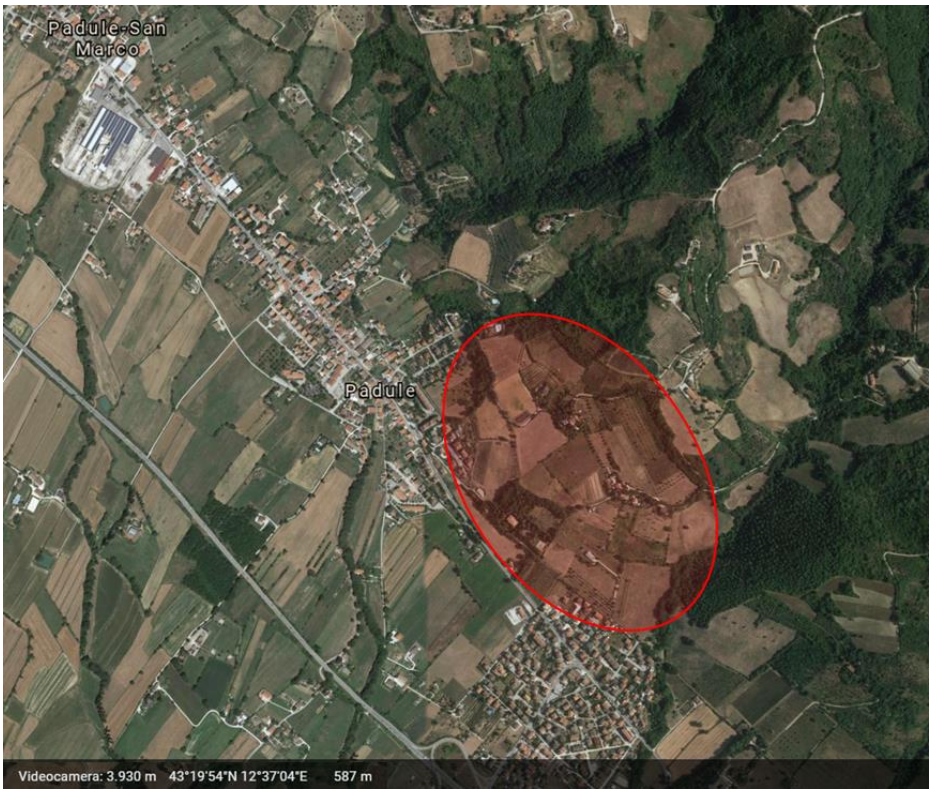

Figure 2.5: Foreseen location in Italy. Image from Google Earth

The reasons of the positioning are various:

- Regarding the field of application selected, the choice made seems to be reasonable. This area is famous at national level for agricultural production. Furthermore, it has a strategic position, being close to the Adriatic transmission line.
- As far the geographic location is concerned, it represents an intermediate situation concerning the forecasted production from PV and wind. To place the plant in the centre of Italy has been done on purpose, since the major part of PV plants and wind turbines are concentrated in the South – specifically Apulia and Sicily. Among the objectives of this work there is the attempt of demonstrating that is worthwhile to invest in this kind of projects also in other locations, even though the natural

resources available are objectively less abundant. In fact, to compensate for this lack it is necessary to design flexible systems in order to access different sources of income and make the project economically feasible.

- Finally, the most important aspect related to the location selection is the compliance with a rather urgent requirement for transmission lines. One the main actions performed by Terna is the congestion resolution. As already mentioned in the paragraph 1.1.1, the TSO often has to deal local with unbalances between production and consumption in the two halves of Italy. For this reason, to have available flexible elements in the middle could be a successful strategy, also from the perspective of the participation of the system to MSD. Terna selects the offers presented on the market, taking only those actually able to solve a problem in the grid. Thus, if the plant has a strategic positioning, the likelihood of operating with profit in the MSD becomes higher than the national average.

It is important to highlight that the model is completely agnostic with respect to the type of application represented by the load profile, it only requires raw power data, no matter the temporal definition[10].

[10] An optional algorithm for data sampling at hourly steps is already embedded in the model, in case input data are not provided in the right discretized sequence yet.

2.3. Prediction model for PV production profile

The solar energy resource is one of the most abundant on Earth; this is valid especially for Italy, where photovoltaic takes up to 20% of the total energy production from renewables [18]. The framework is still now dominated by hydroelectric, which ensures very high energy density but it is also strongly location-dependent, while the solar resource results well-distributed. By heading towards South, the value of solar irradiance justifies the deployment of GW-sized solar plants. Nonetheless, in the area under analysis it still assume acceptable figures to consider photovoltaic technology as valid alternative to fossil fuels.

Two features characterize energy produced by PV: it is not controllable, being totally dependent by the availability of the natural resource, while it is highly predictable in average, since solar irradiance is conditioned by some variables which are fixed once the location is established – for instance latitude, longitude, height above the sea level and so on.

To retrieve a sufficiently precise estimation of the yearly producibility would be enough to make use of historical data of solar irradiance. Nevertheless, it has been decided to bring the developed model to a finer grade of detail by including the aleatory component of cloudiness. For this purpose, solar irradiance values are evaluated through the Bright Solar model [19], [20], which will be discussed in deep later.

Data coming from the above-mentioned model were furtherly processed for the extraction of the solar energy producibility. The whole algorithm is structured in multiple subsequent steps summarized in a block diagram depicted in Figure 2.6.

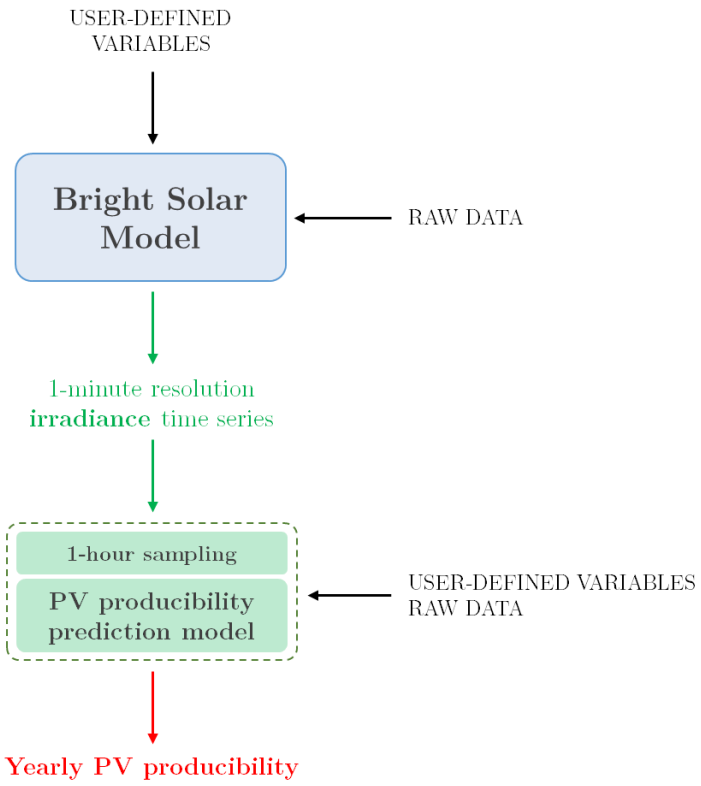

Figure 2.6: Block diagram of PV producibility prediction model

2.3.1. Bright Solar Model description

Solar irradiance varies on a minutely time scale. Such rapid fluctuations are mostly driven by cloud dynamics and atmospheric losses, thus only a finer time discretization allows to capture these effects.

The reason for this kind of model lies in the need to find a valid alternative to 1-minute resolution datasets, which generally lack of consistency and reliability. On the other hand, hourly weather data is widely collected and easy to gather from national meteorological offices [20]. Starting from this information, by employing one of the well-known algorithm for cloud cover stochastic prediction, the model is able to produce multiple 1-minute resolution irradiance time series for any tilt and orientation within a spatial domain [19].

The model is subdivided in two sections:

i. The first generates 1-minute resolution cloud cover map. The pattern is generated with greater complexity than in other models described in literature by using a one-dimensional method that considers cloud height, the speed of the cloud, and the statistical distribution of the horizontal cloud length. A distinct aspect of this methodology is the use of a multitude of Markov chains to stochastically determine future weather condition states of pressure, wind speed, cloud height and okta[11], incorporating the weather variation influence of season, the diurnal dependency and variations caused by pressure.

ii. The latter calculates solar irradiance in three steps: firstly the atmospheric transmission for each minute is determined, secondly the theoretical clear-sky irradiance is calculated based on earth–sun geometry, and finally the irradiance is broken down into its different components in order to obtain irradiance on an arbitrary plane.

It is also possible to retrieve intermediate outcomes from the model, such as clear-sky irradiance, giving the possibility to the end-user to make adjustments, as well as changing the cloud cover generation model, thus validating the outcomes.

The model provides a temporal data series only, and does not include a spatial dimension; for this reason, its application is limited to cases where the spatial element is not integral, such as small-scale PV supply and storage systems, where a single high-resolution irradiance data series input is enough for the systems purpose [20]. Though, an updated version is freely available in case solar irradiance values must be evaluated over a broad spatial domain.

[11] An okta is the representation of cloud amount reported in eighths. Basically, the sky is divided into eight portions and the cloud cover is measured by estimating how many portions of the sky are actually full of clouds. Therefore, zero okta represents the complete absence of cloud, while eight okta a full cloud cover. An additional value of nine okta represents full coverage due to fog or other meteorological phenomena [46].

It is important to underline that the methodology is carried out using 1-minute input observational data from Cambourne (Cornwall, UK), which means the cloudiness evaluated by the model will be representative of a different location with respect to that of interest for the final objective this work. Nonetheless, the assumption proves to be cautionary, since United Kingdom presents higher cloudiness than Italy on a national average.

The model is presented as MATLAB set of algorithms and it requires as input user-defined variables listed in

Time	Starting day of the simulation	01/10/2018
	Ending day of the simulation	31/12/2019
Space	Latitude	43.32° [21]
	Longitude	12.62° [21]
	Height above sea level	535 m [21]
Panel-related data	Azimuth angle	0° [22]
	Pitch angle	33.6° [23]

.

Table 2.1: Input data for Bright Solar Model

Time	Starting day of the simulation	01/10/2018
	Ending day of the simulation	31/12/2019
Space	Latitude	43.32° [21]
	Longitude	12.62° [21]
	Height above sea level	535 m [21]
Panel-related data	Azimuth angle	0° [22]
	Pitch angle[12]	33.6° [23]

The model provides the final outcomes through a vector containing solar irradiance values and offering data visualization by selecting a precise day of those analysed and reporting the corresponding solar irradiance, cloud cover and okta numbers.

[12] It has been employed for the calculation one of the most well-known formula for the evaluation of the tilt angle for a fixed solar panel: $optimal\ tilt = 3.7 + (0.69\ x\ Latitude)$ [°].

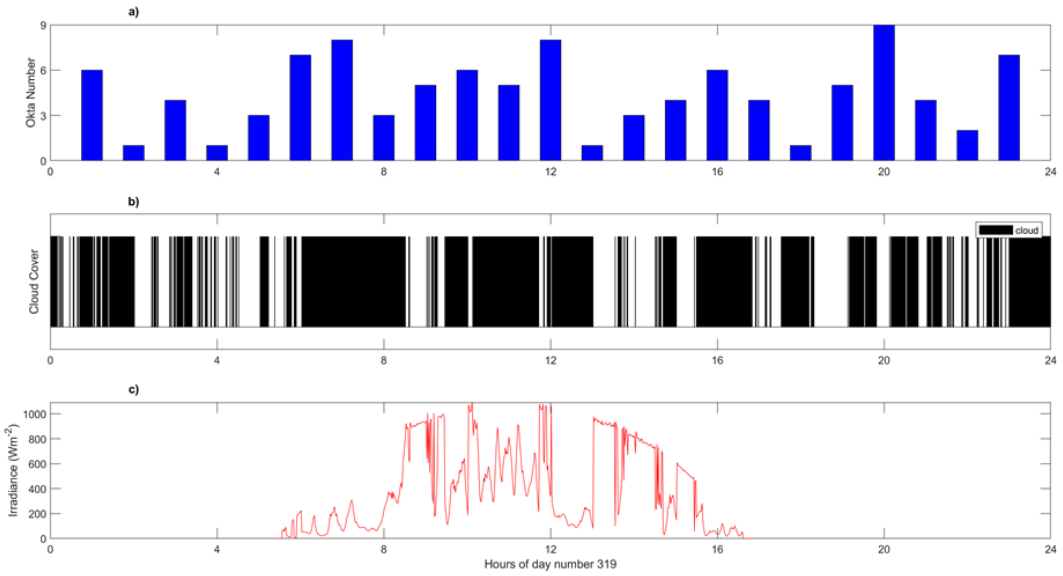

Figure 2.7: Data visualization for Bright Solar Model

2.3.2. PV producibility prediction model

Before the calculation of the yearly energy yield of the system, a pre-processing step is necessary to enable a coherent communication between solar irradiance values coming from the Bright Solar Model and all the other input variable to the main algorithm.

Therefore, a change in temporal resolution of the input data is needed to comply with the requirements coming from Terna and MSD. The management of raw data having different time steps would be too challenging in response to a not relevant improvement of the tool's accuracy. Thus, solar irradiance values has been sampled at 1-hour resolution in MATLAB, by extracting the average of 60 successive values as representative of the corresponding hour.

The irradiance values can be converted in power output by adopting a broad range of models, which have an increasing degree of complexity with the number and type of correlations considered. For this purpose, the model selected is outlined in [24], it takes into account the two most influencing factors for PV plants' yield:

- Electrical losses have direct impact on irradiance values and they are represented through the efficiency parameter η_{el}. This figure includes the power losses due to cables and connection with the central system, while those due to the presence of the inverter has been accounted in the main model described later. Given the electrical layout of the system, the DC power measured at the DC bus is needed, whereas the efficiency of the inverter will be considered when power exchange with the main grid is actually occurring.
- The external temperature influences the functioning of PV panels. This relationship is embodied by the thermal efficiency η_{th}. Starting from the air temperature, it is possible to evaluate this parameter over the whole year, accounting for the seasonal variations. In order to allow the prediction model to reflect more the reality, monthly temperature of the chosen location are kept from updated database [25]. The temperature of the PV panel is then calculated using the following formula:

$$T_c = T_{air} + \frac{NOCT-20}{800} \cdot G\ [°C] \quad (1)$$

Where $NOCT\ (Nominal\ Operating\ Cell\ Temperature) = 45\ °C$ and G is the solar irradiance measured in $\frac{W}{m^2}$.

Finally, the efficiency parameter is evaluated as:

$$\eta_{th} = 1 - \alpha_{th} \cdot (T_c - 25) \quad (2)$$

Where α_{th} represents the loss coefficient due to the temperature and it is set to 0.45%. It must be noticed that the thermal efficiency can have a favourable effect in case the panel temperature does not exceed 25 °C, taken as reference value for the average annual temperature at South European latitudes. Therefore, colder climates help PV power production since does not bring to module overheating [26].

As output of the model, dimensionless values of the power – or rather reported in per unit – are obtained, which will be further scaled with respect to the nominal size of the PV field, expressed in kW_p.

$$\frac{P_{DC}}{P_{nom}} = \eta_{el} \cdot \eta_{th} \cdot \frac{G}{1000} \text{ [pu]} \quad (3)$$

$$P_{DC} = P_{pu} \cdot P_{nom} \quad (4)$$

After the producibility evaluation, it has been implemented a data visualization routine on MATLAB to validate graphically the outcomes of the model.

Figure 2.8 depicts two power profiles evaluated during a generic winter and summer day.

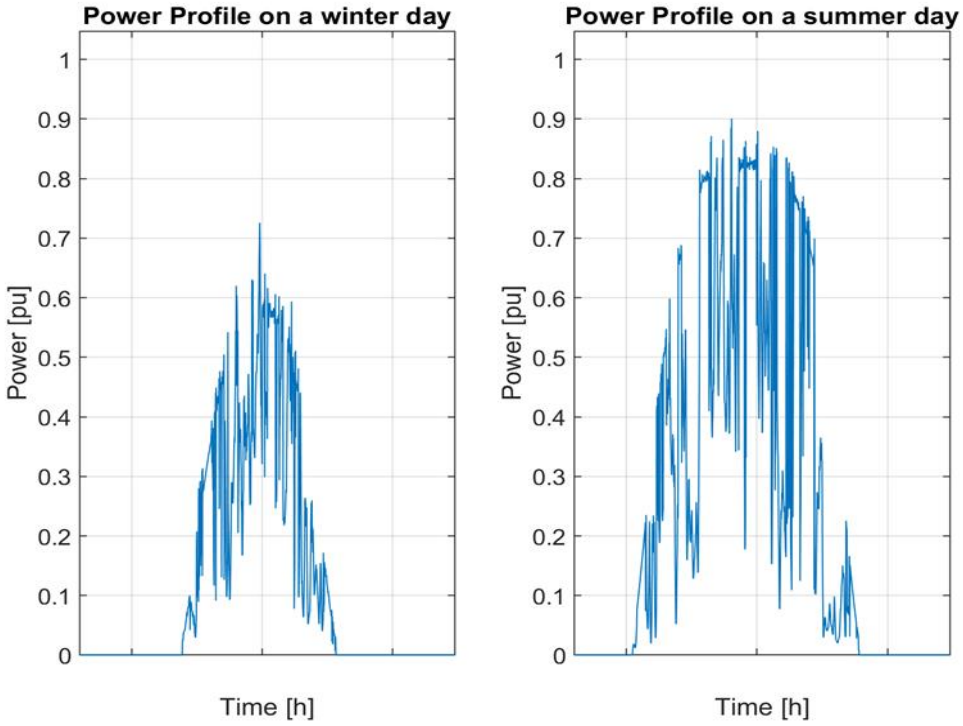

Figure 2.8: Representation of generic PV power profiles

2.4. Prediction model for wind production profile

Wind energy source is a consolidated technology, especially in Southern Italy, where wind farms ensure hundreds of GWh to supply towns and industrial activities. The main tendency clearly states that overall costs of the technology are falling down, which allows to become reasonable its employment in "stand-alone" application for P2P systems. So far, this work considered a single small-size wind turbine, though it is fully trained to be scaled up.

In the framework of the REMOTE project, it was considered a best-selling wind turbine [27], sold by the Danish company Vestas, which ensures 225 kW at full power. The product dominates the market especially in windy locations as Norway, thus it was the best fit for DEMO 4. It presents technical features not compatible with locations which do not ensure abundancy of wind resource. This is clearly the case of Gubbio, which is characterized by an annual average wind speed of 2.35 m/s, a considerably lower value with respect to Rye.

Therefore, a different commercial wind turbine has been selected, mainly on the base of its cut-in wind speed. This parameter represents the minimum wind speed at which the turbine starts generating power, thus products having lower cut-in are more effective on challenging locations. For this reason, the Enercon E33 was chosen, having the German manufacturer an excellent reputation. The turbine is able to produce up to 330 kW as peak power, reached at 12 m/s: its power curve is depicted in Figure 2.8.

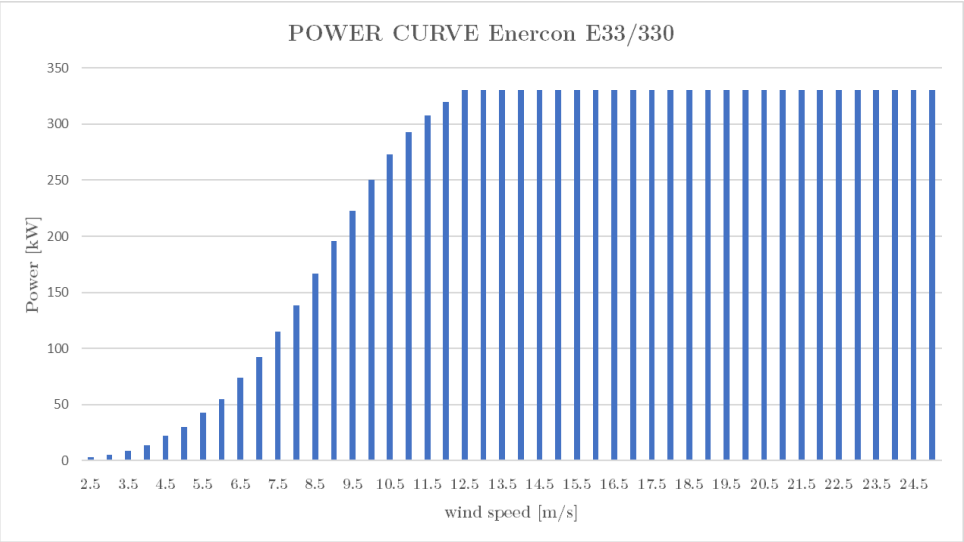

Figure 2.9: Power curve of Enercon E33/330 kW

The technical specifications of the selected products are in Table 2.2 [28].

Table 2.2: Technical specifications of Enercon E33/300 kW

Data	**Value**
Cut-in wind speed	2.5 m/s
Cut-out wind speed	25 m/s
Maximum power	330 kW
Diameter	33.4 m
Area	1963.5 m^2
Hub height	50 m

The annual energy produced by the selected turbine has been evaluated through the following steps:

1. Raw data for the location was imported in the MATLAB script from PVGIS database[13], which provides several meaningful information about the atmospheric conditions of a prescribed, for instance temperature, relative humidity, rather than wind speed and direction, on hourly basis.
2. Another impacting factor is the variation of air density according the actual height of the wind turbine and the air temperature. Vertical changes in density are usually

[13] It is one the most known database, it has been developed by the Joint Research Centre (JRC), the European Commission's science and knowledge service which employs scientists to carry out research in order to provide independent scientific advice and support to EU policy.

considered in annual wind turbine producibility, since power curves provided by manufacturers are evaluated during tests in standard conditions, thus not accounting for specific location characteristics. However, the seasonal variation in air density is forgotten in most of the case, though there are evidences showing that neglecting the dependency could bring to significant errors [29]. In order to not overload the calculation – other relationships can be considered in the model, just by modifying the source script – it has been chosen a semi-empirical formula reported in [30] to evaluate the monthly air density, exploiting the same data used in PV producibility model as far monthly temperature values is concerned.

$$\rho = 3{,}4837 \cdot \frac{\left(101.29 - 0.011837 \cdot (h + h_{hub}) + 4.79 * 10^{-7} \cdot (h + h_{hub})^2\right)}{T_{mon} + 273.15} \left[\frac{\text{kg}}{\text{m}^3}\right] \quad (5)$$

3. The specific location influences the annual producibility accordingly with the conformation of the territory. The presence of obstacles spread on the ground, having both geological and anthropic origin, constitutes a crucial information to retrieve during the design phase of a wind power plant, since the presence of solid bodies at different heights introduces different phenomena which negatively impact wind speed, thus in turn the energy produced will be reduced.
    i. The distributed roughness of the ground is evaluated through the Hellmann coefficient α, which gives an indication of the landscape that surrounds the wind farm. According to different situations encountered, the coefficient increases as the obstacles become denser while goes towards zero in almost flat scenarios, as open sea or wide expanses of ice.

Table 2.3: Hellman coefficient, indication of ground roughness [31],[32]

Terrain typology	**α coefficient**
Lakes, ocean, and smooth hard ground	0.10
Foot-high grass on level ground	0.15
Tall crops, hedges and shrubs	0.20
Wooded country with many trees	0.25
Small town with some trees and shrubs	0.30
City area with tall buildings	0.40

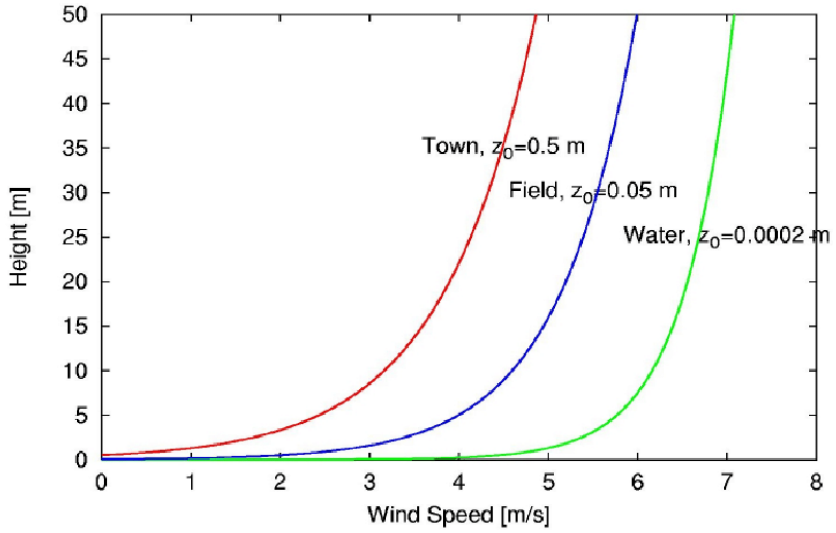

Figure 2.10: Graphical representation of Hellmann coefficient [47]

As it is possible to see from Figure 2.10, the wind speed boundary layer suffers significant modifications according to different terrain typologies. It maintains a not disturbed speed along almost all the vertical direction in particularly flat cases – ice, water or some plains –, while it presents a consistent transition zone in presence of a dense configuration of solid bodies. The considered location presents both anthropogenic obstacles, such as dwellings or factories, and natural elements as trees and bushes. For this reason, it has been taken an intermediate value in the Table 2.3 as Hellmann coefficient: $\alpha = 0.275$ in order to account for the terrain diversity.

ii. The last factor that has to be considered is the impact of localized roughness phenomena. Usually, in correspondence of urban agglomerates made by high buildings, fluid dynamic effects like air recirculation and vortex, which constitute an element of discontinuity with respect to the smooth profile given by the Power Law depicted in Figure 2.10. It is common practice to characterize these localized effects through ad-hoc Computational Fluid Dynamics (CFD) analysis, in case they would be effective for the wind producibility calculation. Nonetheless, this is not the case, since there are not

present solid bodies which could drastically change the original trend imposed by the Power Law calculated with the selected coefficient.

$$v_{wind_{eff}} = v_{wind_{10m}} \cdot \left(\frac{h_{hub}}{h_{10m}}\right)^{\alpha} \quad \left[\frac{\text{kg}}{\text{m}^3}\right] \tag{6}$$

PVGIS provides the hourly wind speed in the prescribed location measured at 10 meters as height. Among many formulas employed to estimate the effective wind speed felt at the wind turbine's hub, the Power Law consists in the best representation of the actual profile of the wind boundary layer [33].

Once evaluated the corrected values of wind speed for the entire year, the characteristic curve of the selected wind turbine has been used to find the value of power produced in the specific hour, thus calculating the whole producibility of the machine by summing up all the hourly contributions. One of the main advantages of the method just described is that it is not necessary to make dubious assumptions to evaluate the actual power capable to generate the wind turbine, since the power curve in Figure 2.9 is directly supplied by the manufacturer as already accounting for the related efficiency chain. The only contingency kept external to the chain is the Capacity Factor, accounting for forced maintenance or unforeseen faults, thus it represents the wind turbine availability. This parameter has been set at $CF = 0.98$ (correspondent to almost 8 days of out-of-service), which constitutes a reasonable guess for a reliable systems as onshore turbines.

The Figure 2.11 below shows the recurring trend of wind power production during a typical summer month.

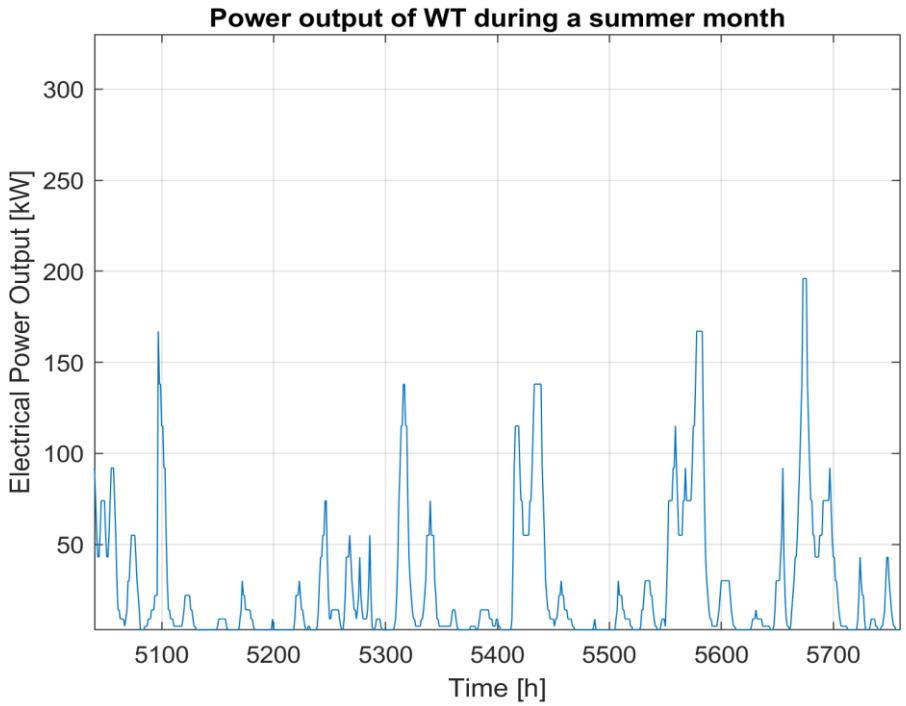

Figure 2.11: Wind power production of Enercon E33/300 kW in a summer month

2.5. P2G system description

The system sub-unit composed by the fuel cell, electrolyzer and hydrogen tank is responsible for the long-term energy storage. A distinction can be made for the components belonging to the sub-unit: the elements empowering the energy conversion are separated from the hydrogen tank.

The **fuel cell** is the machine which converts chemical energy into electrical one. By injecting the right amount of reactants, the ongoing processes occurring inside the components allow the simultaneous incurrence of a flow of electrons together with the establishment of a voltage difference due to the charge separation phenomenon.

The continuative holding of such condition generates a DC electrical power, ensuring high efficiency of conversion for a broad range. Many typologies of fuel cells have been proposed so far, whose differences lie in employed materials for the construction and reactants for the operation phase.

Among the most widespread, Solid Oxide Fuel Cells (SOFC) fit for high performance applications, where the system is able to operate in challenging conditions[14]. Nevertheless, the selected typology is the Proton Exchange Membrane Fuel Cell (PEMFC), which is able to work at much lower temperature – close to ambient conditions – processing hydrogen and oxygen as reactants, still maintaining a relevant efficiency of conversion.

It has been decided to confirm the choice already made for DEMO4 – and for all the other plants of the REMOTE project employing hydrogen-based technologies – to adopt PEMFC due to its compatibility with the microgrids.

This kind of component works in far fewer extreme conditions than SOFC one, thus it requires less effort to maintain and to monitor the expected performance during the operational phase. Moreover, PEMFC ensures a good attitude to power regulation and

[14] SOFC can reach up to 850 °C as optimal operative temperature. At this temperature regime, kinetic process are strongly speeded-up, thus allowing to neglect losses due to transport and activation processes.

poorly suffers frequent start-up and shut-down procedures, which are hardly withstood by high temperature fuel cells[15].

In the framework of DEMO4 plant, they selected a FC module supplied by Powidian[16], having 100 kW of peak power. Fortunately, the fuel cell system architecture is modular, thus allowing to easily perform the scale up of the system while maintaining the same trend in terms of efficiency. For this reason, the maximum achievable power of the fuel cell is set to 270 kW, though this number will be optimized successively.

The efficiency curve reported in Figure 2.3 suffers a lowering towards the extreme points of the range of achievable power, due to kinetic phenomena which slow down the chemical reactions occurring in the machine.

Contextually, the chemical machine just described is intrinsically reversible, thus by imposing an electric power to the electrodes as well as providing pure water to the cells, the machine called **electrolyzer** is able to split H_2O to generate hydrogen having high degree of purity. Most of the concepts already explained for fuel cells are valid for electrolyzers as well, for instance their modularity is confirmed, as well as the preference, for the sake of

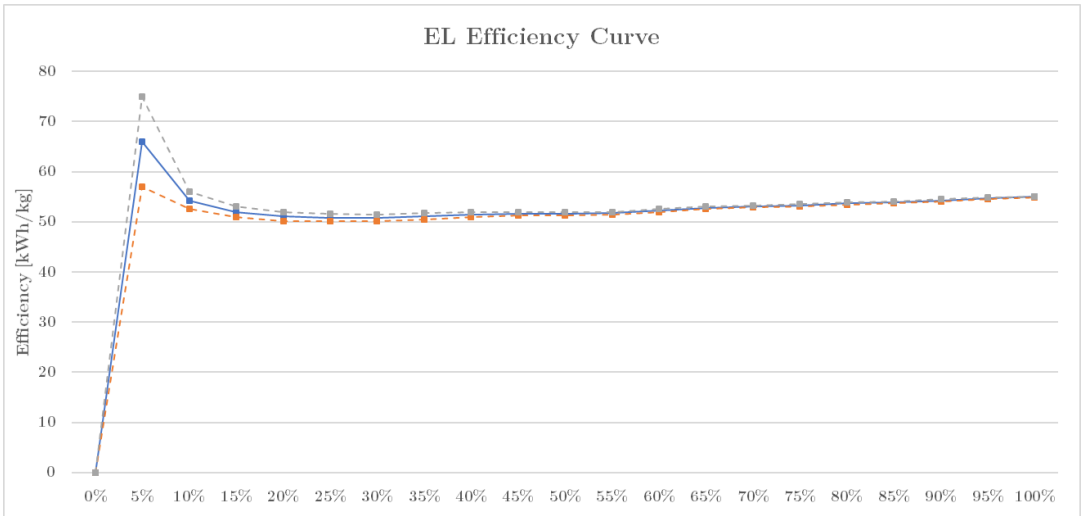

Figure 2.12: Efficiency curves of the electrolyzer

[15] Frequent changes of operating temperature bring to a fast degradation of the active materials contained into the machines.

[16] PowiDian is one the main stakeholders of the entire REMOTE project listed in Table 1.1.

this project, to adopt PEM electrolyzers instead of Solid Oxides technology to exploit the same advantages already described above.

The performance curve depicted in has similar trend with respect to that recurrent for fuel cells, though it presents a more pronounced maximum region around 5% of the nameplate power together with a rising trend towards a full power condition.

In the framework of the developed model, both components are virtually operated avoiding inefficient points of functioning, trying to maintain the efficiency of conversion always close to 50% - which represents a much higher value with respect to state-of-the-art diesel generators, often implied in remote locations, acting as back-up energy system. The peak power consumed by the machine is set to 270 kW as input of the model.

The remaining part of the P2G system is constituted by the element which is responsible for storing the energy under the form of hydrogen produced by the electrolyzer, representing the connection point between the two chemical machines. Nowadays, this component can be considered almost fully standardized, though the huge step forward on Material Science are bringing this technology to be more reliable in terms of structural integrity and cost-effective.

The sizing of this component is tightly dependent to that of the whole P2G system – thus considering the size of fuel cell and electrolyzer – indeed in the developed model has been taken as attempt value a capacity of 75 kg of H_2. Nonetheless, the main objective of the optimization tool described in the final part of this work is to obtain an optimal size of the tank so that the need for external energy source in the system can be minimized, while the revenue streams coming from the MSD participation can be maximized.

In Figure 2.13 is reported a commercial example of state-of-the art hydrogen tank [34].

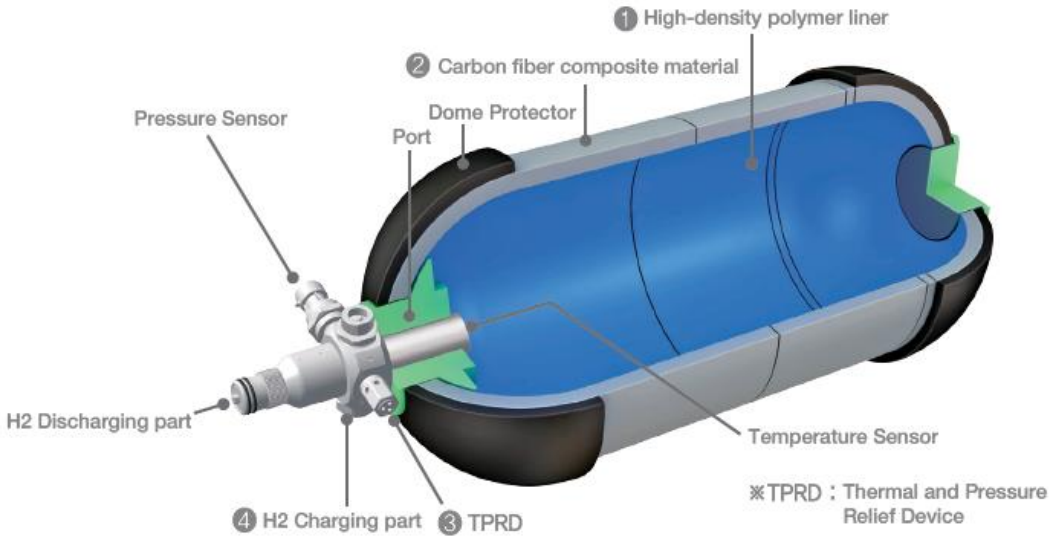

Figure 2.13: Explicative example of a commercial hydrogen tank

3. Simulation Model of the P2P system

3.1. Introduction to the model

The model is composed of a sequence of MATLAB codes, each of them making a specific task along the whole chain. Regarding the decision of employing the programming language MATLAB environment, the main reasons are briefly listed below:

- After a comparative action on different programming languages, the best fit was found with MATLAB, due to the following reasons:
  - Intensive use of vectors and matrices having different dimensions, need for storing and importing partial results along the chain of algorithms.
  - For how the model was built, the language must fluently manage Boolean conditions linked to nested loops. MATLAB proved to be well-suited to perform the specific task.
  - Easy and immediate compatibility with external software such as Microsoft Excel, which has been heavily employed in the section related to the cost analysis and during the handling of input data.
- The software was chosen also looking at the conclusive part of this work, that related to the optimization procedure. MATLAB released additional optimization tools together with the main environment, which are easy to use and provide meaningful results in reduced time.

It is worth to highlight that the developed work has started from an existent backbone represented by a MATLAB script produced for DEMO4 in the framework of the REMOTE project. It was a good starting point; however the entire structure was reorganized and the presented model was fabricated from scratch.

The block diagram presented in Figure 3.1 depicts the whole codes, from the input data – their calculation has been already explained in Chapter 2 – to the final economic assessment of the plant, together with the tools employed to perform some specific tasks.

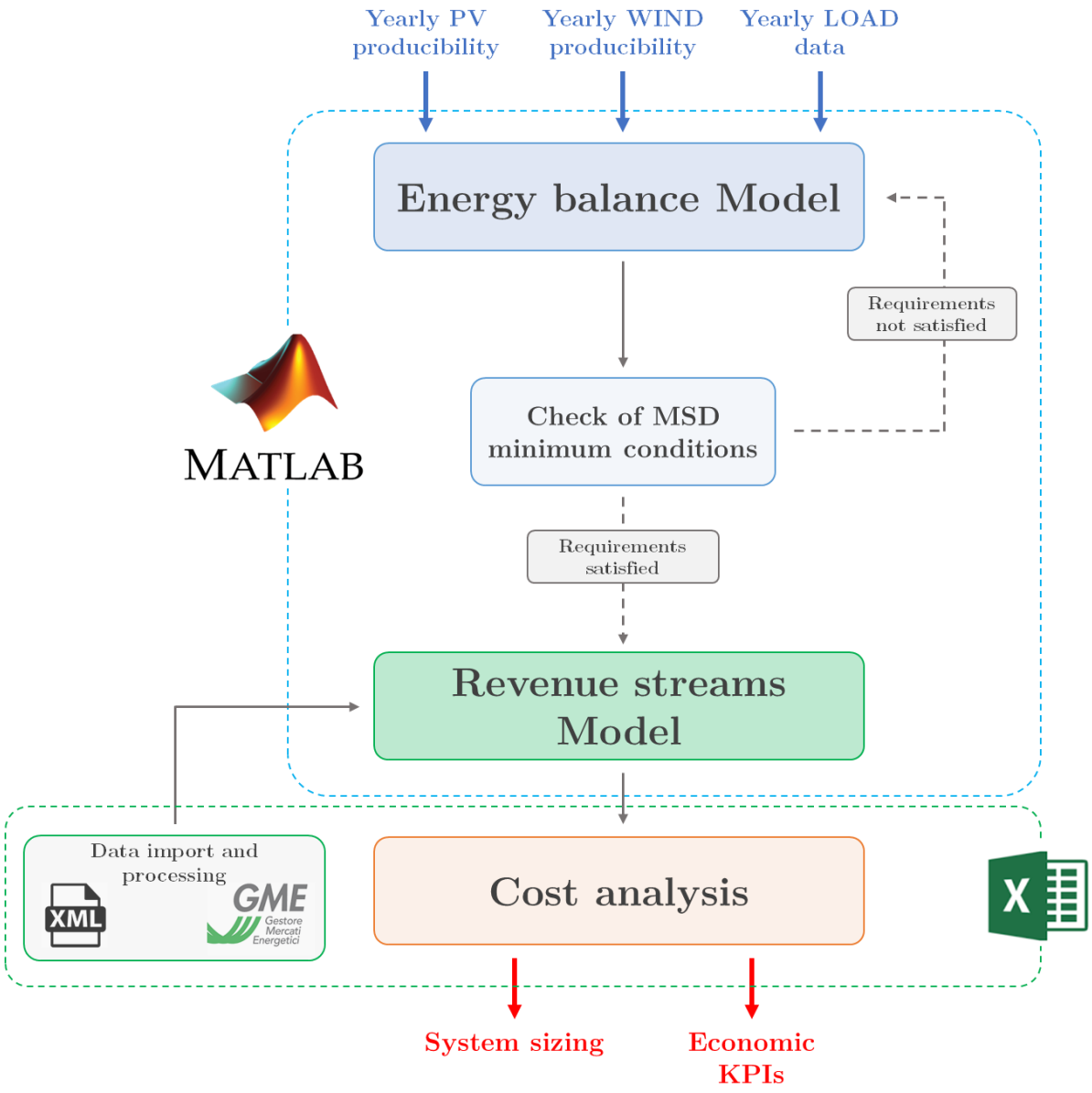

Figure 3.1: Simplified block diagram of the developed model

3.2. Energy balance Model

3.2.1. Pre-processing section

The first section is dedicated to the description of the data import. The outcomes are organized in separated arrays with length equal to the number of hours of a year (namely 8760).

Therefore, the balance measured at the DC bus can be already evaluated, in order to figure out whether the load overcomes the hourly power production from renewables or vice versa. The calculation includes an additional contribution to the load due to the system auxiliaries. Even though the efficiencies of the components are considered separately, a small fraction of the power is implied to drive the Energy Management System[17] (EMS), which is the control system managing the HVAC and the entire electronic part coupled with the machines. The power expenditure from EMS has been quantified to 5 kW, although this variable is highly dependent to the size of the system. For the scenario considered, the above-mentioned value can be considered a reasonable guess.

The establishment of the power sign – or thinking in terms of power flow, the direction – is the first main branching in the energy balance model, since it drives the behavior of all the system's components.

But first it is necessary to define the technical specifications and the simulation choices of the P2G system.

- As far the fuel cell is concerned, the range of operation is expressed as fraction of the nameplate power of the machine. The selected interval is [10% ÷ 100%], in order to avoid operating points characterized by too poor efficiency of conversion. Contextually, from the limits in percentage were calculated the absolute values

[17] The EMS is the software part of the energy systems. It actuates the control logic, which can be fixed in advance by the plant controller or it is driven by predictive algorithms, which adapt the behaviour of the system according to the trend of other external factors.

which bound the power produced. Finally, the efficiency curve was imported as MATLAB function, since it changes according to the power required by the system.

- Regarding the electrolyzer, also in this case the range of operation is expressed as fraction of the nominal power of the machine. The chosen interval is [10% ÷ 100%], to avoid working out of the optimal field of operation. Contextually, from the limits in percentage were calculated the absolute values which bound the amount of hydrogen produced. Finally, the efficiency curve was imported as MATLAB function, since it changes according to the power required by the system. In this particular case, the electrolyzer manufacturer has provided information as percentage of hydrogen Lower Heating Value (LHV), expressed on $\left[\frac{\text{kWh}}{\text{kg}}\right]$, thus it was made a further step to evaluate the punctual efficiency.

$$LHV_{H_2} = 119.96 \ \left[\frac{\text{MJ}}{\text{kg}}\right] \tag{7}$$

$$\eta_{EL} = \frac{LHV_{H2} \cdot \frac{10^3}{3600}}{\eta_{EL_{\%LHV}}} \ [\%] \tag{8}$$

- Regarding the hydrogen storage, the target mass of hydrogen contained into the tank is not the only meaningful information for the model, but the limits of operation must be defined as well. The amount of hydrogen present in the tank can be represented by the dimensionless variable State of Charge (SoC): for the sake of simplicity, it was considered in the model a direct relationship between the just mentioned variable and the actual pressure of the gas within the containment. In this way the limits detection becomes straight-forward, since it is related to the maximum and minimum pressure allowed in the tank – which are specified by the manufacturer as well.

$$p_{max} = 28 \ \text{[bar]} \tag{9}$$

$$p_{min} = 3 \ \text{[bar]} \tag{10}$$

$$SoC_{max} = 1\ [-] \tag{11}$$

$$SoC_{min} = \frac{p_{min}}{p_{max}} = 0.1071\ [-] \tag{12}$$

$$m_{H_{2_{min}}} = SoC_{min} \cdot m_{H_{2_{nom}}} = 8.036\ [\mathrm{kg_{H_2}}] \tag{13}$$

It is important to underline the relevant assumption made, since the system cycling brings the capacity of the hydrogen tank to a substantial decrease over its lifetime [35]. In the model was not accounted the capacity fade effect on a yearly basis, but it is surely an insight for future developments. The corresponding energy content is evaluated as function of the hydrogen mass as follows:

$$E_{ACC} = \frac{m_{H_2}}{LHV_{H_2} * \frac{10^3}{3600}}\ [\mathrm{kWh}] \tag{14}$$

Moreover, the model needs to be initialized properly. The initial guess related to the initial SoC of the hydrogen tank is set at 0.5 in order to guarantee a symmetrical option of charging/discharging the tank. Besides, the vectors which will be updated at each step of the loop must be allocated *a priori*, to be successively fulfilled once at a time.

3.2.2. Outlook on efficiency chains

Before proceeding with the explanation of the rationale behind the model, it is important to clarify the efficiency chains applied to systems' components, so that the energy balance would be respected over the whole year.

As already pointed out in section 2.2, the selected load profile is derived from experimental measurements at the DC-side of the electric node, thus it accounts for the constant contribution given by the inverter and the eventual copper losses along the cabling system.

The PV field and the wind turbine do not need a further penalty on the amount of energy produced, since the correspondent models provide the DC power at the node, already accounting for the all the losses.

The machines belonging to the P2G system could work at different voltage according to the different equipment manufacturer. The different voltage level is mainly due to how many cells – the elementary unit of the electro-chemical machine – are linked in series. Depending on various needs, the voltage coupling could be different. Therefore, it was foreseen an element of voltage conversion in the model to account for this add-on. Nonetheless, bi-directional DC/DC converters ensure very high efficiency, as it is possible to notice in Figure 3.2, thus their inclusion does not deeply affect the producibility of the system.

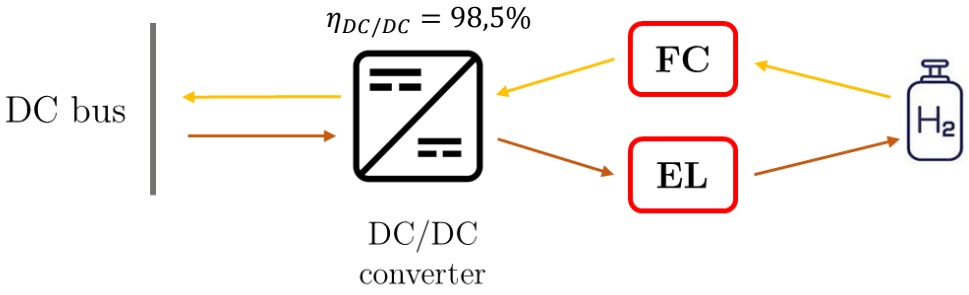

Figure 3.2: Efficiency chain of the P2G system

A similar approach has to be applied to power exchange with the national electricity grid. Obviously, it is important to consider the right factors which affect the functioning of such system since the power extract from the grid has a non-negligible cost, thus accuracies of the economic assessment strictly depends on the detailed representation of the power chain.

It is important to highlight that, since the model accounts for the different efficiency chains impacting each component, during the model development it has been necessary to make the distinction between the variables referred properly to the specific component and their correspondent when measured at the DC electric node.

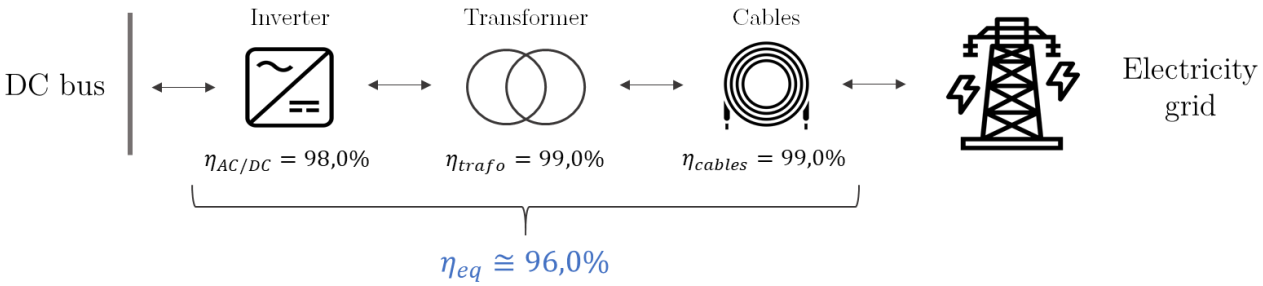

Figure 3.3: Efficiency chain of the connection system with the national grid

For instance, the Figure 3.3 can help to figure out which are the components accounting for the efficiency chain reported in the algorithm.

3.2.3. Algorithm description

As already stated in the previous section, the first step of the model is performed out of the main loop is the determination of the power sign. This step is performed to understand if the system works with a power deficit or with a surplus. The logic condition is implemented in the model as depicted in Figure 3.4.

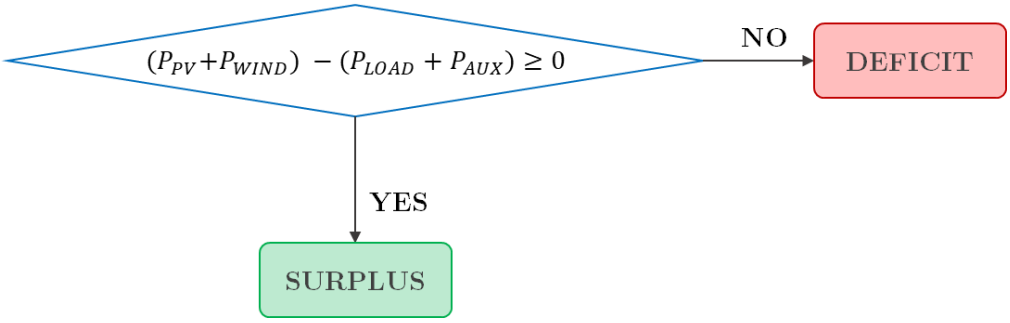

Figure 3.4: Block diagram surplus/deficit

Nevertheless, the way the system behaves changes according to the time slot: during the time interval which spans from 2 P.M. and 8 P.M. of each day, the authority ruling the UVAM obliges it to present an offer on the market corresponding to at least its qualified power. The commitments observance is then checked on a separated MATLAB script, when all the hourly variables are calculated.

Therefore, the control system needs ad-hoc adjustments for these spots, thus it consists in a further branching of the algorithm.

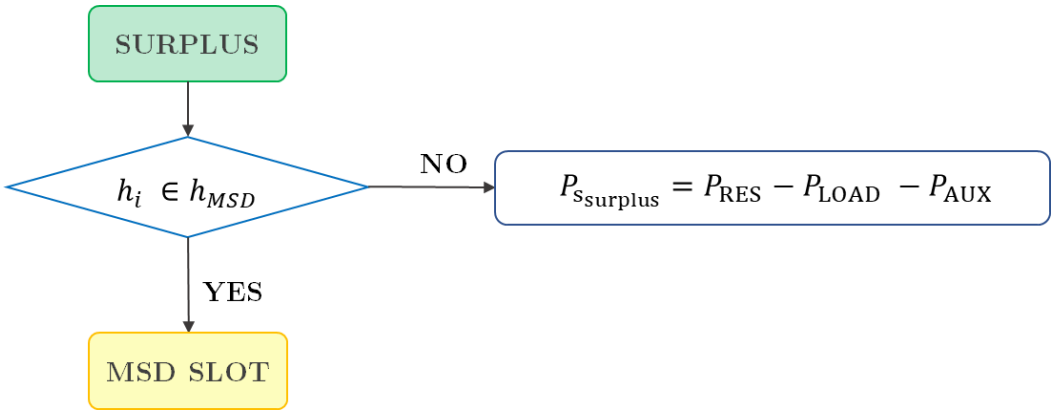

Figure 3.5: Block diagram MSD participation "surplus case"

Within the *MSD slot* block are available several alternative configurations of the system:

- The requirement imposed by the regulator matches with the time interval which records the highest production from solar and wind energy sources. For this reason, as primary choice, the system tries to cover the entire power requested by the market with only the exceeding hourly value. This condition is verified whether the power surplus overcomes the threshold value of 200 kW – the rationale behind the choice has been already outlined in section 1.1.1. Obviously whatever value observing the above-mentioned condition will be committed to the MSD market without further sub-division, this action is consistent with the economic principle of constantly pursuing the most valuable market asset, valid at each step of the loop.
- The power surplus does not match the threshold imposed by the MSD: in this case the fuel cell activation is needed. The algorithm accounts for the limits already imposed regarding the range of operation; thus, if the power requested is below the activation threshold, the fuel cell will not intervene. Nevertheless, the likeliness related to this case is only 10% and cannot be enhanced, since if the fuel cell cannot intervene, the lack of power supply will be penalized by Terna. Assuming to ensure the fuel cell start-up, two different situations can occur:
  - There is **enough hydrogen in the storage** to allow the fuel cell intervention. The condition on the tank SoC[18] is verified with success, therefore the remaining fraction of load covered by the fuel cell.

$$P_{L_{FC}} = P_{threshold} - P_{surplus}\ [\text{kW}] \tag{15}$$

$$P_{FC} = \frac{P_{L_{FC}}}{\eta_{DC/DC}}\ [\text{kW}] \tag{16}$$

[18] There are several equivalent conditions to verify the fullness and emptiness of the hydrogen storage. That referred to the SoC or the energy available, for instance, are surely the most straight-forward and they are the preferred choice for the model.

$$P_{ACC} = \frac{P_{FC}}{\eta_{FC}} \ [kW] \tag{17}$$

The variable calculated in (17) is the hourly power under the form of hydrogen chemical energy which must be available in the tank to ensure the power $P_{L_{FC}}$ at the electric node in the prescribed hour.

The routine which is in charge with updating the variables related to the storage energy content consists in evaluating the chemical power consumed, then to update the energy accumulated and the SoC for the successive time instant, as reported in eq. (18) and (19).

$$E_{ACC}(i) = E_{ACC}(i-1) + P_{ACC}(i-1) \cdot \Delta t \ [\text{kWh}] \tag{18}$$

$$SoC_{H_2}(i) = \frac{E_{ACC}(i)}{E_{ACC_{max}}} \ [\text{pu}] \tag{19}$$

As already reported, the time interval considered in the model was 1 hour, while the sign convention states negative power when hydrogen is taken out from the tank to be employed in the fuel cell, and vice versa.

- The **gas storage is empty**: this does not allow the intervention of the electro-chemical machine. This condition is verified when the SoC of the hydrogen storage is below the minimum threshold defined in section 3.2.3. Thus, the SoC remains the same, as well as the energy accumulated, while the unmet value of power is counted for the penalties which the plant controller will pay to Terna. It could occur an intermediate situation, when the storage is approaching the emptiness, but still a small quantity of hydrogen is available to drive the fuel cell. In that case, the fuel cell is activated and the value of power subjected to the penalties from the regulator would be only the remaining unmet part of the power.

The Table 3.1 gathers the different cases taken into account by the model. Each scenario has been identified a code to give a comprehensive view to the reader.

Table 3.1: Description of the cases analyzed by the model

Case	Description
Surplus_1a	Surplus – MSD block hours – surplus
Surplus_1b	Surplus – MSD block hours – surplus + fuel cell
Surplus_1c	Surplus – MSD block hours – surplus, penalties (storage empty)
Surplus_1d	Surplus – MSD block hours – surplus, penalties (below activation threshold)
Surplus_2a	Surplus – out of MSD block hours – curtailment committed to the MSD market
Surplus_2b	Surplus – out of MSD block hours – electrolyzer activated
Surplus_2c	Surplus – out of MSD block hours – storage full, no power absorbed
Surplus_2d	Surplus – out of MSD block hours – surplus not exploited (empty storage)
Surplus_2e	Surplus – out of MSD block hours – electrolyzer below the activation threshold
Surplus_2f	Surplus – out of MSD block hours – maximum electrolyzer power activated
Deficit_1a	Deficit – MSD block hours – deficit below the maximum fuel cell power
Deficit_1b	Deficit – MSD block hours – deficit above the maximum fuel cell power
Deficit_2a	Deficit – out of MSD block hours – deficit below the maximum fuel cell power
Deficit_2b	Deficit – out of MSD block hours – deficit above the maximum fuel cell power
Deficit_2c	Deficit – out of MSD block hours – storage empty, no power supplied
Deficit_2d	Deficit – out of MSD block hours – Deficit, unmet load due to the empty storage
Deficit_2e	Deficit – out of MSD block hours – fuel cell below the activation threshold

Moreover, Table 3.2 reports the acronyms identifying the different variables employed in the model. This recap table should help the understanding of the schemes reported in this section.

Table 3.2: Summary of the notation used for the model implementation

Variable	Description
P_{FC}	Operative fuel cell power
$P_{L_{FC}}$	Operative fuel cell power, measured at the electric node
P_{EL}	Operative electrolyzer power
$P_{s_{EL}}$	Operative electrolyzer power, measured at the electric node
P_{LOAD}	Internal load power
P_{AUX}	Auxiliaries power consumption
P_{RES}	Power produced by renewables
P_{thresh}	Threshold value of the power committed to the MSD market, set to 200 kW
P_{cover}	Requested power to achieve the minimum power committed in the MSD market
$P_{L_{deficit}}$	Power deficit, measured at the electric node
$P_{s_{surplus}}$	Power surplus, measured at the electric node
h_{MSD}	If the selected hour is comprised in the MSD block hours
$P_{FC_{max}}$	Fuel cell nameplate power
$P_{EL_{min}}$	Electrolyzer nameplate power
P_{MSD}	Power committed to the MSD market
P_{pen}	Power subjected to penalties that the BSP will pay to Terna
P_{ACC}	Chemical power which represents the consumption of hydrogen during fuel cell activation and its creation during electrolyzer functioning
E_{ACC}	Energy available in the hydrogen tank
$E_{ACC_{min}}$	Minimum energy available in the hydrogen tank
SoC_{H_2}	State of Charge of the hydrogen tank
SoC_{H_2min}	Minimum State of Charge of the hydrogen tank
Δt	Time resolution of the model, set to 1 hour
η_{eq}	Equivalent efficiency

The block diagram depicted in Figure 3.6 helps summing up the different cases taken into account by the model.

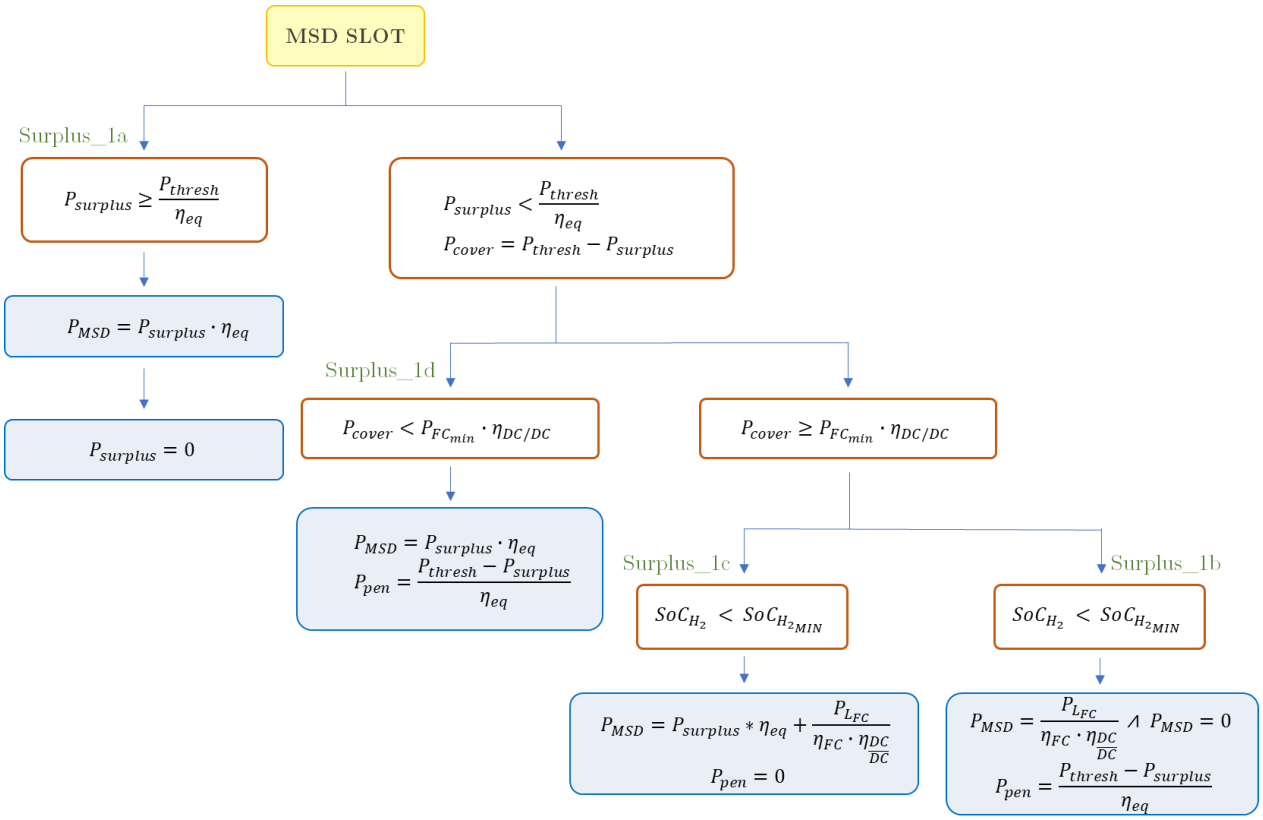

Figure 3.6: Block diagram MSD slot and related branching

When the time interval is outside the MSD block hours, the energy surplus cannot be instantaneously employed to perform grid services, though it is absorbed by the P2G system by means of storing this energy under the form of hydrogen.

To do that, the electrolyzer has to be turned on, if the power surplus is high enough to overcome the activation threshold. The electrolyzer operating power has been calculated as the minimum value among:

I. The **surplus power**, that is the most recurrent option, since it is selected in all the common situations.
II. The correspondent power which would bring **the hydrogen tank to fill up** completely. This condition occur the time instant right before filling up completely the hydrogen tank, thus in this case the electrolyzer will work at partial load.

III. The **maximum nameplate power** of the electrolyzer. In that case, the surplus overcomes the electrolyzer potentiality and there is no other possibility than power curtailment for the exceeding part of energy which cannot be exploited. One of the design choices of the model is the adding of an exception to the main rule: although the time interval is not comprised in the block hours in which it is mandatory to present at least an offer for the MSD market, there is nothing to stop the corresponding plant BSP to make such offer during the rest of the day, of course at different hourly prices. For this reason, in the event that the curtailed power verified the condition below:

$$P_{curt} \geq \beta * P_{thresh} \quad [\text{kW}] \qquad (\beta = 0{,}9) \tag{20}$$

The power is rerouted to the electricity grid and sold to the MSD market. The parameter β has to be subject of a sensitivity analysis, since its value determines a more or less aggressive strategy of intervention into the MSD market. A lower value of β implies that the system has a higher probability to employ otherwise wasted power in a profitable way, but at the same time it enhances the penalties paid by the BSP to Terna. This is due to the fact that the gap with the threshold value cannot be supplied by the system, thus it is subjected to Terna's penalties. It has been explored during the project the possibility of providing the remaining part by driving the electrolyzer, though it would lead to further discharge the hydrogen tank, which would require an expensive oversizing, making not convenient the option analysed. The same is valid vice versa for the value of β.

As far the electrolyzer control is concerned, the same "safety options" already seen for the fuel cell are proposed for the inverse electro-chemical machine, namely the maximum SoC of the hydrogen tank verification, as well as the lack of intervention in case the power surplus is below the activation threshold of the electrolyzer.

The block diagram shown Figure 3.7 explains which are the alternative operation modes of the system in case of power surplus.

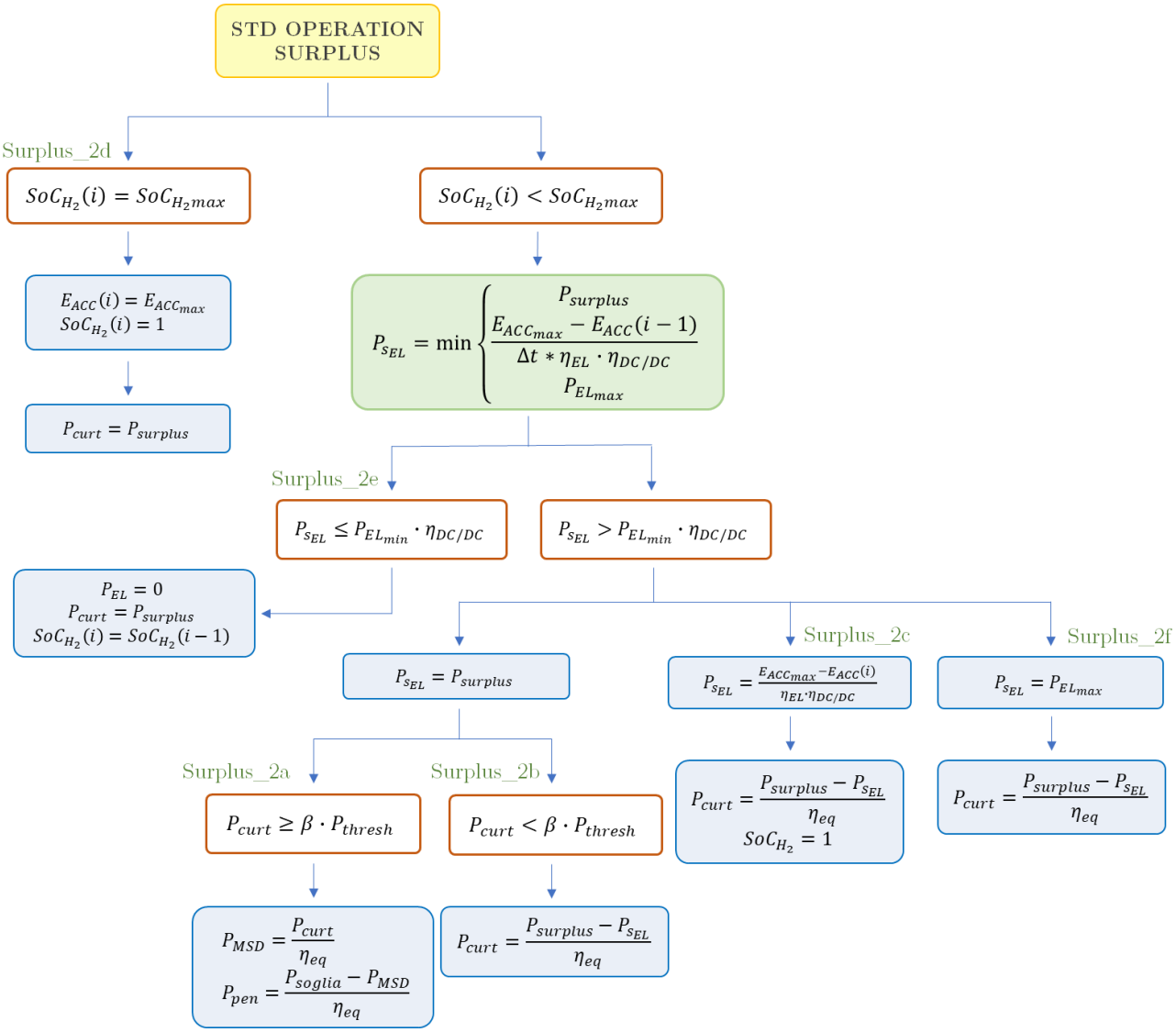

Figure 3.7: Block diagram standard operation "surplus case"

After having analysed all the possible alternatives for the "surplus case", the model examines the other situation which can occur during the operation: especially in the nighttime, the power produced by renewables does not manage to match the load requested by the end user, thus triggering the **"deficit case"**.

Even in the "deficit case", the first branching made by the model is whether the system has duties towards the MSD market in that time interval or not, thus the logic condition is the same already seen for the "surplus case" early in this section.

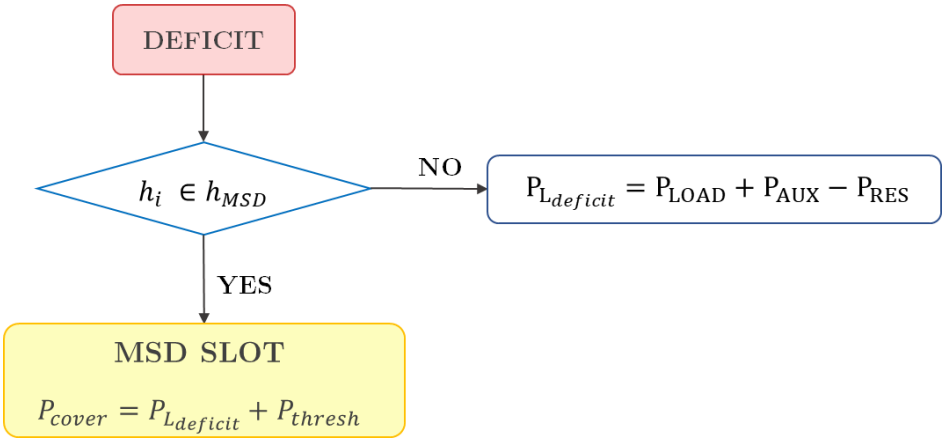

Figure 3.8: Block diagram MSD participation "deficit case"

The participation to the MSD market when the condition of power deficit occurs at the electric node proves to be much more simplified than in the previous case. Since the power sign is negative yet, it is just necessary to boost the power produced by the fuel cell to keep up with the novel demand. Therefore, the only limit imposed is related to the maximum power allowed by the electro-chemical machine.

$$P_{L_{FC}} = \min\left(P_{cover}\,;\, P_{FC_{max}} \cdot \eta_{DC/DC}\right) \quad [\text{kW}] \tag{21}$$

The fuel cell functioning splits into two alternatives:

- It manages to match the entire requested power load in a time interval: the produced power is correctly shared between the internal load of the P2P system and that requested from the MSD market, without the intervention of the external source of energy.
- The positive amount of power supplied is bounded by the size of the electro-chemical machine. In this framework, a precise design choice was made: the maximum power generated is rerouted as much as possible towards the fulfilment of the dispatch order coming from Terna, at the expense of not matching the

internal load coming from the holdings/factories. This decision has an economic foundation, since the lack of supply to the internal load can be fixed by the external source through the dedicated power line. The expenditure associated to the supply will be always lower to the corresponding remuneration gained if such power is committed to the MSD market. The margin obtained will be dependent of the price fluctuations of the above-mentioned market. This choice could be counter-intuitive from a physical point of view, but it can pay consistent dividends if evaluated on a long-term horizon.

The success of this strategy strongly relies on the correct sizing of the electro-chemical machine. Although it is very unlikely that the model falls on this specific branch, given that the MSD block hours has a good fit with the period of maximum power production from renewables, if the fuel cell can reach a maximum power too close – or even lower than – to the market threshold, very often the BSP will be obliged to pay penalties to Terna, making no more smart and profitable the strategy. In both cases, the hydrogen availability in the tank must be checked in order to be sure to provide the service.

$$E_{ACC}(i) = E_{ACC}(i-1) - \frac{P_{L_{FC}}}{\eta_{FC} \cdot \eta_{DC/DC}} \quad [\text{kWh}] \tag{22}$$

If the storage limitation occurs, the penalties will rise to the whole threshold value, obviously this is the situation that has to be avoided the most, the sizing of the fuel cell, together with that of the hydrogen tank, has to comply with this design need.

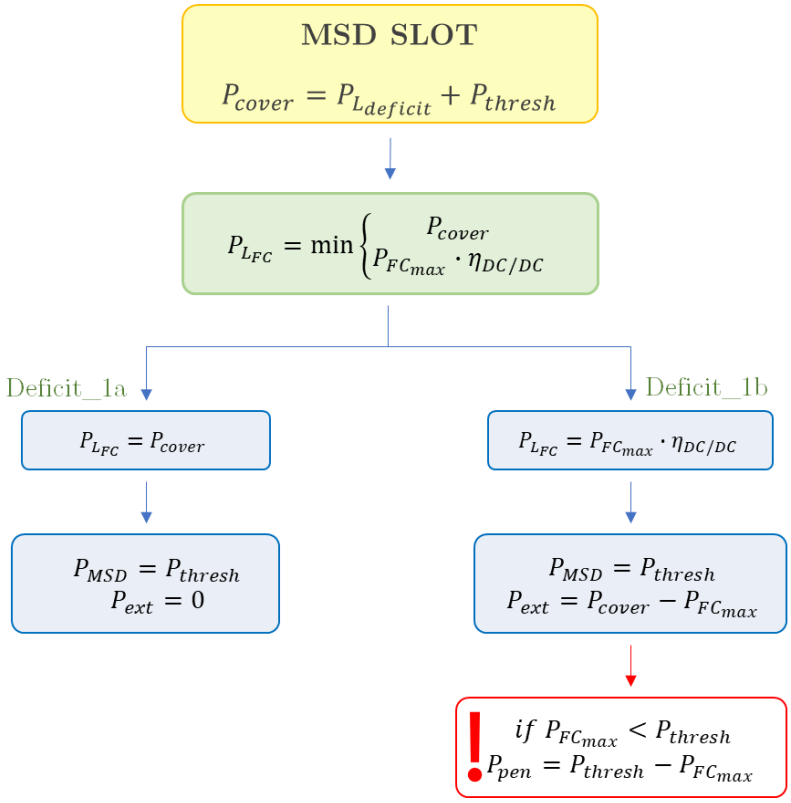

Figure 3.9: Block diagram MSD slot and related branching in "deficit case"

Looking outside the MSD block hours, the model settings are similar to those just described for the electrolyzer intervention. They are briefly summarized below:

- First of all, the power deficit has to be enough to activate the electro-chemical machine. If this condition is not fulfilled, there is no other to do than providing the power through the external source of energy.
- Then, once verified that there is enough hydrogen in the tank to drive the fuel cell, it assumes the following value of power:

$$P_{L_{FC}} = \min\left(P_{deficit}\,;\, P_{FC_{max}} \cdot \eta_{DC/DC}\right) \quad [\text{kW}] \tag{23}$$

The mechanisms embedded in the model are the same already seen in the "surplus case", just transposed for cases in which the sign of power flow is reversed. The "deficit case" outside the MSD block hours is described in Figure 3.10.

The loop just examined scans each hour of the year. When the calculation is completed, the developed model performs further elaborations on the variables related to the yearly energy produced or consumed by the components.

For the sake of verification, the model contains a short MATLAB routine which ensures

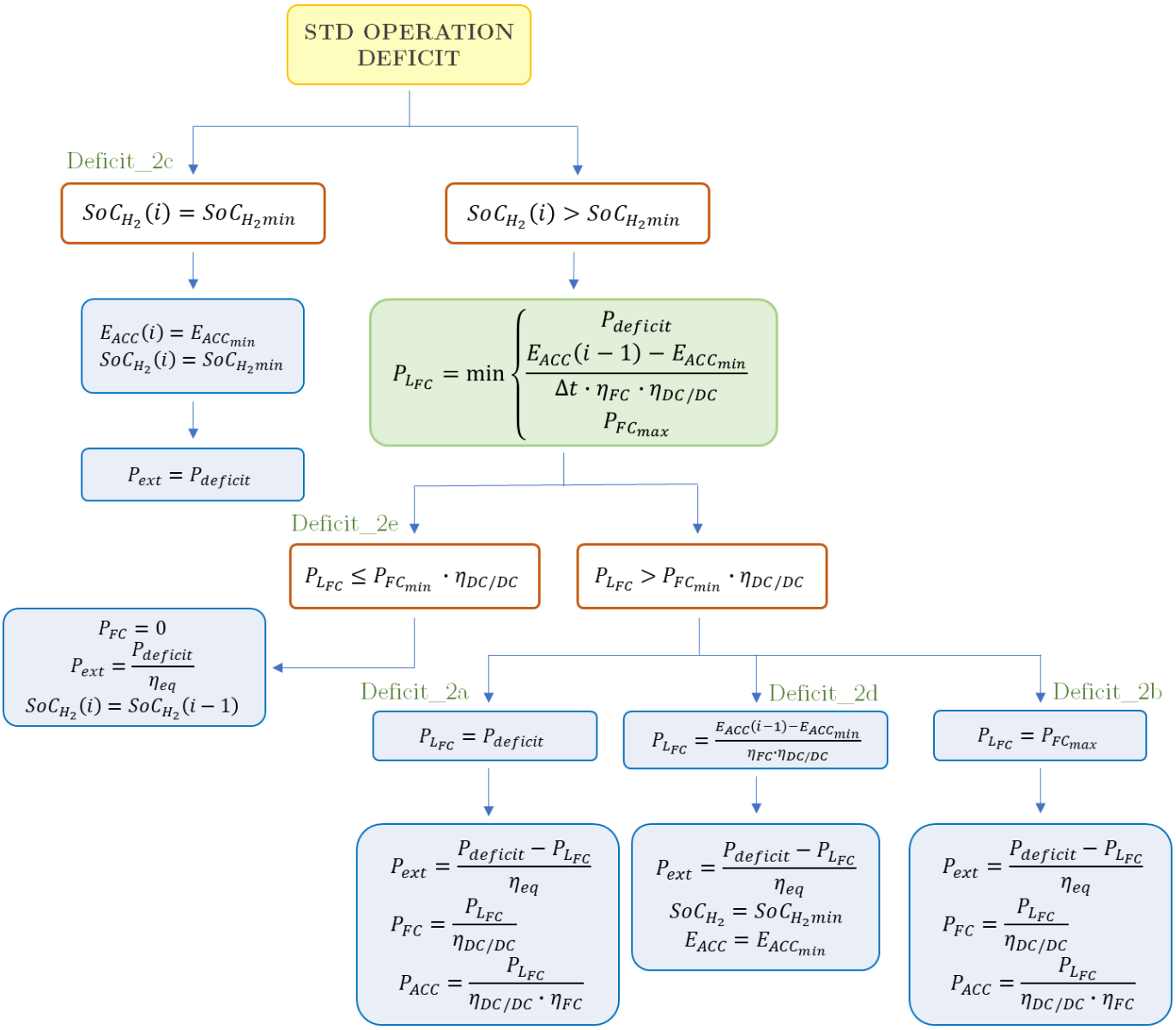

Figure 3.10: Block diagram standard operation "deficit case"

the energy balance at the electric node is respected. The DC bus of the system, which acts as central unit and interconnection channel for all the components, consists in a **net zero energy entity**, since it is not able neither to generate nor to absorb electricity, therefore

the entire amount of energy passing through it during the whole year must be in perfect balance.

The verification is assessed as successful if the following equation is satisfied:

$$\left(E_{load} + E_{s_{EL}} + E_{curt} + E_{MSD}\right) - \left(E_{PV} + E_{wind} + E_{L_{FC}} + E_{ext}\right) = 0 \ \text{[MWh]} \tag{24}$$

It has been already checked that the equation is actually verified, thus confirming the validity and consistency of the developed model.

As support of what has been illustrated in this chapter, in the next pages are depicted – and briefly elucidated – few examples of how the model actually works, putting the focus on the more intricated branches of the algorithm.

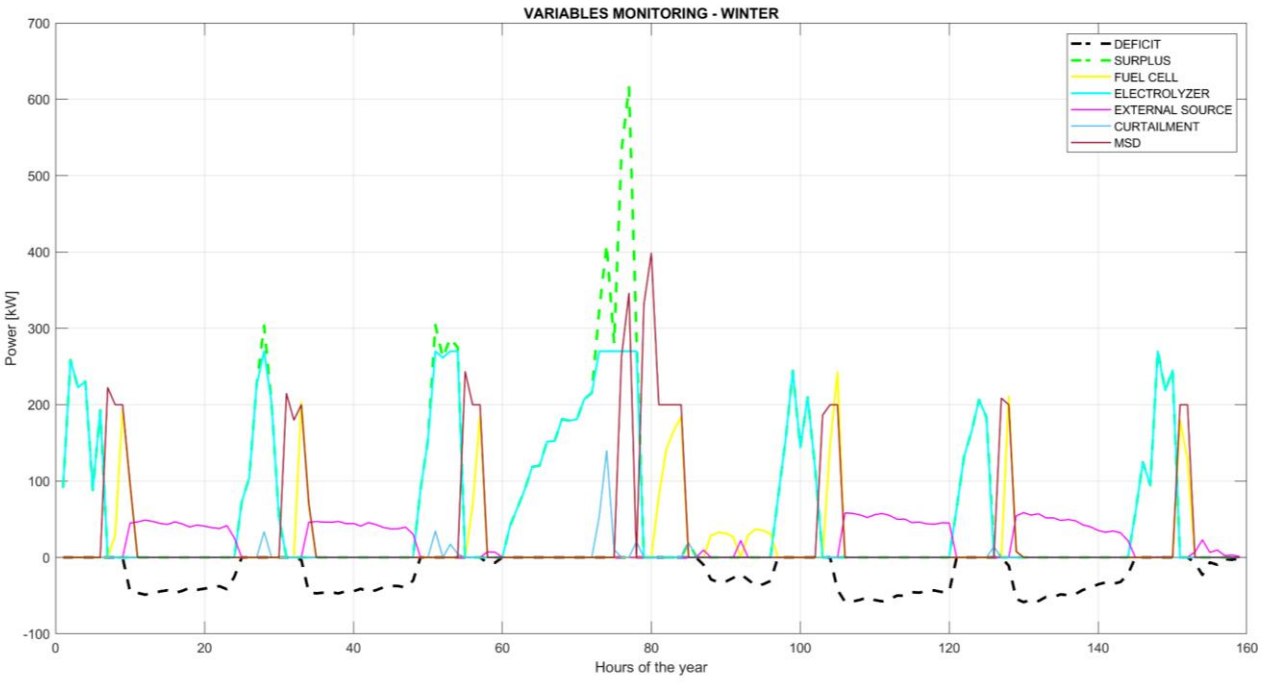

Figure 3.11: Overview of the main energy variables - typical trend in winter

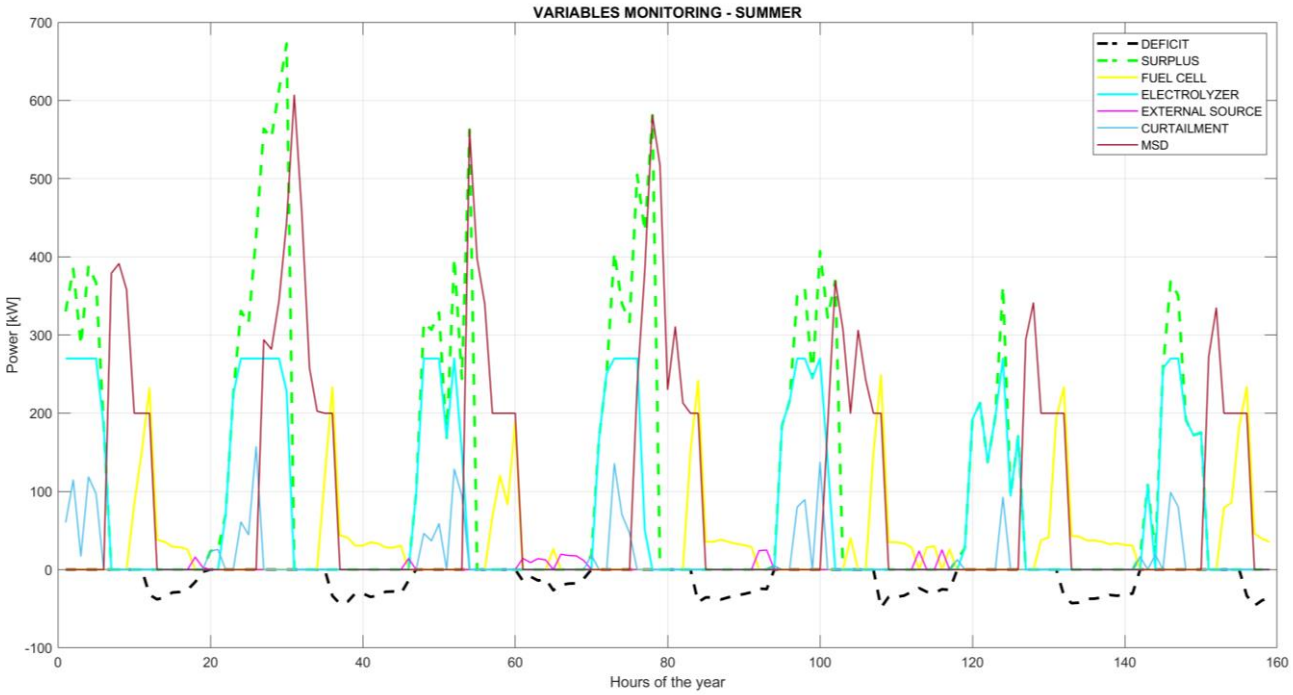

Figure 3.12: Overview of the main energy variables - typical trend in summer

From the Figure 3.11 and Figure 3.12 above it is straight-forward to perform a comparison between the typical situation occurring in summer and winter. Of course the main difference which can be noticed is the amount of energy produced by renewables, which indirectly reflects the energy surplus highlighted in dashed green in the figures.

During winter, the internal load has to be almost fully covered the external source, since there is not enough hydrogen in the tank to drive the fuel cell in the evening hours, given that it was used to comply with the dispatch orders from the MSD market. Conversely, during summer the energy surplus is so large that the system manages to charge the tank through the action of the electrolyzer and at the same time send a considerable power to the grid, generating a substantial source of income.

The dark red solid line represents the power offered in the MSD market by the P2P system: in Figure 3.11, the system struggles to reach the 200 kW threshold, ensuring the minimum

amount foreseen by the grid service[19], while in Figure 3.12 the market participation is extended on a temporal basis as well as following the peaks of energy surplus.

It is possible to notice that the power curtailed remains under control in winter, when the fewer energy has a more rational use, while in summer 100 kW or more peaks of power curtailed are registered. This happens when the system is approaching the contemporaneous peak power for both the renewable energy sources, which implies a considerable waste. However, the system sizing should not be performed on the potential peak power of the PV field and wind turbine, given the very short time interval within the year in which they can ensure it. The most profitable solution will be a trade-off between the size of renewable energy sources and the correspondent maximum power allowable by the P2G system, in order to guarantee the best exploitation of the hydrogen tank.

[19] Terna pointed out in the UVAM regulation a set of requirements on a monthly basis which must be observed by the system qualified for the service. The observance of these rules is checked on the following step of the developed model and it will be explained in detail in the following paragraph.

The dynamics which control the P2G system are graphically visualized in Figure 3.14 and Figure 3.13.

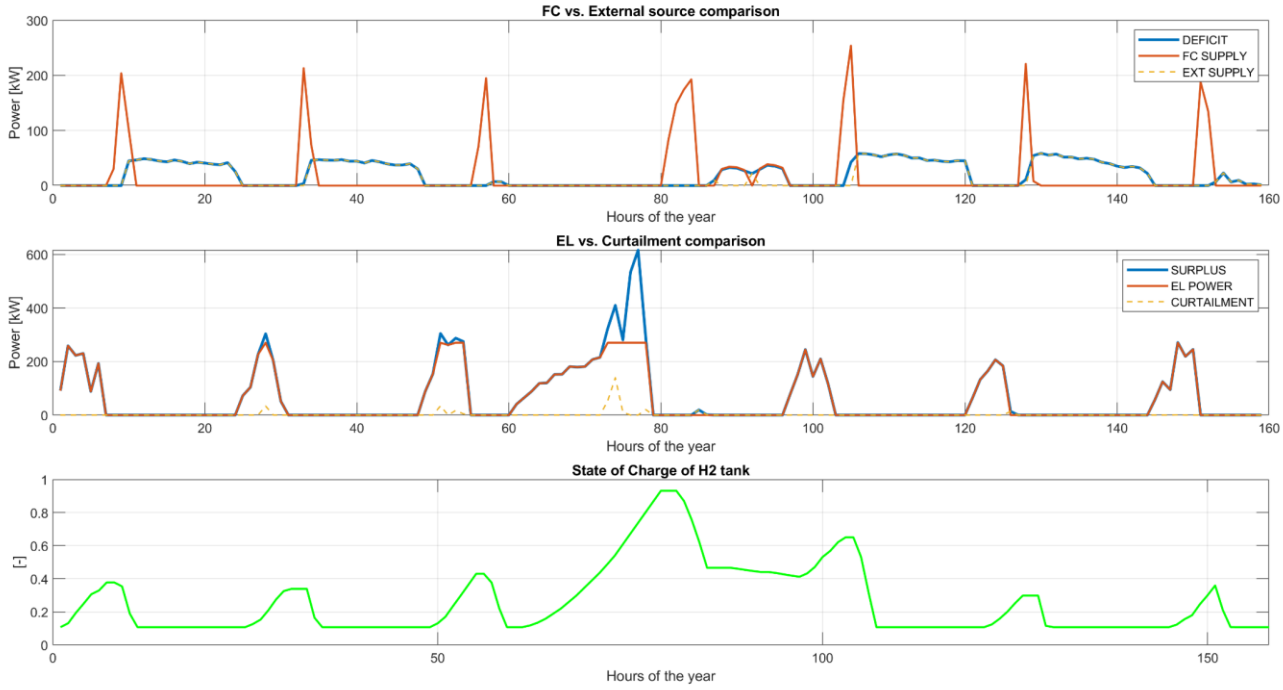

Figure 3.14: Overview of the P2G system functioning – typical trend in winter

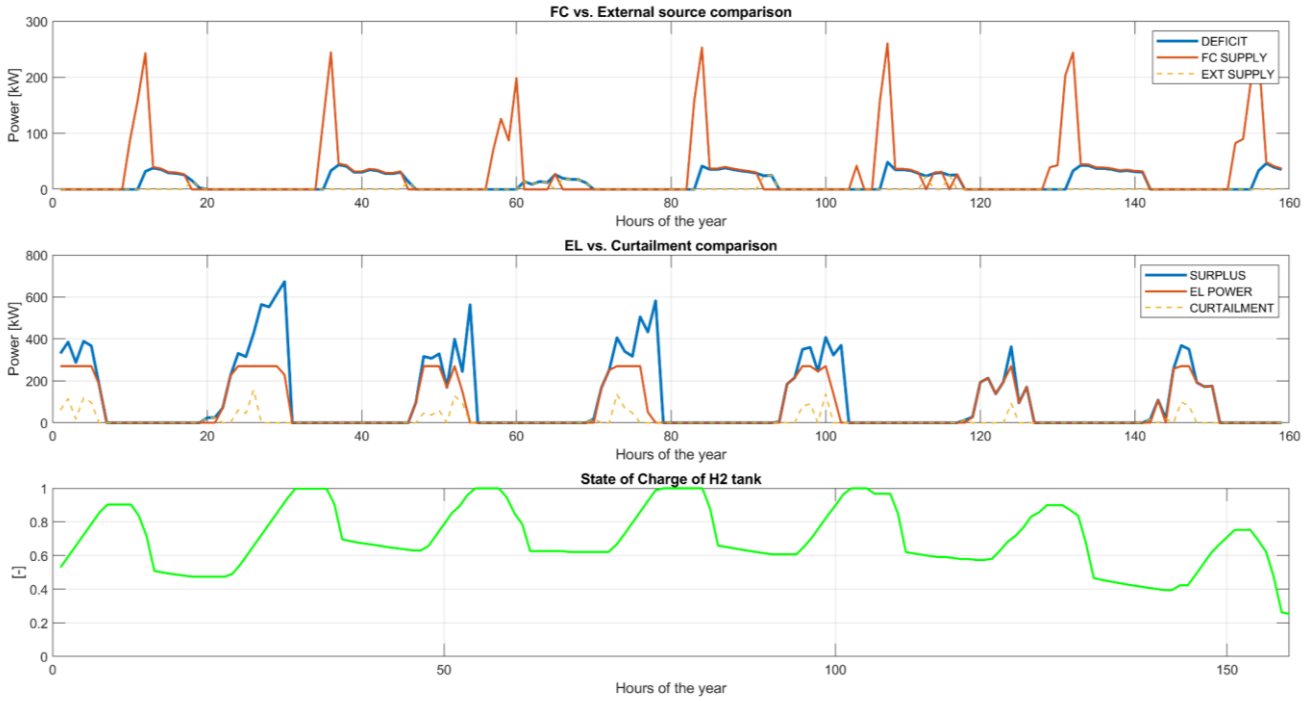

Figure 3.13: Overview of the P2G system functioning – typical trend in summer

In Figure 3.14 and Figure 3.13. is highlighted the behaviour of the P2G system in two different situations: during winter, the power deficit has to be satisfied for the major part by the external source of energy. As we can see from the curve in solid green, the SoC of the hydrogen tank is often below the minimum value, except for unusual peaks of surplus power. In the nighttime the tank is empty: when it start filling up early in the morning, the fuel cell has enough hydrogen to sustain the internal load from the factories. However, every day at 2 P.M. begins the MSD block hours, so the fuel cell employs the remaining hydrogen to provide the service for the national grid.

This scenario is partially avoided in a typical summer week, as depicted in Figure 3.13. The average SoC of the hydrogen tank is higher, energy surplus allows the electrolyzer to work at full power for the whole central part of the day, therefore the combination of renewables and fuel cell manages to accomplish all the objective set, resulting still in a considerable energy curtailment, though much lower than the amount spent for useful purposes.

The hydrogen tank, evaluated in this specific system, acts as daily storage asset instead of performing only a function of seasonal backup (as it is in a more structured configuration – comprising the Battery Energy Storage System (BESS) as well). By keeping a limited size of the tank and the same time taking out batteries, the system strongly cuts the upfront costs, in the attempt of being profitable and economically attractive right from the beginning, in anticipation of the deep technological advancement involving the system's components.

3.3. Requirements check Model

Upon completion of the Energy balance Model, the vectors containing the information regarding the market participation and the potential penalties associated with it are imported in a separated MATLAB script to be furtherly readjusted.

The separation has been mandatory in order to not weigh down the main model. The check of the regulation can be done ex-post, then the input parameters can be modified and the model rerun, provided the requirements are not satisfied.

The main model tries to control the system so that it must present an offer to the MSD market in each hour within 2 P.M. and 8 P.M. of each day of the year. Nonetheless, the official regulation states that *the UVAM are obliged to present at least one offer for 4 consecutive hours within the MSD block hours.* This condition sets the minimum amount of energy that the UVAM must exchange with the national grid in the framework of the MSD market, the authority has set at **70%** the energy threshold below which the system is suspended and consequently its action will not be remunerated.

$$E_{min_{MSD}} = \frac{P_{thresh}}{10^3} \cdot \frac{n_{days}}{year} \cdot 4\frac{hours}{day} \qquad \left[\frac{\text{MWh}}{\text{year}}\right] \tag{25}$$

After the rearrangement of the vector containing the market offers, the corresponding energy must be higher than the 70% of $E_{min_{MSD}}$, otherwise the system sizing has to be rethought.

The Requirements check Model is based upon the fact that the system will need to take out some hours during winter, sticking to the 4-hours threshold, while in case of abundant energy production from renewables the system is able to provide grid services even outside the prescribed temporal window. In other words, the correction performed by the sub-model is particularly meaningful in autumn and winter, allowing to drastically reduce the penalties imposed by the regulator.

The rationale behind this sub-model is summarized in the Figure 3.15.

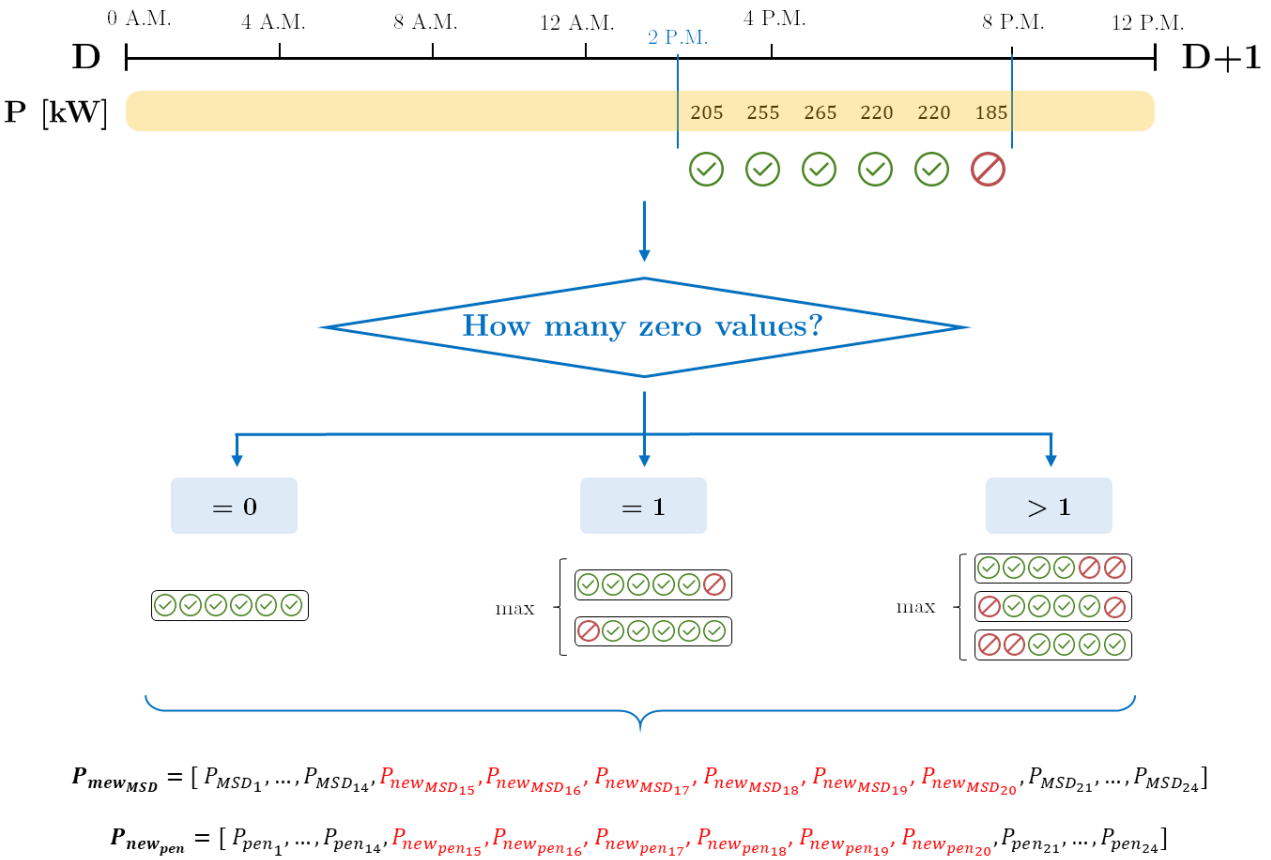

$$\boldsymbol{P_{mew_{MSD}}} = [\, P_{MSD_1}, \dots, P_{MSD_{14}}, P_{new_{MSD_{15}}}, P_{new_{MSD_{16}}}, P_{new_{MSD_{17}}}, P_{new_{MSD_{18}}}, P_{new_{MSD_{19}}}, P_{new_{MSD_{20}}}, P_{MSD_{21}}, \dots, P_{MSD_{24}}]$$

$$\boldsymbol{P_{new_{pen}}} = [\, P_{pen_1}, \dots, P_{pen_{14}}, P_{new_{pen_{15}}}, P_{new_{pen_{16}}}, P_{new_{pen_{17}}}, P_{new_{pen_{18}}}, P_{new_{pen_{19}}}, P_{new_{pen_{20}}}, P_{pen_{21}}, \dots, P_{pen_{24}}]$$

Figure 3.15: Conceptual scheme of the Requirements check Model

The MATLAB algorithm is based on a loop recalled in a mobile window sliding every day of the year, within the 24 hours, it analyses only the MSD block – as already said, from 2 P.M. to 8 P.M. – and it keeps unchanged the power values referred to all the other time intervals.

First, it verifies how many zeros are present in the vector containing six power values: a null value means that the system has not been able to comply with the dispatch order imposed by Terna in a certain time interval. However, the regulator is tolerant with the BSP, lowering the threshold to *four consecutive out of a total of six hours* when at least the minimum qualified power must be supplied by the UVAM to the national grid.

Figure 3.15 gives an outlook of how the sub-model works: starting from the left-hand side, if the first verification retrieves a positive outcome – there is no zero value within the vector – the sub-model reconstructs the original vector and moves forward without modifications.

Conversely, if the vector contains only one zero value, the algorithm performs a second check on the actual position: if it is located in position 3 or 4, the algorithm fully discards the vector, making not valid the whole daily supply. This happens because the regulator imposes at least four hours of *consecutive* power supply, thus if the shortage occurs in the central hours the consequences are particularly economically damaging.

Nonetheless, the situation described above occurs rarely during the year, since shortage case are typical of the extremes hours of the block. Just to name a few scenarios, during winter the sun goes down way ahead of 8 P.M., in case of significant and diffuse cloudiness[20] or when there are wind anomalies due to external factors. One of the just named situation, together with fuel cell shortage, is enough to cause the failure of supply to the MSD market.

The selection of which value to discard is based upon the energy criterion: the combination which yields the maximum amount of energy is selected[21]. Contextually, the vector is modified by keeping the right vector containing the zero value in the "optimal" position, while putting a zero value in the correspondent position in the penalties vector.

This is the most important action performed by the sub-model, since it allows to take out a pretty expensive 200-kW penalty. The latter case is based upon the same rationale, it simply requires checking out a higher number of combinations. As depicted in Figure 3.15, the final step is to reconstruct the final vectors related to the power committed in the MSD market and the penalties.

As conclusion, the sub-model evaluates whether the system configuration is actually compliant with the rules imposed by Terna, through the comparison between the energy offered to the MSD market and eq. (25).

[20] Where the OKTA number is higher than 6, a drastic decrease of PV productivity is recorded [19].

[21] Looking at how the model has been set from the beginning, it is coherent to define the sum of several power values as energy: this because each value belonging to it is in turn a value of energy. Though it is valid if and only if the model has 1-hour time resolution, which allows to make the equivalence between a power value measured in kW and its corresponding energy value expressed in kWh. Be careful in case the time step ruling the model does not allow to perform the equivalence, in such case the sub-model must be adjusted accordingly.

$$\gamma = \frac{\sum P_{new_{MSD_i}}}{E_{min_{MSD}}} \geq 0.7 \tag{26}$$

As far the system analysed is concerned, the γ value is calculated twice – the former does not account for the correction, while the latter considers the modifications as well as including the power values out of the MSD block hours – so that it can be acknowledged the relevant effect brought by the sub-model, and in eq. (27) and (28).

$$\gamma_{old} = \frac{\sum P_{MSD_i}}{E_{min_{MSD}}} = 1.18 \tag{27}$$

$$\gamma_{new} = \frac{\sum P_{new_{MSD_i}}}{E_{min_{MSD}}} = 1.61 \tag{28}$$

Figure 3.16 brings a visual impact of the modifications brought by the sub-model.

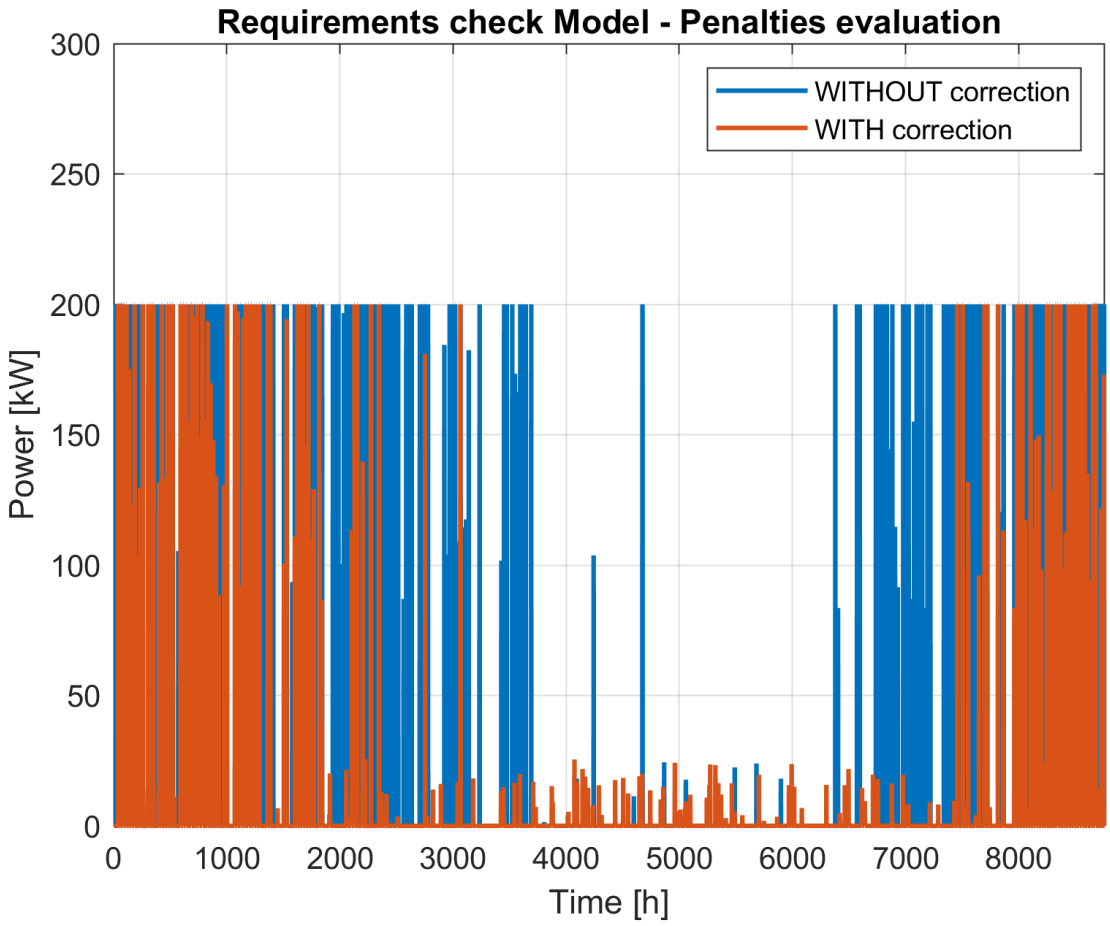

Figure 3.16: Modification of the power committed to the MSD market after the deployment of the Requirements check Model

3.4. Revenue streams Model

3.4.1. Data import and processing

Once evaluated the power profiles of the different components belonging to the P2P system, it is necessary to employ them to assess the economic profitability of the system. To do that, realistic assumptions need to be formulated, which will complement the information coming from the regulator.

It has been decided to make use of the historical data coming from the public repository of the authority in charge of the management and legislation upon the Italian energy and natural gas markets. This entity is called ***Gestore dei Mercati Energetici (GME)***, it cooperates with Terna to ensure fair competition among the market players together with elevate quality standards related to the electricity supply.

Among the duties borne by GME, there is the obligation to publicly disclose all the data and information of the market actions, for the sake of transparency [36]. For this reason, it is possible to download a wide variety of historical data from its website under the form of Extensible Markup Language (XML) files.

It has been chosen to employ the data from the year 2018, being the most recent year for which the complete set of variables is available and it is not affected by anomalies in energy demand – according to the website information.

Before importing it in the MATLAB sub-model, it has been manipulated in order to have available only the information which are useful for the purpose. From the GME website it is possible to download hourly data with one month as maximum time extension, thus it was used Microsoft Excel to merge together the separated table as well as selecting only the columns having the data related to the zone of interest – which is labelled as "CNOR" representing the North-Central part of Italy.

The information requested are the hourly energy sold and bought in the specific zone, expressed in MWh, the hourly sell and buy price, differentiating the corresponding

maximum, minimum and average value. This was repeated both for data related to MSD and MB market, since the latter is used for determining the penalties.

3.4.2. Remuneration schemes

At this stage it is all set to be imported in the MATLAB sub-model, as far the remuneration coming from the MSD market is concerned, four different compensation schemes were suggested:

1. The power exchanged with the grid is always sold at the **strike price**, which is equivalent to **400 €/MWh**. This is the most optimistic scenario and also the less realistic one, it does not reflect a feasible situation than can occur during the whole year, since the strike price is verified only in unusual situations. Nevertheless, the figure calculated by considering this situation can be useful to set an upper cap which helps figuring out the order of magnitude of the system profitability.
2. While the first scenario forecasts a flat price, the information regarding the actual trend of the MSD market prices was imported in the sub-model to put in place a realistic scheme of remuneration. To do that, it was used the **hourly trend of the average selling price relative to the North-Central macro-zone**. Therefore, if the UVAM would have been up and running since 2018, it would have generated – on average – money incomes following such scheme.
3. The scenario just described can be evaluated as conservative, since nowadays the MSD market is still dominated by fossil power plants, which are still obliged to provide grid services for the TSO. If the pilot projects carried out concurrently by Terna and ARERA would bring to the expected results, there would be a drastic change in the Italian energy market, resulting in a positive impact on renewable energy systems' profitability. For this reason, it seems reasonable to employ the **hourly trend of the maximum, instead of average, selling price relative to**

the North-Central macro-zone, in the perspective of a probable economic growth of the sector. Nonetheless, the difference between the last two scenarios is not so relevant, thus the overestimation of the money income is avoided.

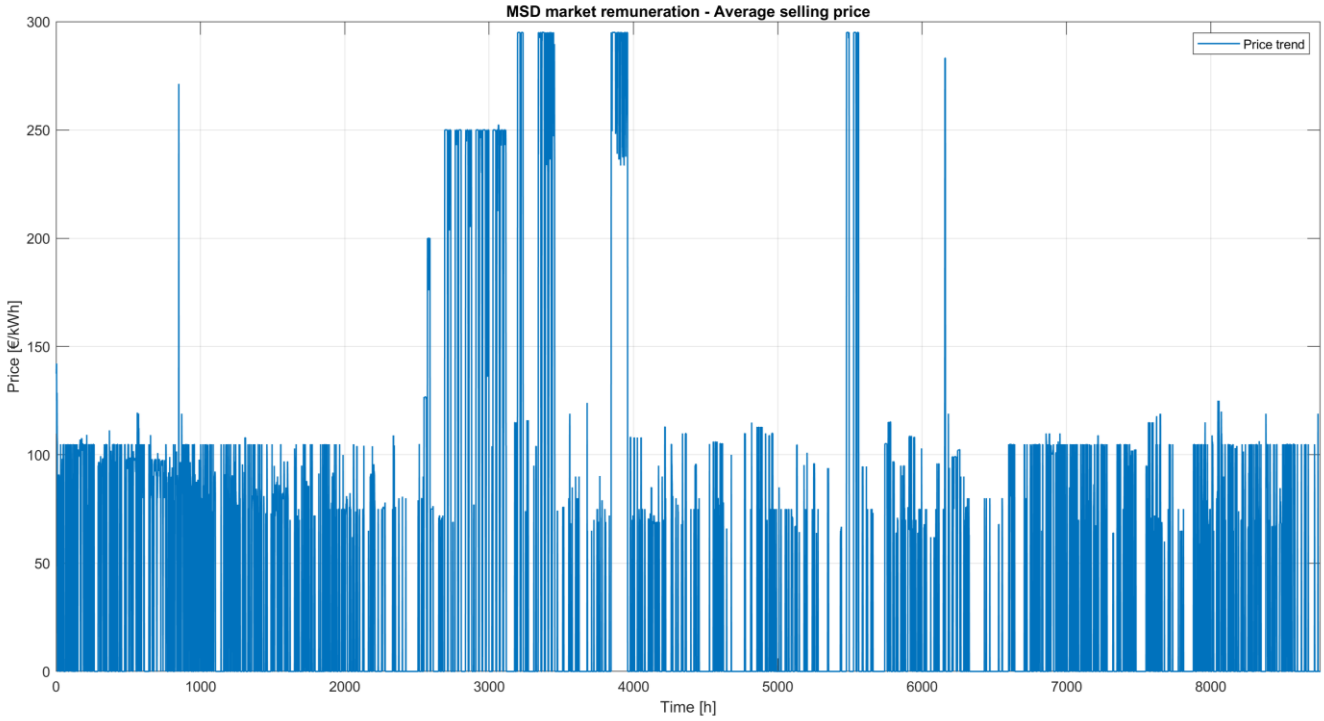

Figure 3.18: Remuneration scheme #2 - Average selling price

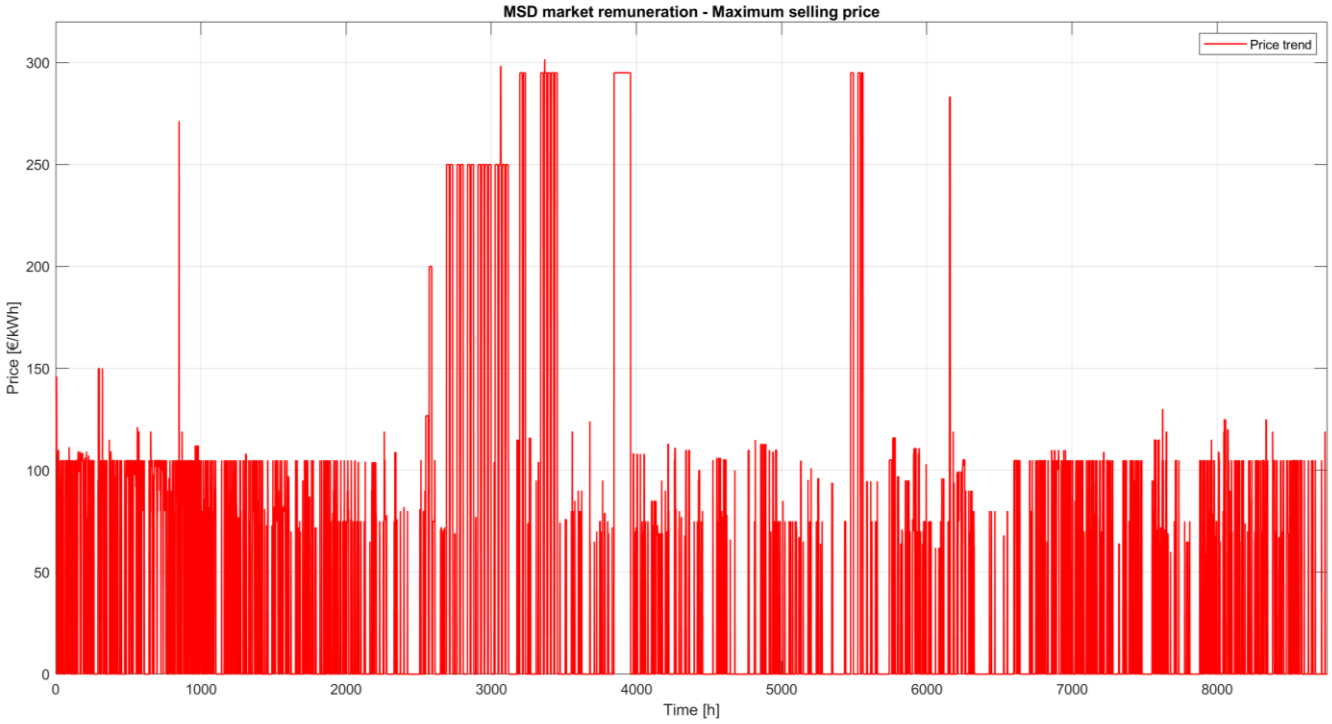

Figure 3.17 Remuneration scheme #3 - Maximum selling price

4. Finally, this last scenario can be assumed as feasible when the UVAM regulation will become the state-of-the-art, together with the market participation from any aggregate of distributed energy sources. The more systems that obtain the market authorization, the more there will be a tendency towards price stabilization. Therefore, the scenario considers a **flat price** equivalent to the overall **mean of the non-null average selling price within the MSD block hours**. This situation aims at simulating the possibility, at the hands of Terna, to guarantee a constant remuneration to the system providing grid services in the most energy-demanding time interval of the day.

   This aspect surely would encourage companies to invest in the sector, given that nowadays the most cumbersome barrier is the economic uncertainty behind such systems. The development is hindered due to the impossibility of performing reliable long-term estimations regarding the revenue stream generated by the plant.

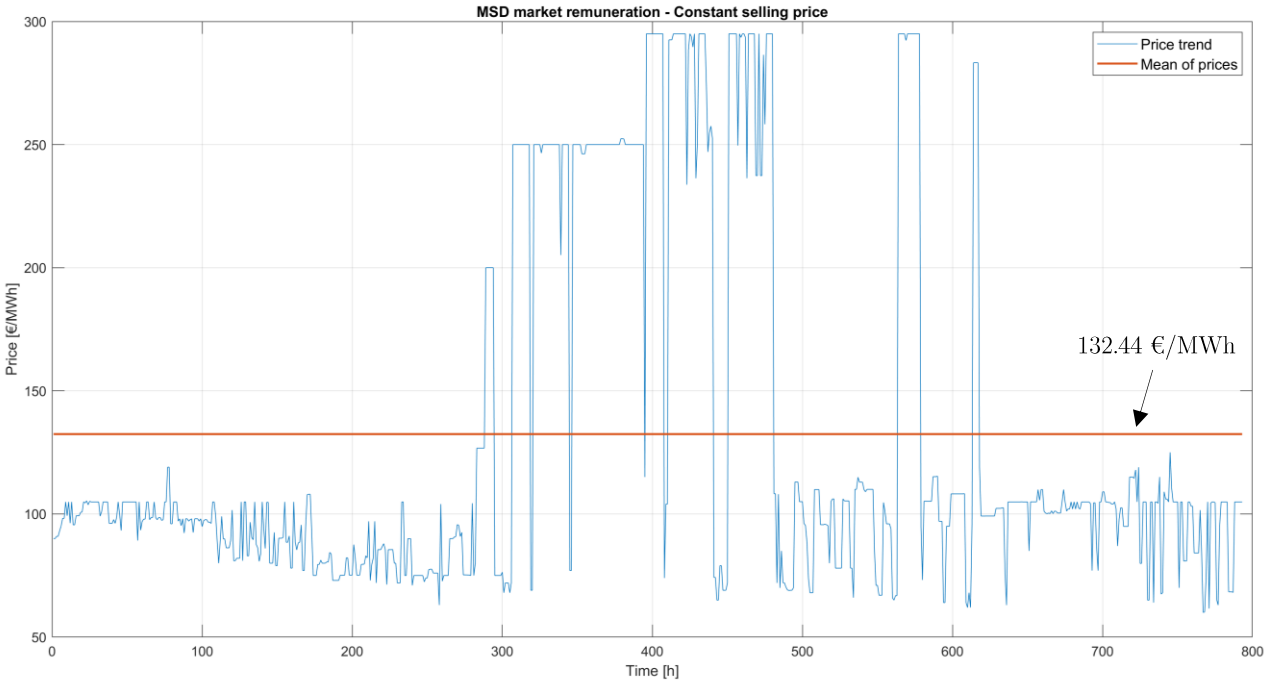

Figure 3.19: Remuneration scheme #4 - Constant selling price

3.4.3. Penalties evaluation

The data imported from the GME website allows to calculate the penalties which the BSP must paid to Terna at the end of the year. What is called for the sake simplicity "penalty" in this work, in the official regulation is reported as *Corrispettivo per il mancato rispetto delle quantità accettate sul MSD*. Therefore, the BSP is obliged to pay a toll if it is unable to comply with a dispatch order that it committed to respect, but it did not.

The developed model approaches the P2P systems in a simplified way: what actually happens is that the BSP controlling a certain UVAM must communicate the system's **baseline** to the TSO, namely the expected "normal" power profile – it could have both positive and negative sign – at least one day before the actual power delivery. Then the BSP receives the dispatch order, under the form of set points array for each hour of the corresponding day of delivery. Obviously, the imposed set points will always remain under the maximum qualified power. If the system is not able to follow the hourly set points, the BSP will be penalized according to the entity of the unbalance generated.

The described rules can be applied to the P2P system as well, since there are mandatory requirements to comply with and the qualified power coincides with the minimum threshold imposed by the regulation. In this way, the BSP is sanctioned only when it does not respect a mandatory order, whereas it is considered any difference between the actual power produced by the system and that communicated by the BSP to Terna, so as not to make the model too complicated. If this assumption stands, it is not possible that the BSP is charged for disrespect of the orders out of the MSD block hours.

The official regulation clearly explains how to compute the penalties and, as already said, they are directly proportional to the unbalance between the dispatch order and the actual energy supplied to the grid, as shown in eq. (29) and (30).

$$Q_{MSD}(i) = \sum q^{sell}_{EX-ANTE}(i) + \sum q^{sell}_{MB}(i) \tag{29}$$

$$Sbil_{UVAM}(i) = Ene_{mis}(i) - Q_{MSD}(i) \; < \; 0 \tag{30}$$

In case of negative unbalancing, as shown in eq. (30), it means that the system has not been able to successfully respond to the dispatch order coming from the regulator. Terna subdivides the penalties according to the entity of the unbalance: if it has to deal with a **small unbalance** the BSP pays the failure of energy supply at the average price, weighted upon quantities, of the accepted selling offers to the MSD market.

$$if \;\; \frac{Sbil_{UVAM}(i)}{Q_{MSD}(i)} < 5\% \quad \rightarrow \quad Tax = Sbil_{UVAM}(i) * \bar{P}^{UVAM}_{MSD\uparrow} \tag{31}$$

On the other hand, in case of a **large unbalance** the BSP pays the failure of energy supply at the maximum value between the above-mentioned price and the highest price for the accepted selling offers to the Mercato del Bilanciamento (MB).

$$if \;\; \frac{Sbil_{UVAM}(i)}{Q_{MSD}(i)} \geq 5\% \quad \rightarrow \quad Tax = Sbil_{UVAM}(i) * max\left(\bar{P}^{marg}_{MB\uparrow}; \bar{P}^{UVAM}_{MSD\uparrow}\right) \tag{32}$$

This choice has a precise meaning: when the unbalance occurs, part of the power that was promised is not delivered to the grid – and vice versa happen with the consumption units – therefore Terna must retrieve the missing power elsewhere. The ultimate resource of provision for the TSO is MB, where the power exchange happens nearly real-time. Though it is evident that these assets are the most valuable in the market and thus the most expensive. For this reason a large unbalance brings a deep expenditure for the BSP, so it must be avoided at any cost.

Finally, the cumulative hourly penalties constitutes the overall compensation of which the BSP is liable towards Terna, the figure just computed will be added to the cost analysis as yearly fee.

3.5. Cost analysis

The final objective of this work is the assessment of the economic suitability of P2P systems in grid-connected configuration.

It is important to emphasize that some technologies belonging to these energy systems are in the process of continuous development and evolution. The expected technological progresses will not only allow to improve system's performance and efficiency, but also to drastically reduce the production cost.

It is possible to claim, with no fear, that the likelihood with which this will happen is substantial, not just looking at historical data to extrapolate forecasted trends, indeed by acknowledging the dominant direction chased by the policies carried out by the most powerful nations worldwide.

The need for the energy transition and grid decarbonisation is urgent and cannot wait any longer. The path to follow seems clear and challenging, it will take the highest level of commitment, but something started changing.

The premise was necessary to open the chapter regarding the economic analysis, since the outcome of the model are based on reputable data coming from different literature source, instead of optimistic long-term predictions. It can be confirmed that the major part of provisions made by professional merely a decade ago have been successfully overcome by the data available in the current year. Once again this represents a huge step forward towards the impactful rollout of such technologies.

3.5.1. Model description

The variables evaluated into the MATLAB code, which have been considered as relevant for the cost analysis were imported in Microsoft Excel. This tool is commonly used to perform the financial sector, since it allows to easily handle large tables, as well as has embedded ad-hoc functions able to compute the most known economic indicator. The cost analysis has been organized in six different sections:

a) Input project data

The general data of the project have to defined in this segment. It was assumed the official starting of the simulated project the year 2021 and a 20-years duration. This condition is compatible with the average lifetime of the system components and it reflects the mainstream choice in projects involving renewable energy sources.

Another important time interval to set is the amortization period, namely the total length of time it takes a company to pay off a loan. To comply with the upfront costs brought by the plant, the company needs to ask for a loan; if it chooses a long amortization period, it will have lower monthly payments but pay more interest overall. This figure was set to 20 years – the same of the project duration – in order to ensure a positive net cash flow every year of the project.

Then, the actualization – or discount – rate has been computed following two alternative procedures:

- Employing the common procedure of the Weighted Average Cost of Capital (WACC), suggested as preferred solution by NREL [37]. It evaluates the actualization rate as weighted average between the shares of equity ($\%_E$) and debt ($\%_D$) – taking for simplicity an equal subdivision, mostly common for this kind of projects – considering as weights the corresponding interest rates for both equity and debt.

$$WACC = \%_D * \frac{0.5 \cdot C_{debt}}{C_{debt} + C_{equity}} + \%_E * \frac{0.5 \cdot C_{equity}}{C_{debt} + C_{equity}} \quad (33)$$

- Alternatively, the actualization rate can be also computed by performing the sum of the interest, inflation and risk rates.

$$i_{act} = i_{int} + i_{inf} + i_{risk} \quad (34)$$

The discount rate determines which is the value of money during time.

b) Data import sheet

It gathers all the technical data related to the system, which are the main outcomes of the MATLAB model. It also contains the external data regarding the unitary costs of the components. The information contained in this section are acquired by reports, benchmark analyses and journal articles from the most internationally recognised organizations and research centres. Therefore, the figures reported below represents a reliable source to assess the average economic trend related to such systems.

- The upfront cost of **PV** technology is the one that is driving down the most. Always keeping the estimation conservative, it has been considered the value of 350 €/kWp only for the PV modules, while the Balance of Plant (BOP) was quoted to 250 €/kWp [38]. The solar inverter cost is obviously excluded from BOP[22]. The replacement cost has been set in relationship with the system capital cost, namely 45% of the whole PV field expenditure every 20 years, which is a reasonable value considering the current degradation rate of commercial PV modules. The cost related to Operation and Maintenance (O&M) are estimated at around 15 €/kWp, around 2% of the total cost of the system.

[22] The inverter has been considered as a separated component, since it is in charge of performing the conversion in AC at the electric node for the whole system, not just for the PV field.

- The **inverter** cost is size-dependent, too. However, since it is not associated to the PV system alone, the sizing is not made according to the solar peak power: indeed, it has been considered the maximum power exchanged with the grid – in both directions – during the whole year, adding a safety factor equal to 1.25. The calculation retrieved nearly 200 kW, which are multiplied to the unitary cost of 60 €/kW state in [38]. As far the replacement cost is concerned, it actually comes very close to the initial investment: after approximately ten years is recorded its full depletion and it must be changed in bulk, keeping only the associated wiring, which accounts for an almost negligible part of the cost.
- The cost of the **wind turbine** is of course dependent to the specific model. However, many reliable sources estimate a comprehensive construction cost for a wind farm within [700 ÷ 1300] €/kW range [39]. Within this interval, it has been chosen to pick 850 €/kW, as indicated in [40]. Also in this case, the replacement cost is substantial; however, the average lifetime of a wind turbine operating at the forecasted conditions can last from 20 to 25 years. Therefore, the consistent expenditure does not impact the business case. The typical value set to estimate O&M costs is expressed in percentage with respect to the upfront cost, a most-known value is 2% and it will be replicated for the P2G components as well.
- The **Power-to-Gas system** components are those weighing in on the total investment cost the most, according to the sizes considered in the standard configuration. As already said previously, they are not consolidated technologies yet, though they need a consistent technological advancement on Material Science to conclusively break down the market barriers and trigger a worldwide rollout.

Table 3.3: Fuel cell and electrolyzer data for the cost analysis

	PEM Fuel Cell [41]	**PEM Electrolyzer** [42]	
Unitary capital cost	714.29	781.5	€/kW
% of CapEx for replacement	35%	35%	-
Replacement cost	250.00	273.53	€/kW
Replacement time	5	5	years
% of CapEx for O&M	2%	2%	-
O&M cost	14.29	15.63	€/year
Lifetime of the component	20	20	years

Table 3.4: Hydrogen storage data for the cost analysis

	HYDROGEN STORAGE [43]	
Unitary capital cost	300	€/kg_{H2}
% of CapEx for replacement	90%	-
Replacement cost	20250	€
Replacement time	30	years
% of CapEx for O&M	2%	-
O&M cost	450	€/year
Lifetime of the component	30	years

c) Capital Expenditure sheet

It gathers the information related to the investment costs of system components. It is common practice to handle the CapEx using the amortization/depreciation procedure. The depreciation is an accounting convention that allows a company to write off an asset's value over its useful life. If a component has a useful life longer than the lifetime of the project, it will ensure a residual value for the owner, thus the actual expenditure charge by the owner is lower the longer is assets' useful life.

Depreciation is used to account for declines in the carrying value – the different between the original cost and the accumulated depreciation – over time.

The selected amortization procedure is the so-called *straight-line method*, which considers a constant contribution of depreciation named *depreciation* rate. This is easily computed by taking the amortization value of a prescribed asset and dividing it for the number of years correspondent to the amortization period.

It is important to remark that the depreciation concept is only related to system accounting, though it does not represent an actual variation of the incoming or outgoing cash flows. Therefore, the project owner still has to pay in advance – at year "zero", as indicated in common cash flow analysis – for the infrastructure, but the expenses are diluted over the amortization period in order to generate a net positive income from the very beginning of the project.

As alternative way to account capital expenditures, the entire amount is considered at year "zero", without accounting for a yearly negative cashflow. In this way, the project's cash flow analysis starts with a deep liability at the beginning, subsequently it generates a series of positive net incomes which bring the positive cash flow to rise and eventually to overcome the zero-threshold, thus generating a profitable investment.

d) Operational Expenditure sheet

Each component belonging to the P2P system involves a cost to ensure that it works fine over the whole duration of the project. The seamless functioning of the system is guaranteed whether ordinary and extra-ordinary maintenance is carried out, along with the component replacement if a substantial performance degradation is noticed during the time[23].

[23] Usually the replacement time and the corresponding cost are set for these kind of project, given that the components suffer a different type of degradation which is going to infer their performance. The figures

Therefore, OpEx are evaluated as yearly payments which include the O&M cost – generally expressed in relative terms with respect to the upfront cost of the component – together with a replacement charge, with cadence dependent to the specified time interval.

It is crucial to point out – given that it avoids a consistent expense – that if the need of replacement falls in the closing year of the project, of course this is not carried out. The renewal of an asset which then will be either dismantled or reused for other purposed would negatively impact the economical visibility as well as performing a useless activity for the project's sake.

e) Revenue streams sheet

It collects the hypothesized set of yearly revenues earned in the MSD market, which have been already described in the section 3.4 of this work.

The fixed remuneration mechanism ensured by Terna guarantees a constant positive income for the system, which will be summed up with the variable part that is dependent on the energy committed in the MSD market, as well as on the assumption made on energy pricing during the considered year.

Later in the chapter will be assessed the economic profitability of the plant by considering different combinations of revenue streams in order to figure out which scenario has solid economic basis to be pushed forward.

considered in this work are generally recognized as educated guesses for the purpose. Obviously, it is up to the specific equipment manufacturer to specify the recommended replacement time.

f) Business case overview sheet

This Excel sheet summarizes all the most important information coming from the just described sheets and with these it performs a straightforward cash flow analysis. As already said, there are two alternatives bringing to the same outcome, the mainstream approach is to consider the CapEx all at once, carrying only the OpEx as yearly negative cash flow.

The variables computed in this section are listed below:

- *Yearly net cash flow*: it is calculated by subtracting the total liabilities from the revenues streams. Its sign determines if the project has a profit or a loss.
- *Discounted cash flow*: the value of money is not equal throughout the time, thus the cash flows suffer a write-off by multiplying the discount factor – which has been computed using the WACC early in the chapter – with the corresponding net cash flow.
- *Cumulated cash flow:* it is the cumulated sum of all the previous cash flows, and it represents the overall economic trend of the project.

The calculation of these parameters allows to evaluate common economic indicators attesting the profitability of the investment, as shown in eq. (35), (36) and (37).

The NPV is the sum between the upfront cost and the summation of cash inflow-outflows over a period of time. It measures the monetary return of investment for a specific project, as shown in eq. (35).

$$Net\ Present\ Value\ (NPV) = -C_{inv} + \sum_{t=1}^{n} \frac{R_t}{(1+i)^t} \tag{35}$$

The PBT refers to the amount of time the plant's owner takes to recover the cost of the investment, namely when the discounted cash flow shifts from negative to positive and the investment stop being at a loss and start producing tangible earnings.

$$Payback\ Time\ (PBT) = \frac{C_{inv}}{R_t} \tag{36}$$

The IRR is the actualization rate which sets at zero the NPV. This value is a direct indicator to assess the economic profitability of a specific activity. The project worth the investment whether the IRR is higher than the standard actualization rate computed with the WACC procedure. Put in other words, the project is economically successful if the investor has the possibility of earning more money investing in it instead of putting them in the bank. The IRR presents some limits of applicability and requires the observance of a set of rules from the cash flow series.

$$Internal\ Rate\ of\ Return \rightarrow NPV = -C_{inv} + \sum_{t=1}^{n} \frac{R_t}{(1+IRR)^t} = 0 \qquad (37)$$

Given the simplified approach of this cost analysis, this indicator has enough reliability to be considered. Nevertheless, projects with a high innovation content such as the one analyzed in this work need tailor-made metrics not only regarding the financial aspect, which are able to highlight strengths and weaknesses.

3.5.2. Key Performance Indicators (KPIs)

The KPIs selected for the system evaluation must present some imperative features which allow to perform an unbiased assessment.

First of all, they have to be as representative as possible, covering all the relevant aspects of the analysis. For this reason, it has been decided to consider indicators related to both the energy and financial management of the system.

It is the author's duty to clearly state the meaning associated with each parameter, in order to immediately link up figures with tangible implications.

The indicators elected for the purpose are listed below:

1. **Energy ratio**. It aims at checking if the system performs an optimal use of the renewable energy sources. It is a good indicator of whether the plant has been correctly sized or not. A low value means that the energy curtailment is low, but of

course this has to be compared with the actual size of PV field and wind farm. It is a common practice in KPI analysis to make use of ratios or, more in general, dimensionless parameters, which are able to describe a system's feature regardless the change in size[24].

$$\gamma_{RES} = \frac{E_{curt}}{E_{RES}} \tag{38}$$

2. **Mean SoC of the P2G system**. This parameter is mainly focused on rating the rational employment of the P2G system. Also in this case, a dimensionless indicator is the best option, since during the sensitivity analysis will be varied the sizes of the fuel cell, electrolyzer and hydrogen tank. A well-sized P2G system should manage to maintain the average SoC of its hydrogen tank around the central SoC[25], which can be evaluated as:

$$SoC_{H_2MEAN} = \sum_{i=1}^{8760} SoC_{H_2}(i) \tag{39}$$

This is due to the fact that if the SoC is as close to the middle value as possible, the system will have a higher probability to intervene, either absorbing extra power through the electrolyzer or providing it via fuel cell. On the other hand, if the parameter is too close to the SoC boundaries, the system will experience more frequent periods of unavailability, resulting in less profitability of the plant as a whole.

$$SoC_{H_2CENTRAL} = \frac{SoC_{H_2max} - SoC_{H_2min}}{2} \tag{40}$$

3. **P2G system efficiency**. This parameter is an attempt to quantify the overall efficiency of the P2G system. Of course, there is not a univocal way of representing

[24] This concept becomes particularly relevant when carrying out the sensitivity analysis, where the objective is to evaluate the behaviour of the system by varying its representing variables. Its outcomes are reliable the more significant and even-handed KPIs are set.

[25] Be aware that central SoC is not always equal to 50%, indeed it depends on the specific Depth of Discharge (DoD) of the system. If the DoD is symmetric with respect to 50% the figure is confirmed, otherwise it has to computed separately.

it. The most straightforward way consists in performing the average of the single average efficiencies of the two electro-chemical machines. The indicator is extremely important, as explained in section 2.5, to evaluate the quality of the system's sizing, since the operational efficiencies are related to the power regime of the above-mentioned machines. Particular attention was given to the P2G system, clearly it is not by chance, but because one of the main objectives of this work is to assess whether it constitutes a reliable stand-alone storage asset or it is necessary the integration of batteries to handle daily variations.

$$\eta_{P2G} = \frac{\eta_{FC_{mean}} + \eta_{EL_{mean}}}{2} \tag{41}$$

4. **Off-grid factor**. This KPI concerns the ability of the system to perform the island-mode functioning. To achieve the goal, it was calculated the amount of time the system does not need the grid intervention to accomplish its tasks. The indicator could be particularly useful in case of specific locations having strict requirements in terms of grid connection and availability.

$$OGF = \frac{h_i(P_{ext} = 0)}{h_{tot}} \cdot 100 \tag{42}$$

5. **Investment factor**. The indicator aims at assessing the economic profitability of the investment. It carries a double dependence: the former is the capital expenditure which investors must address to finance the project, while the latter is the total energy committed in the MSD, which represents a measure of the potential revenues deriving from the market participation. It adds to the set of economic parameters already described in section 3.5.1.

$$IF = \frac{C_{inv}}{\sum_{i=1}^{8760} P_{MSD}(i)} \tag{43}$$

4. Assessment of the P2P system potential

In this chapter will be presented the main outcomes of the complete model just described in *Chapter 3 - Simulation Model of the P2P system.*

Firstly, the results coming from the preliminary sizing will be presented and briefly commented, then it will be outlined the sensitivity analysis carried out to gain insights on how to improve the efficiency along with the profitability of the plant during the design phase. The preliminary sizing is the output of a trial-and-error process, which has brought to a well-run configuration, though it is not optimized.

4.1. Key outcomes of the Simulation Model

As far the Energy Balance Model, some of the main trend outlined in the post-processing phase are depicted in section 3.2.3, whereas the purpose of the current is to present the main findings of the work as effectively as possible.

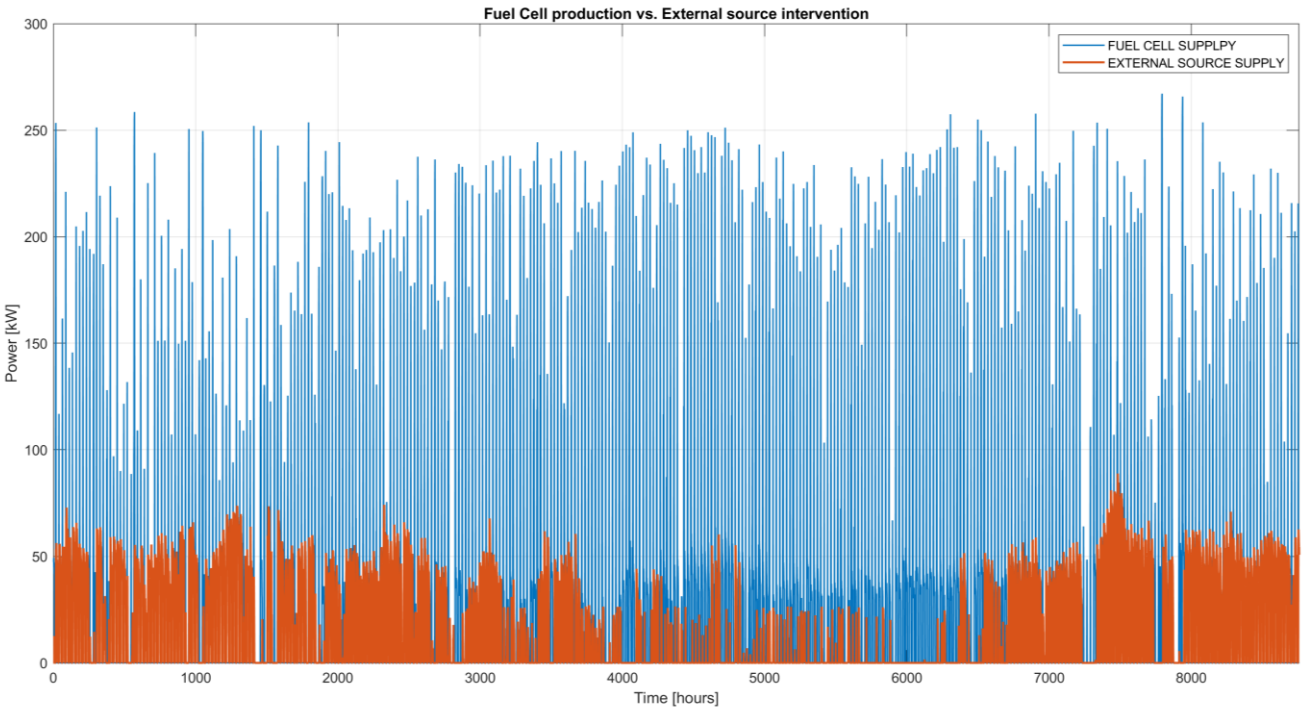

Figure 4.1: Comparison between fuel cell production and the external source supply

The Figure 4.1 highlights the intensive use of the fuel cell throughout the entire year. Most of the time the electro-chemical machine works close to its maximum power value, since often it must intervene to make available the offer to the MSD market. It is evident from the Figure 4.1 that the fuel cell manages to cover the internal load only for a short time interval during summer, when the power surplus coming from renewables is at its highest, while the rest of the year the intervention of an external source is needed.

This behaviour can be justified by the fact that the activation threshold of the fuel cell is often higher than the hourly internal load. Lowering the threshold would bring to the less efficient operation of the fuel cell. This aspect has a relevant importance and it must take into account during the design phase and one of the objectives of the sensitivity analysis is to figure out which is the best configuration minimizing the need of an external source of energy, thus allowing the system to work in off-grid mode for as long as possible.

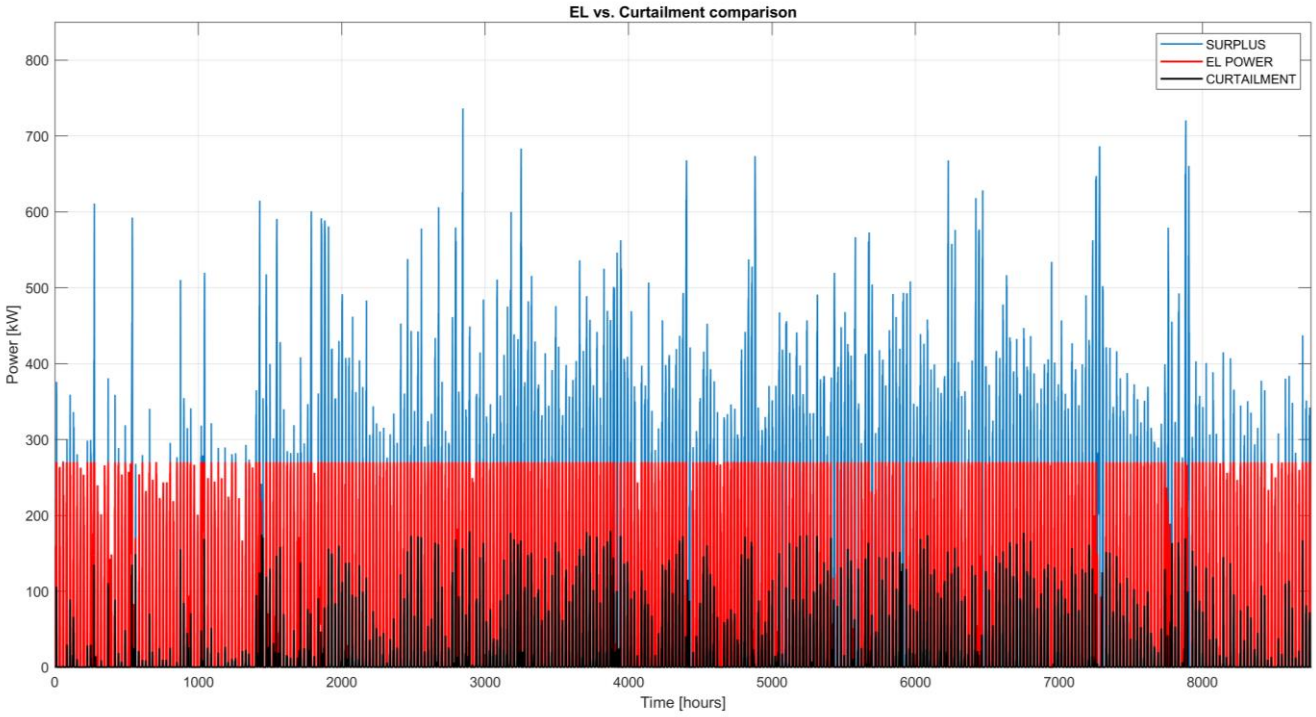

Figure 4.2: Overview of power surplus utilization

In Figure 4.2 is illustrated the management of the power surplus between the P2G system, the portion committed to the MSD market and the remaining part which will suffer the curtailment.

The first aspect which can be noticed at a first glance is the underestimation of the electrolyzer nameplate power, given that it is not able to absorb the frequent peaks of energy produced by renewables, especially during summer. This brings to frequently curtail the power, even though the absolute value of wasted energy is contained to 73.8 MWh per year.

On the other hand, this size implies an intensive, indeed the energy absorbed by the electrolyzer to produce hydrogen stands at 528.5 MWh on yearly basis.

Given the nameplate power of the fuel cell, it is an impressive number, however it does not address the most problematic characteristics of such systems. Renewables ensure significant peaks during daytime, which help carrying out the dispatch order coming from Terna, even though the electrolyzer does not manage to store enough energy to be then employed by the fuel cell to drive other system's activities.

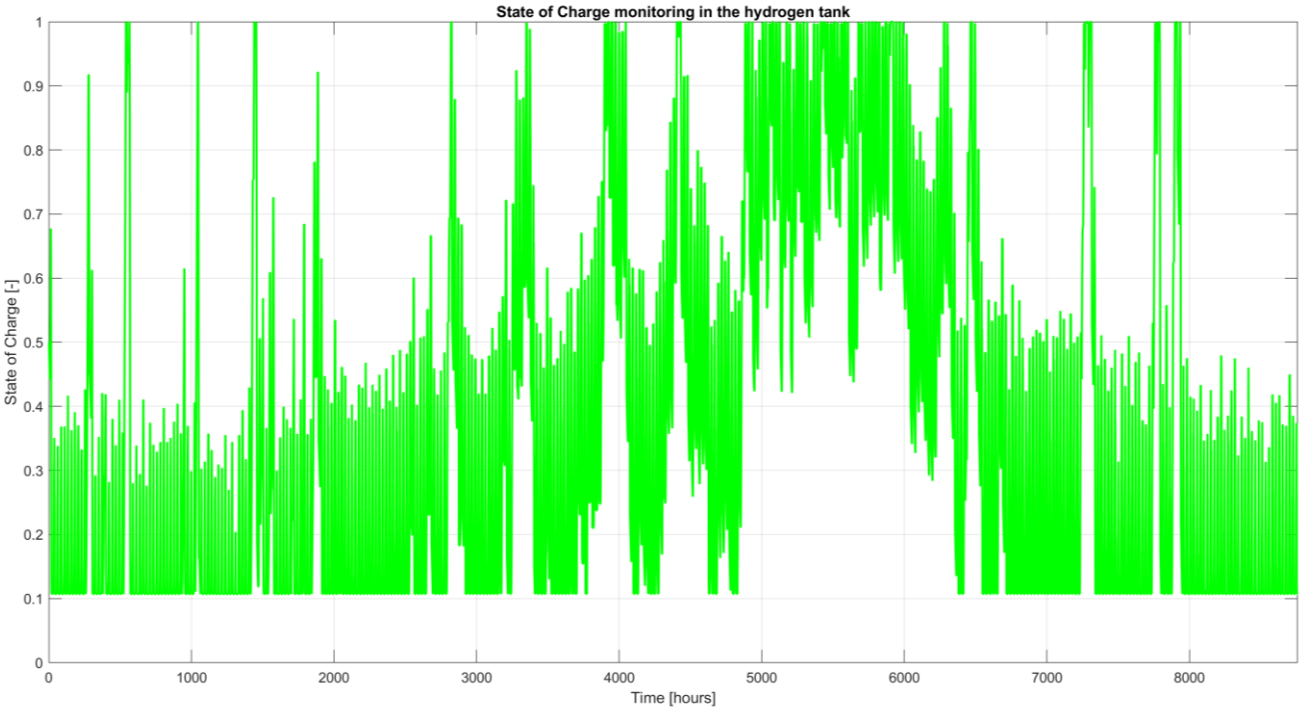

Figure 4.3: State of charge in the hydrogen tank

Figure 4.3 depicts the trend of the energy content in the hydrogen tank. Steep peaks and falls are recorded due to the reduced dimension of the hydrogen tank, namely 75 kg of

hydrogen as maximum content, with respect to the nameplate power relative to the electro-chemical components. This aspect brings the SoC to its minimum value very often.

From the trend reported in Figure 4.3 it is evident which is the main target of the hydrogen storage: it has to act as both daily and seasonal storage, trying to remain as close to the central SoC as possible. If batteries were present, the SoC oscillations would be much smoother than the steep variations depicted in Figure 4.3. Besides, the number of interventions of the P2G system would be less than in case of a single storage asset as well as it would be responsible of accumulating the excess of energy available in summertime.

Finally, Figure 4.4 highlights the overall trend of the hourly power the system is able to offer in the MSD market. It is possible to notice how the lack of power delivered to the market – indicated in solid black – is more concentrated during autumn and winter, while in summertime the system is able to provide a substantial quantity of energy to perform grid services.

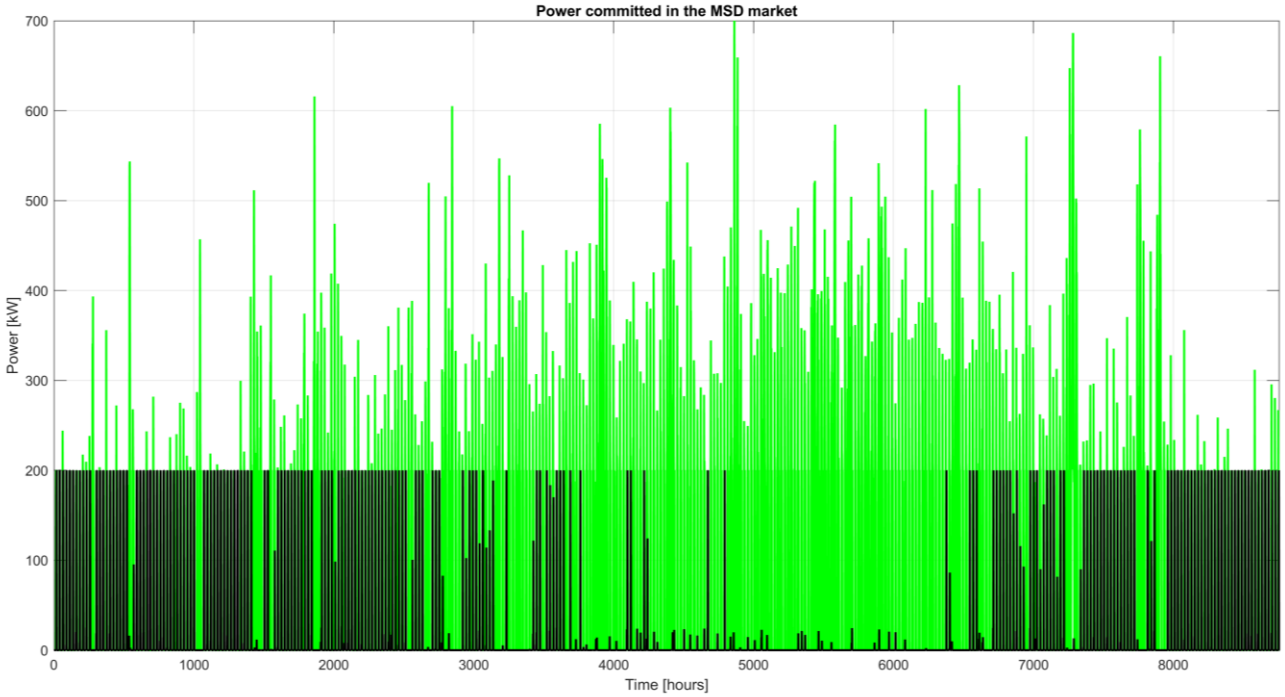

Figure 4.4: MSD market participation of the P2P system

Although the minimum energy requirement with regard to the above-mentioned market are satisfied, as already confirmed in section 3.3, it is preferable to have a more balanced distribution, which is one the desired outcome of the optimization algorithm developed in this work.

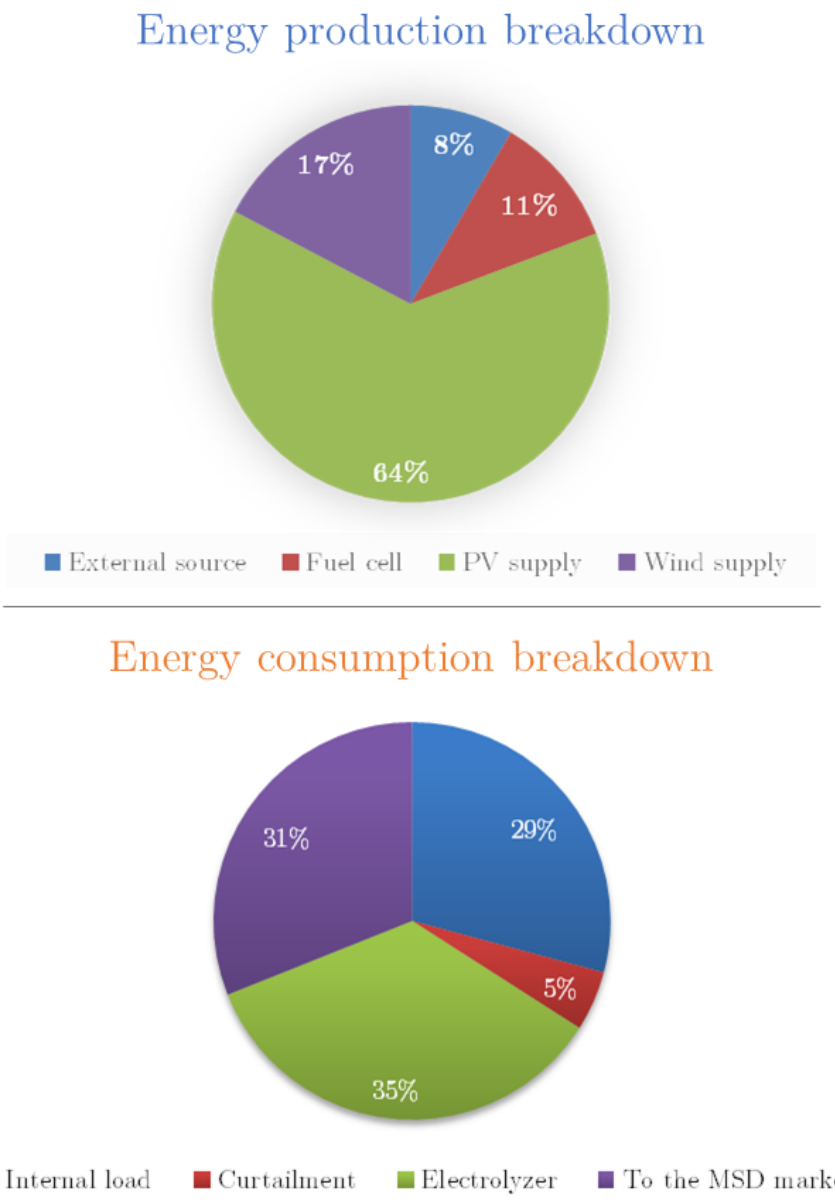

Figure 4.5: Yearly energy balance at the electric node

Figure 4.5 illustrates, by means of pie charts, the subdivision of the power exchange at the electric node. It is possible to notice that nearly 31% of the energy consumed by the system is committed to the MSD, thus it is able to generate revenues. This number is

fundamental to positively assess the suitability of an energy project involving a P2P system.

The most important variables related to the energy analysis are reported in the Table 4.1.

Table 4.1: Sum up table of the Simulation Model – standard configuration

Label	Value	Unit
Power WIND turbine	330.00	kW
Power PV field	600.00	kW
Power FC	270.00	kW
Power EL	270.00	kW
Mass of H2 storage	75.00	kW
Max power to the grid	88.87	kW
Average SoC	37%	-
FC mean efficiency	51%	-
EL mean efficiency	62%	-
Off-grid hours	5649	hours

This set will be then evaluated for each configuration selected for the sensitivity analysis, since they represent the most relevant energy variables relative to the P2P system.

As far the cost analysis is concerned, the main outcomes are reported in the

Table 4.2: Sum up table of the Cost analysis – standard configuration

Label	Value	Unit
Internal Rate of Return	2 %	-
Net Present Value	- 361'246.90	€
Payback Time	n.c.	-
En. Curtailed / En. RES	0.058	-
Average SoC	36.85%	-
P2G system efficiency	56.77%	-
Off-Grid Factor	64.49%	-
Investment Factor	1.870	k€/MWh

The Cost Analysis was simulated selecting only a unique hypothesis made regarding the revenue streams, mainly for two reasons: considering all the four attempts explained in section 3.4.2 would bring the elaboration to a too high level of complexity, given that the varying parameters are already numerous. Secondly, it is already evident from the first run of the Simulation Model that the two scenarios which take into account the actual fluctuations of the MSD market price retrieve too poor revenues to be competitive at this stage.

Nonetheless, one of the main purpose of the work was the construction of the model, when more aggressive remuneration policies will come, it will be crucial to have available a tool which manages to capture the best value from the market by knowing in which time intervals is worth to intervene. This possibility will help to improve the business case of such projects.

On the other hand, the first scenario highlighted in the section 3.4.2, that considering as selling price the maximum allowed – namely the strike price – was not even considered, since it is representative of any realistic situation, now as in the future.

Therefore, the assumption made in the section 3.4.2 on the revenues generated by the system consists in assuming a fixed average price as remuneration for grid services, at least in the most intensive block hours of the day.

This scenario aims at pushing the MSD market towards the standard energy market, which is characterized by a higher price stability and, more in general, it guarantees a more certain source of income, even if with less margin comparing to that of MSD.

Among the future development of this work will be also included the need of building alternative scenarios to those analysed so far, given that the context in which the P2P system are inserted could change deeply according to the specific situation.

Analysing the results of Figure 4.5, the P2P system has proven its effectiveness in terms of energy performance for the accomplishment of the tasks set in advance. This is not in the same way valid under the financial point of view, given that the economic KPIs report a loss-making investment.

The IRR has to overcome the interest rate accounted for the project – it has been set at the beginning to 7 % - as a consequence, the project will not generate a positive income measured at the final year, indeed the Net Present Value presented in Table 4.2 is heavily negative.

It is trivial to say the project, considering this configuration, not worth the investment. The sensitivity analysis and the optimization procedure aims at improving the framework presented; however, there are still significant barriers to overcome.

Firstly, such system are enabled to generate multiple sources of income, thus performing a revenue stacking process, by providing additional grid services as well as finding alternative ways to optimize *behind-the-meter* utilization.

In addition to a more structured model, the provision regarding the revenue streams would account for a more aggressive strategy proposed by the authorities in the years ahead.

The UVAM-related pilot projects will be activated in 2021 with an expected duration of five year. Though if they would retrieve successful results, consequently they would stimulate even further the transition to renewable energy sources integrated with storage assets.

4.2. Sensitivity analysis

The most relevant outcomes of the sensitivity analysis are summarized in this section. The procedure was performed by setting a *for loop* on a MATLAB script which runs sequentially the elements belonging to the Simulation Model and automatically reports the results in a dedicated Excel sheet gathering all the outcomes of the economic model.

The main findings of the analysis are divided according to the parameter considered as variable and they are reported in the following subsections.

4.2.1. Capacity of the hydrogen tank

Firstly it was analysed how the variation in the size of the hydrogen tank may affect the performance of the system.

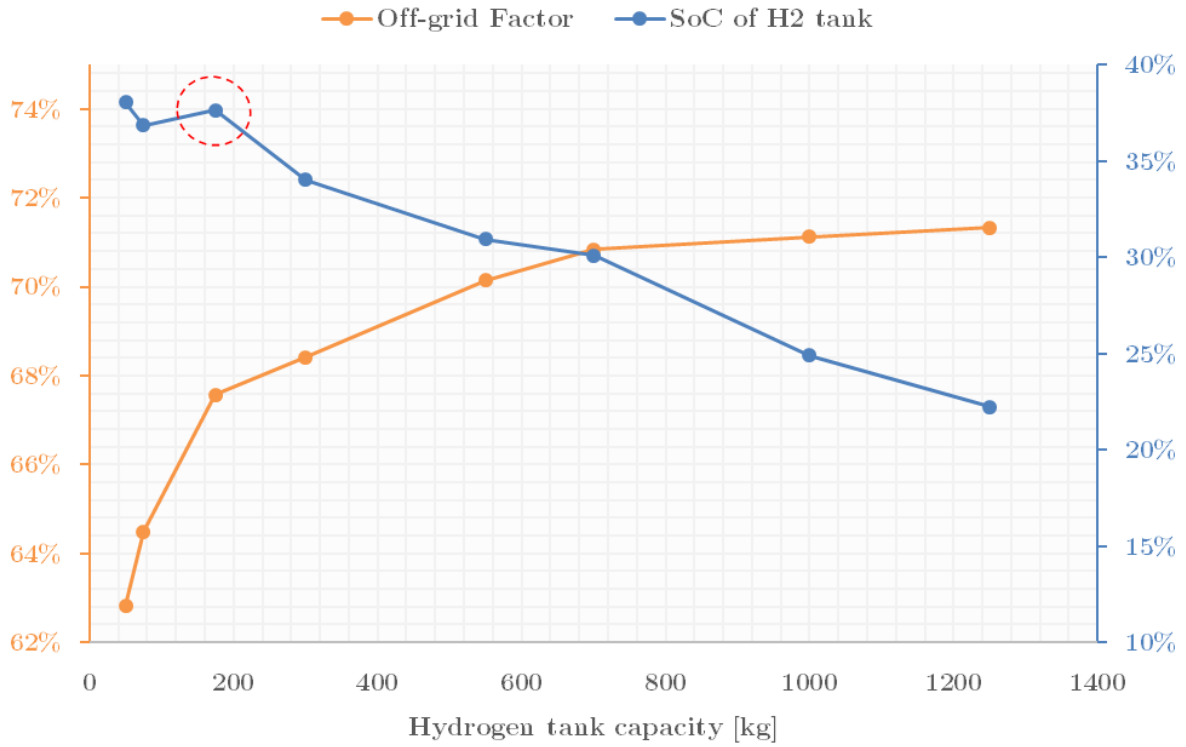

Figure 4.6: Sensitivity analysis on hydrogen tank capacity – OGF and average SoC

As it is possible to notice from the Figure 4.6, keeping constant the nameplate power of the electro-chemical machines, the average SoC of the hydrogen tank records an overall decline, heading away from the optimal condition. This is due to the fact that above a certain

threshold, the Fuel Cell is no more able to refill the tank at the pace the hydrogen is employed by the Electrolyzer. However, the growth on tank's dimension corresponds to an increase of the Off-grid Factor, this behaviour could be interpreted as counter intuitive, though the tank is emptier on average, it is more capable of accumulating the excess of energy produced during summer, acting better as seasonal storage. Another useful insight is represented in circled red in Figure 4.6: if the size of the Fuel Cell and Electrolyzer are fixed, the highlighted point can be seen as maximum of the curve, providing a first indication on which could be the optimized system's size. As a matter of fact, the above-mentioned point appears early in the graph, meaning that an excessive increase of tank's dimension is not advantageous for the project sake, also due to the peculiar yearly energy distribution provided by renewables, which makes useless an excessive oversizing of the tank. This aspect is fully reflected looking at the trend of the financial KPI depicted in Figure 4.7. Project's requirements are fundamental: if the need to work independently from an external energy supply is an imperative, it would spend more for a hydrogen tank with higher capacity.

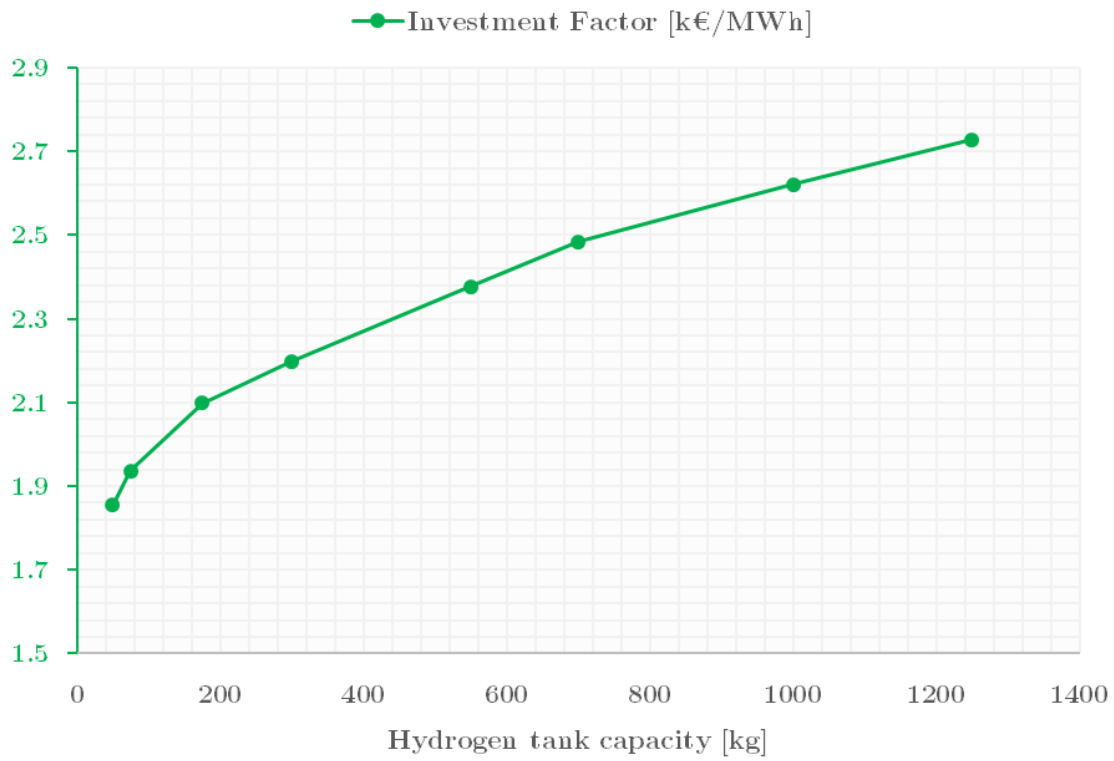

Figure 4.7: Sensitivity analysis on hydrogen tank capacity – Investment Factor

4.2.2. Fuel cell nameplate power

One of the objectives of the sensitivity analysis is to figure out which variables influence more the overall performance of the system and to assess the magnitude of their contribution. In the current case, the variation of the Fuel Cell nameplate power does not cause significant improvement of the business case.

In fact, as it is possible to see in Figure 4.8,the results of the model affected by the variation are the energy supplied to the MSD market and that requested by the external source.

Both depict a concave shape, but paying attention to the scales, it can be noticed that the variations are negligible, thus an excessive increase of the achievable Fuel Cell power surely does not justify the raise on Capital Expenditure.

It is worth specifying that this trend is not helped by the still very high unitary cost associated to electro-chemical technologies, as already discussed in section 3.5.

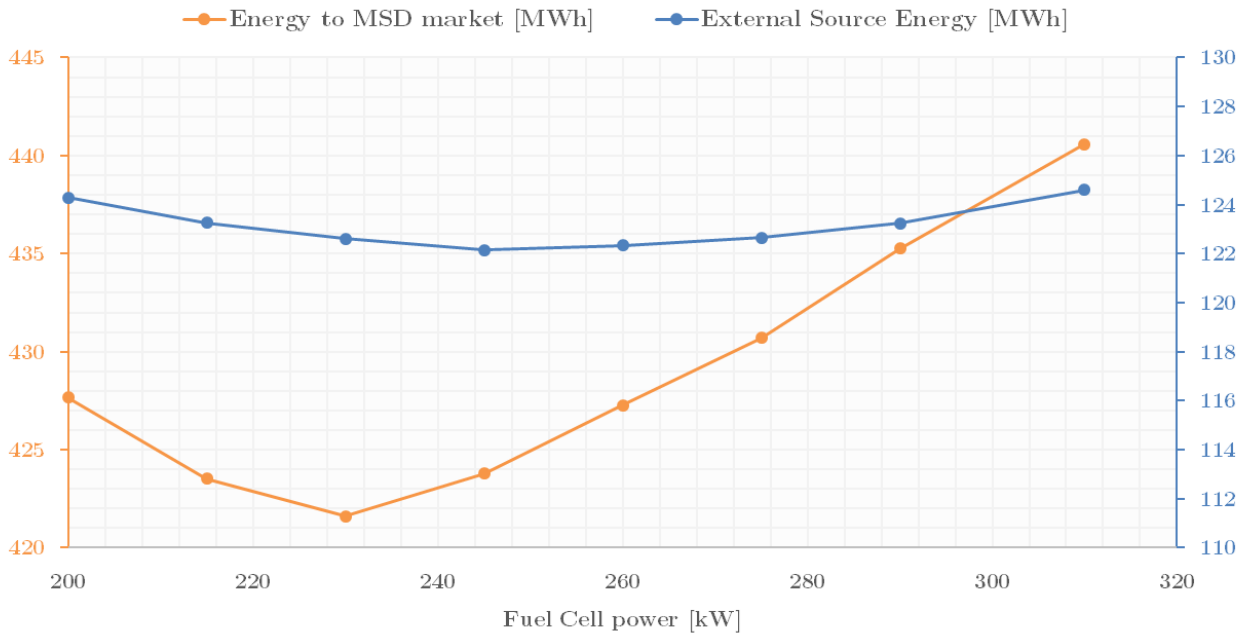

Figure 4.8: Sensitivity analysis on Fuel Cell power – MSD market and External source energy

In Figure 4.8 is possible to point out a slight decrease of the power devoted to the MSD market as the Full Cell maximum power rises; nevertheless, the corresponding rise in

revenue streams coming from the MSD market is overshadowed by the weighty boost in machinery cost, that makes useless the size upgrade of the system.

This concept is rightly recorded by analysing the Investment Factor in Figure 4.9.

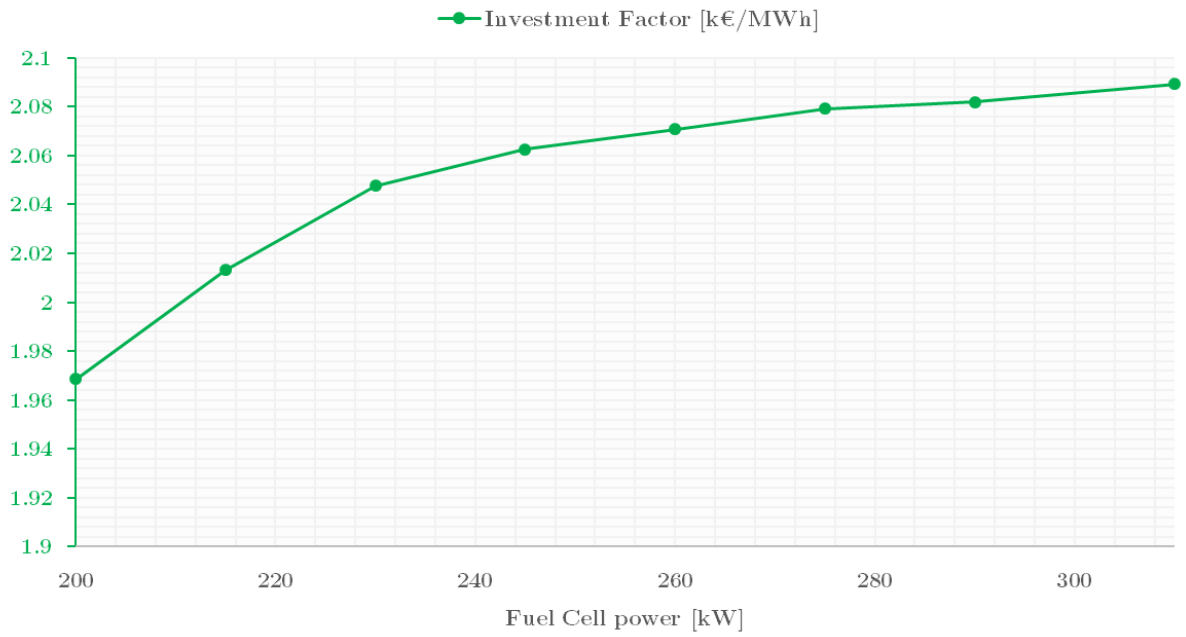

Figure 4.9: Sensitivity analysis on Fuel Cell power – Investment Factor

4.2.3. Electrolyzer nameplate power

Unlike what has been learnt for the Fuel Cell, by varying the nameplate power related to the Electrolyzer it is possible to obtain relevant benefits even keeping fixed the remaining configuration of the system.

The most accredited reason rely on the efficiency chain which characterizes the P2Gsystem: the Electrolyzer oversizing is necessary, given that the round-trip efficiency of the set comprised by FC+EL+H_2 tank is considerably low.

In other words, the electrical power absorbed by the Electrolyzer at the node is retrieved at the same place only after a double step of conversion – from electrical to chemical, and vice versa – and the loss due to hydrogen storage, which can be neglected as first approximation. Almost all the simulation performed during this sensitivity analysis retrieved a values of the energy KPI representing the overall efficiency of the P2G system equal to $\eta_{P2G} \cong 57\%$, thus round-trip efficiency:

$$RTE = (\eta_{P2G})^2 \cong 32.5\,\% \tag{44}$$

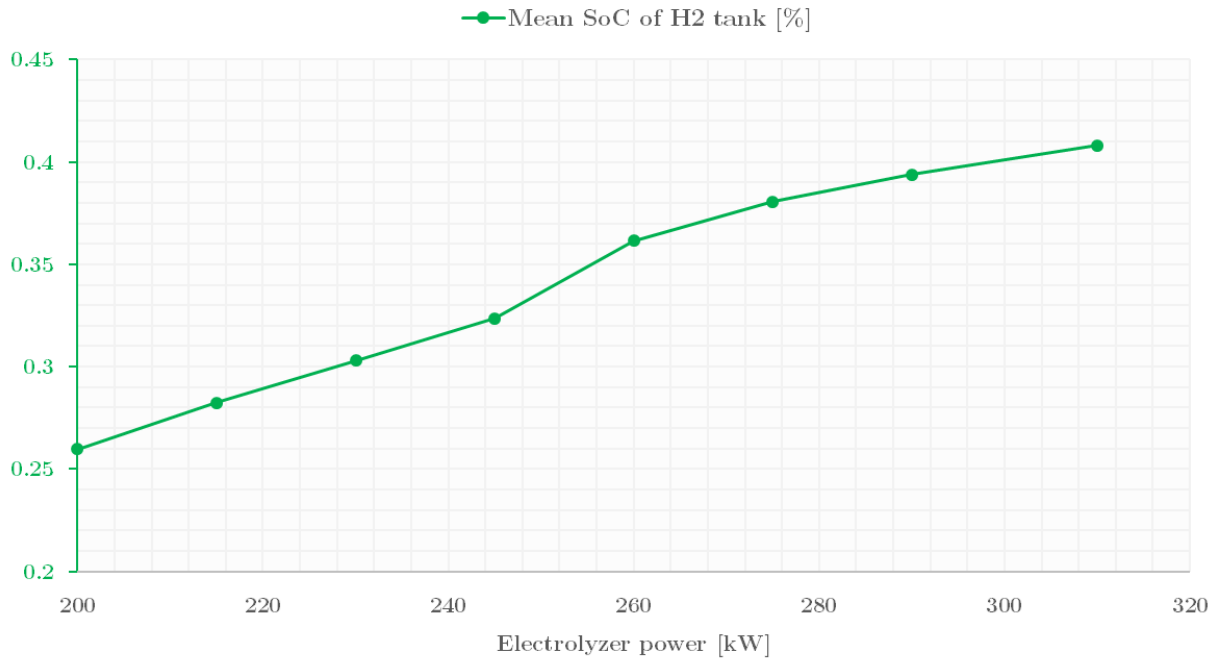

Figure 4.10: Sensitivity analysis on Electrolyzer power – Average SoC of the hydrogen tank

The considerable waste of energy in the process is the price to be paid for the production of a valuable energy carrier as hydrogen is.

Having said that, Figure 4.11 highlights the evident advantages brought by an increase of the Electrolyzer size. Surely, the yearly energy absorbed by the machine at the node increases as the nameplate power does the same, whereas it declines the energy curtailment – which otherwise would be substantial during summer – since the machine manages to convert more power if assessed in an hourly basis.

As a direct consequence, a consistent rise in the yearly average SoC of the hydrogen tank, as depicted in Figure 4.10.

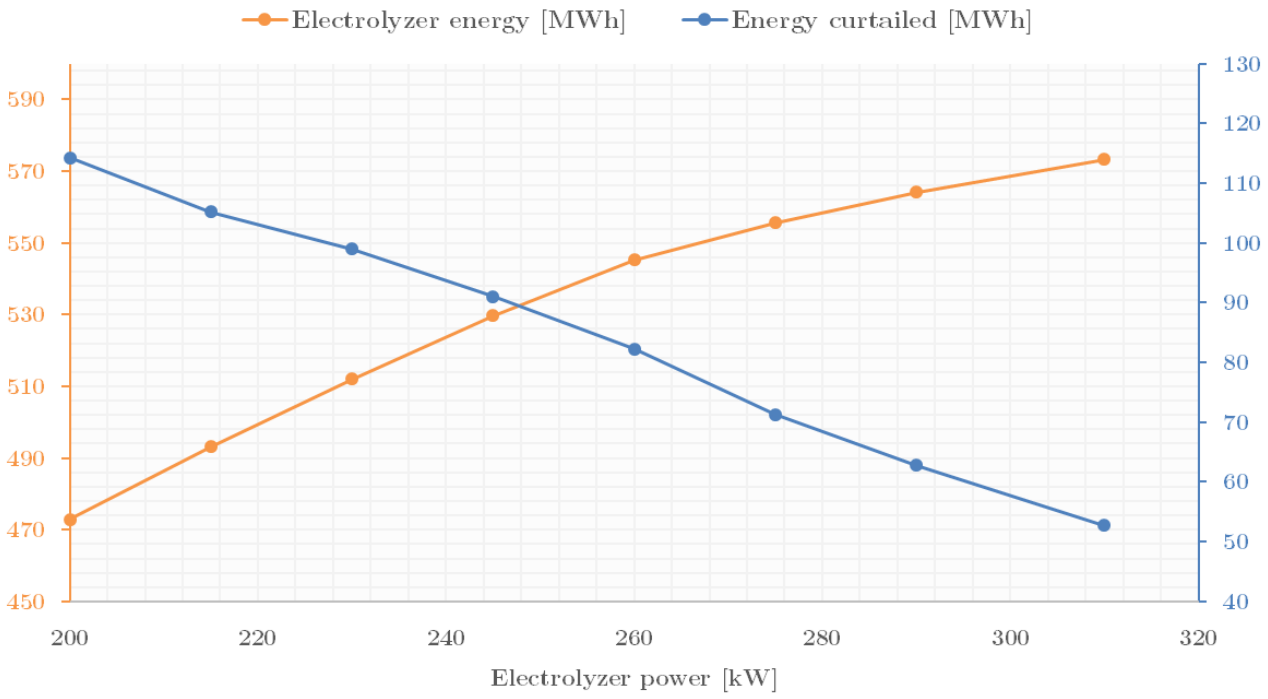

Figure 4.11: Sensitivity analysis on Electrolyzer power – Energy produced by the machine and curtailed

4.2.4. Renewable Energy Source and capacity of the hydrogen tank

In the last part of this analysis, the objective was to evaluate the impact on the overall performance of the system considering renewable energy sources of different size.

Regarding the PV field, it was just necessary to vary the peak power in the sub-model described in section 2.3 to obtain the wanted scaling of the system. Instead, the energy produced by the wind turbine was computed assuming the machines employed were ruled to exact the same power curve of that considered in section 2.4[26]. Contextually, the dimension of the hydrogen tank must change as well, since the higher yearly energy needs more capacity for the storage.

Therefore, the simulations was performed by varying a set composed by three data, as reported in Table 4.3:

Table 4.3: Description of the analyzed scenario

Scenario	Wind power [kW]	PV power [kWp]	Mass of H_2 [kg_{H2}]
1	250.00	400.00	100.00
2	300.00	500.00	200.00
3	350.00	570.00	300.00
4	400.00	650.00	400.00
5	450.00	720.00	500.00
6	500.00	800.00	600.00
7	550.00	870.00	700.00
8	600.00	950.00	800.00
9	870.00	970.00	900.00
10	900.00	1000.00	950.00
11	930.00	1040.00	1000.00
12	970.00	1080.00	1050.00
13	1010.00	1150.00	1100.00
14	1050.00	1200.00	1150.00
15	1080.00	1240.00	1200.00
16	1120.00	1300.00	1300.00

[26] The simplification made does not compromise the accuracy of the results presented in the analysis, given that the power curves characterizing the wind turbines are very similar to each other, except for slight changes on cut-in and cut-out speeds, which drive wind turbines to specific fields of application.

The numbers indicated in the first column are used to better identify the system configuration in the following graphs.

The first relevant insight gained by the sensitivity analysis was regarding the average State of Charge of the hydrogen tank. As it is possible to see in Figure 4.12 , the percentage rises steadily while increasing the producible power of the system, this trend represents a more efficient exploitation of the P2G system.

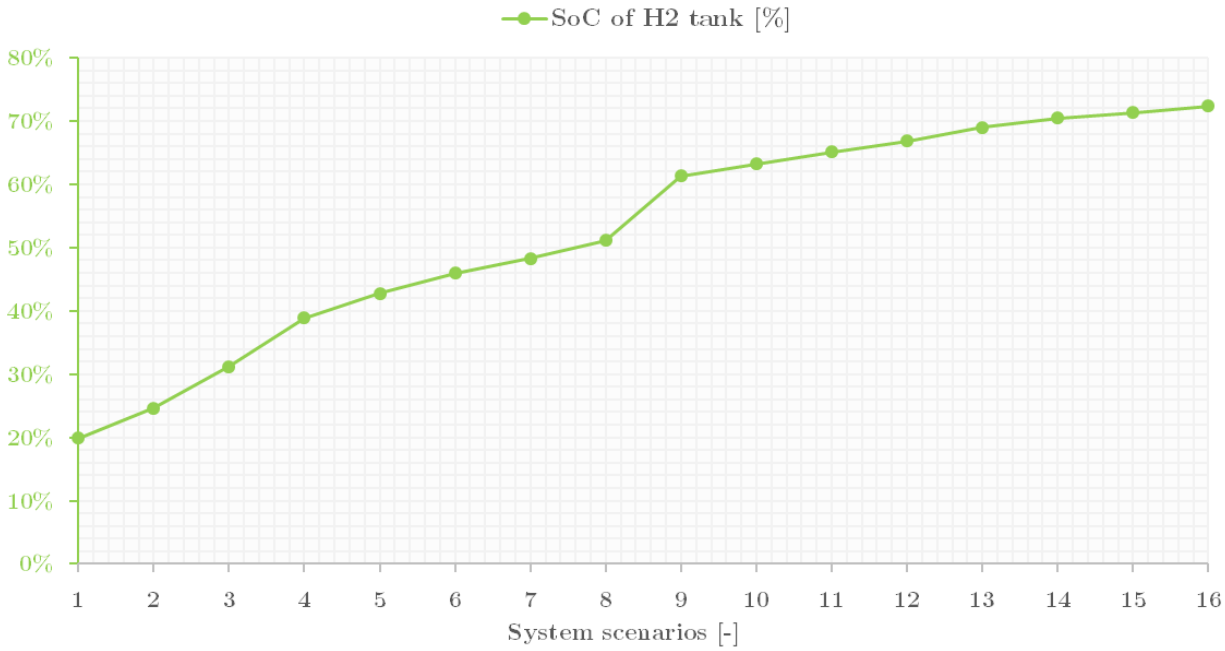

Figure 4.12: Sensitivity analysis on RES system – Average SoC of the hydrogen tank

The reason of this growth is twofold:

- An increase of hourly power coming from the wind turbine is imposed, this guarantees a more homogeneous distribution of the output throughout the day, helping out the Fuel Cell to keep up with the requests coming from the internal load.
- At the same time, more solar energy produced is going to fill the hydrogen tank faster than the Fuel Cell manages to discharge it, thus provoking the ascending trend.

During the design phase, it must be paid attention to limit the reverse effect, because too high SoC values block the intervention of the Electrolyzer and they are indicative of an under-sizing of the P2G system. The best solution is the product of a trade-off which the optimization model tries to address.

As far the exchanges with the electricity grid is concerned, the trends depicted in Figure 4.13 – together with the ones already described above – clearly state that the first sizing made for the system to perform the first of the Simulation Model presented an heavy unbalance toward the P2G system: this has made it neither efficient from the performance point of view, nor cost-effective.

After a first rise, the energy curtailed starts decreasing as RES produce more power: if the P2G system were sized well, the highlighted trend should have been in contrast with the expected behaviour of the results, since at a certain point the energy available could not be processed by the electrolyzer.

It is possible to record instead a decline in both the energy curtailed and the one requested from an external source, which surely benefits the profitability of the system as a whole.

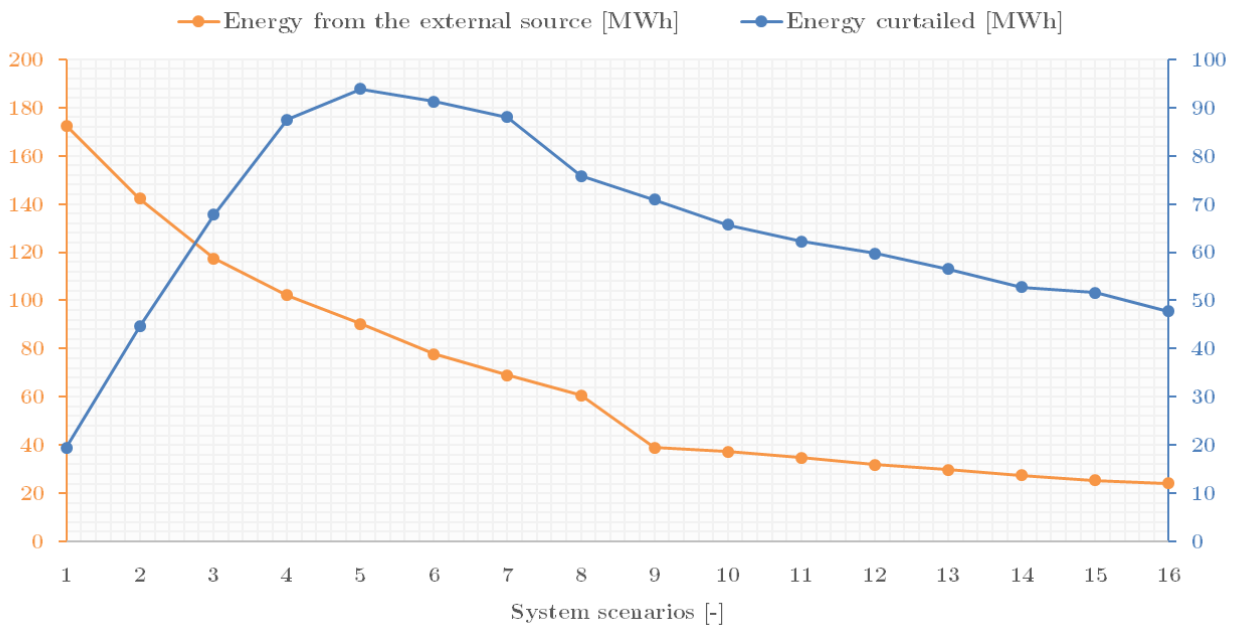

Figure 4.13: Sensitivity analysis on RES system – Energy curtailed and from the external source

The P2P system records a considerable gain from the MSD market participation with the growth of RES system dimension.

As it is evident from Figure 4.1, Figure 4.2 and Figure 4.4, the main contribution to the market is at the hands of the PV system, the steep power peaks during the sunniest hours of the day allow the BSP to sell the energy surplus were the prices are at their highest. The more spread powers exceeding along the year allow to drastically bound the situations of supply failure, thus limiting the penalties accruing to the regulator.

Figure 4.14 shows a steady growth of the power devoted to the MSD market, which will have an extremely positive impact on the evaluation of the business case related to the project.

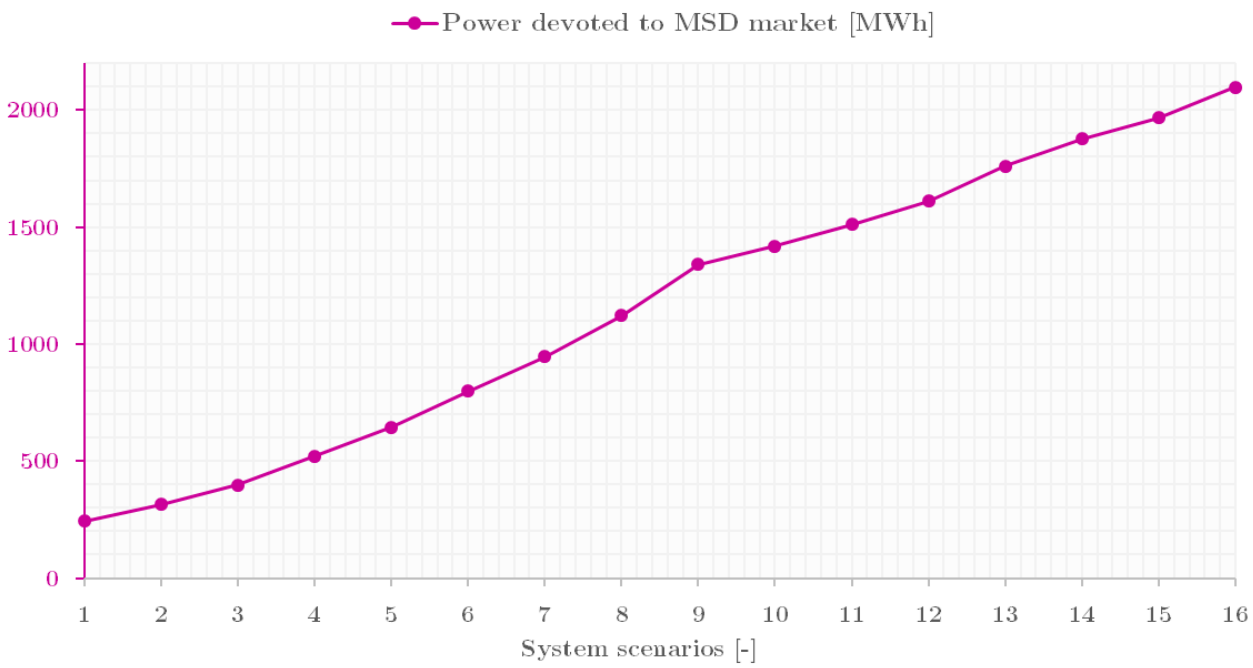

Figure 4.14: Sensitivity analysis on RES system – Power devoted to the MSD market

The overall improvement of the system performance influences the financial part of the analysis as well. The two parameters selected to assess the economic profitability (i.e. IRR and IF) of the project both show promising indications for the P2P technology rollout.

The first system configuration capable of retrieving an *Internal Rate of Return* higher than the assumed discount rate corresponds to the scenario #8 in Table 4.3– as it can be noted in Figure 4.15 – from that point on, the investment made is profitable since it generates a positive Net Present Value at the 20th year with the assumption made.

The *Investment Factor* (IF) as well is reported in Figure 4.15, the lower its value, the smaller will be the expense sustained to offer 1 MWh to the MSD market, which represents the absolute measure of the earning that the system is actually able to capture.

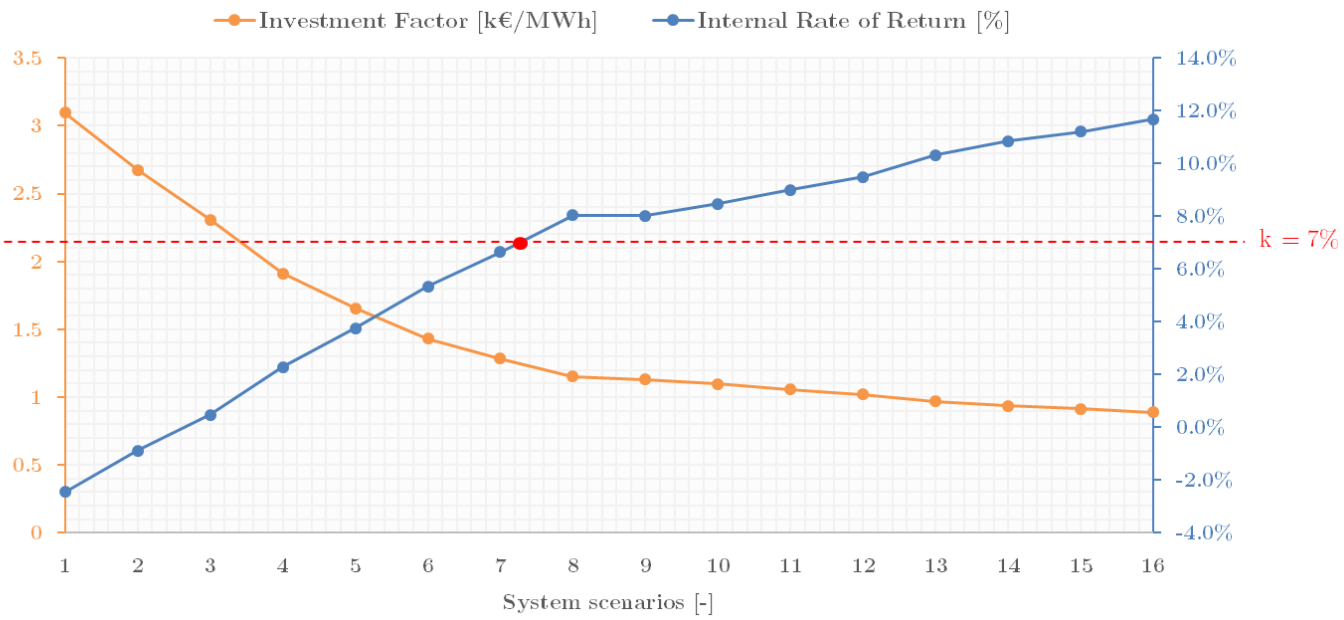

Figure 4.15: Sensitivity analysis on RES system – Financial parameters

The last remark to make regarding the economic assessment of the system is that up to now the reasoning has been made only on relative terms, though the evaluation of an investment also depends on the absolute amount of the expenditure to be incurred.

To witness that renewables still ensure competitive business model to be ready for a massive rollout is taken for granted and it is not the aim of this work. The evaluation must be made for P2P plants, where the cardinal point is the presence of a hydrogen-based energy storage infrastructure and still this scenario is not competitive, as a matter of fact.

4.3. Optimization Model

4.3.1. Overview of the Optimization Model

The last part of this work investigates the possibility of providing an insightful tool able to support the design phase of P2P systems.

The most effective way to perform it is making use of optimization algorithms which help figuring out which configuration of the system fits better with the specific project's needs.

The first concept to learn is that the optimal layout of the system in absolute terms does not exist: these procedures must be fine-tuned so that they are able to retrieve a solution complying with the requirements imposed.

In the previous section were presented the results of a sensitivity analysis: it is a rude example of optimization procedure, since the objective is to look for the best setup of the system's components, but without any structured logic behind the process, just applying a trivial trial-and-error scheme.

The step forward was to perform a consistent optimization by employing the Genetic Algorithm to the already described Simulation Model.

Before entering in the operative part, it is worth to specify that there are multiple reasons justifying the choice of the GA – which will be presented later on – however it is not the only optimization method suitable to address this kind of problems. The implementation of alternative procedures was saved for future developments of this work.

4.3.2. Genetic Algorithm

Belonging to the set of heuristic methods, the Genetic algorithm is able to solve both constrained and unconstrained optimization problems based on a natural selection process that mimics biological evolution [44].

The selection process applied in the algorithm is inspired by Charles Darwin's theory of natural evolution: starting from an initial population[27], only the fittest individuals belonging to it are selected for reproduction in order to perpetuate the species [45].

The following generation of individuals (the so-called *children*) is selected starting from a specific set of individuals (defined as *parents*) from the current population, those presenting higher fitness scores than others.

Fitness scores are calculated by evaluating the fitness function on the set of variables each individual aims at representing in other words the fitness function determines the ability of an individual to compete with other individual. The higher fitness score gained, the more likely it will be selected for reproduction.

The reproduction mechanisms can be different; the more employed (also combined together) are:

- **Crossover**:

  It is among distinctive features of the Genetical Algorithm. Crossover children (called *offsprings*) are created by combining pairs of parents in the current population. At each coordinate of the child vector, the default crossover function randomly selects an entry, or *gene*, at the same coordinate from one of the two parents and assigns it to the child.

- **Mutation**:

  The algorithm creates mutation children by randomly changing the genes of individual parents. While the modification involved two parents in the crossover phase, mutation influences the single member. It is a fundamental step along the process since it adds the component of randomness which allows to reach a more

[27] Usually this action is performed randomly, in order to create an initial set of variables which is as unbiased as possible. Structured algorithms like this are equipped with specific condign parts which control if the solution space is explored in a coherent and homogeneous way

reliable solution, trying to avoid the eventual meeting of local minima in the solution space.

- **Elite children**:

  The individuals in the current generation with the best fitness values, thus they are the closest to the optimal solution. These individuals automatically survive to the next generation.

The differentiation on selection criteria makes Genetic Algorithm particularly robust and reliable, especially when the problem to address is highly non-linear or involves discontinuous functions.

The problem addressed by the Simulation Model introduces peculiar characteristics which make the major part of the optimization models not suitable for the purpose.

First of all, it cannot be depicted by means of a whatever explicit function, since the results of the model must comply with the evolution of time as well as it must be respected the *"sequentiality"* of the problem. In few words, the outcome related to the n-th time instant is wholly dependent to the behaviour of the system from the beginning of the simulation to *n-1*-th time (i.e., the system has memory).

Given the extreme level of non-linearity and the number of dependent variables, the need for a robust algorithm was essential and the GA is able to achieve acceptable accuracies of the solution provided after a relatively small number of iteration, if properly sharpen according to the problem features.

Finally, to carry out the optimization procedure it was necessary an algorithm able to embrace the function as it was (i.e., a "*black box*"), where the input variables introduction would trigger the simulation, then the fitness function would be retrieved by combining the output.

The rationale behind Genetic Algorithm fits perfectly with the peculiar structure of the problem and hence it was selected as tool to perform the optimization process.

4.3.3. Model implementation

The algorithm was implemented using MATLAB software – in order to ease the integration with the already fully developed Simulation Model – by means of the specific Optimization Toolbox embedded in the MathWorks® package.

It is equipped with a very intuitive User Interface which allows to clearly state the condition imposed to the problem and keep track of the most relevant outcome of the simulation.

The optimization process was carried out by setting up a separated MATLAB function containing the sub-models described in Chapter 3, then the most relevant options required for the simulation were configured in the tool. In particular, the parameters moved out from a default setting were:

- The number of variables was set to five, namely the FC and EL nameplate power, as well as the peak power achievable from PV and wind sources and the dimensions of the hydrogen tank.
- Initial population site was set to 30: it is dependent by the heaviness of the function recalled, but it represents a good guess to maintain the simulation feasible in terms of time burden.
- The same necessity drives the decisions regarding the stopping criteria: the number of generations was capped to 100, while the tolerance applied to the fitness function was considerably raised (5e-3) with respect to the default value (1e-6), given that for the KPIs evaluation such high accuracy is not needed.

As already outlined in the introductory paragraph, the optimal configuration of the system is dependent to the selected driving factor: therefore, it were performed three simulation runs, in the attempt of picturing various scenarios which can be faced during the design phase.

Need to work in island mode

Section 2.1 has been already presented how P2P systems would be able to interface with the electricity grid and the way a separated connection between end-users (internal to the microgrid) and a hypothetical external energy source.

Usually, the state-of-the-art asset employed in microgrids worldwide is diesel generator, due to its reliability and its capacity of turning on when it is actually needed.

In the perspective of accomplishing the full transition to carbon-free technologies, generators could be replaced with alternative source of energy which are controllable and capable to cover the shortcomings of the P2P systems.

However, the cost per energy of such technologies, also considering their utilization factor is relevant. Therefore, among the most urgent needs during the project design would be to make the system working with as less intervention as possible from external generators as possible, in order to reduce the associated expenditure.

The first optimization procedure was performed looking for the configuration of the system retrieving the highest value of the Off-grid factor (OGF), the KPI defined in section 3.5.2.

Of course, by increasing the peak power of renewables it would be obtained a substantial improvement, but the focus of the analysis is regarding the ability of the P2G system to ensure an island-mode functioning.

For this reason, the cumulated size of PV + wind turbine aggregated was locked, letting to vary the Fuel Cell and Electrolyzer nameplate powers as well as the hydrogen tank dimension.

$$P_{PV} + P_{WIND} \leq \ 800\ [kW] \tag{45}$$

The remaining constraints imposed to the procedure are summarized in Table 4.4.

Table 4.4: Main constraint imposed to the Off-grid Factor optimization

Component	Lower bound	Upper bound
PV field	400 kW	1000 kW
Wind turbine	300 kW	800 kW
Fuel Cell	10 kW	500 kW
Electrolyzer	10 kW	500 kW
Hydrogen tank	10 kg	2000 kg

The outcome of the optimization process are presented in Table 4.5,which gathers the figures related to the best configuration considering the chosen objective function, and Figure 4.16, where it is presented the approach process to the solution of the algorithm.

Table 4.5: Results of the optimization regarding the Off-grid Factor

Component	Optimal size
PV field	453,8 kW
Wind turbine	330,6 kW
Fuel Cell	267,8 kW
Electrolyzer	424,6 kW
Hydrogen tank	256,9 kg

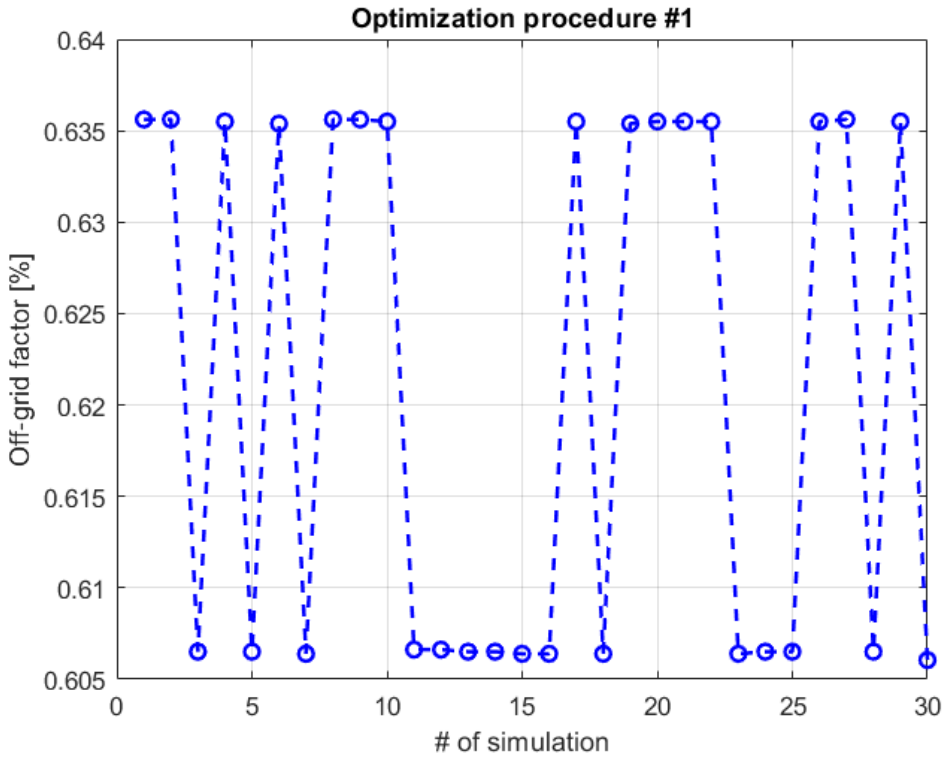

Figure 4.16: Graphical evaluation of the optimization regarding the Off-grid Factor

It is evident an oscillatory behaviour heading towards the optimal solution of the problem. It is worth to notice that even the solution has not reached the complete stabilization, the values respects accuracy requested.

Optimal energy management

Another aspect that is gaining more and more importance in the current energy framework, namely the rational use of the resource available.

Nowadays, the actual value of an investment in infrastructures has to be assessed also accounting for its comprehensive footprint, paying extreme attention to not waste scares resources and operate as efficiently as possible.

In this perspective, the parameters selected to represent at best this concept was already depicted when talking about the possible KPIs to evaluate P2P systems, namely the *energy ratio:*

$$\frac{E_{curt}}{E_{PV} + E_{wind}} \ [pu] \tag{46}$$

The objective of the second optimization procedure is to figure out which configuration of the system retrieves the minimum value of the ratio, since it measures the relative amount of wasted energy with respect to the actual potentiality of renewable assets.

The constraints imposed to the problem are the same reported in Table 4.5, there were no need to change them since they still represent an interesting case to examine.

The results of the optimization model are reported in Table 4.6 and Figure 4.17.

Component	Optimal size
PV field	424,1 kW
Wind turbine	315,2 kW
Fuel Cell	71.0 kW
Electrolyzer	448,2 kW
Hydrogen tank	744,3 kg

Table 4.6: Results of the optimization regarding the energy management factor

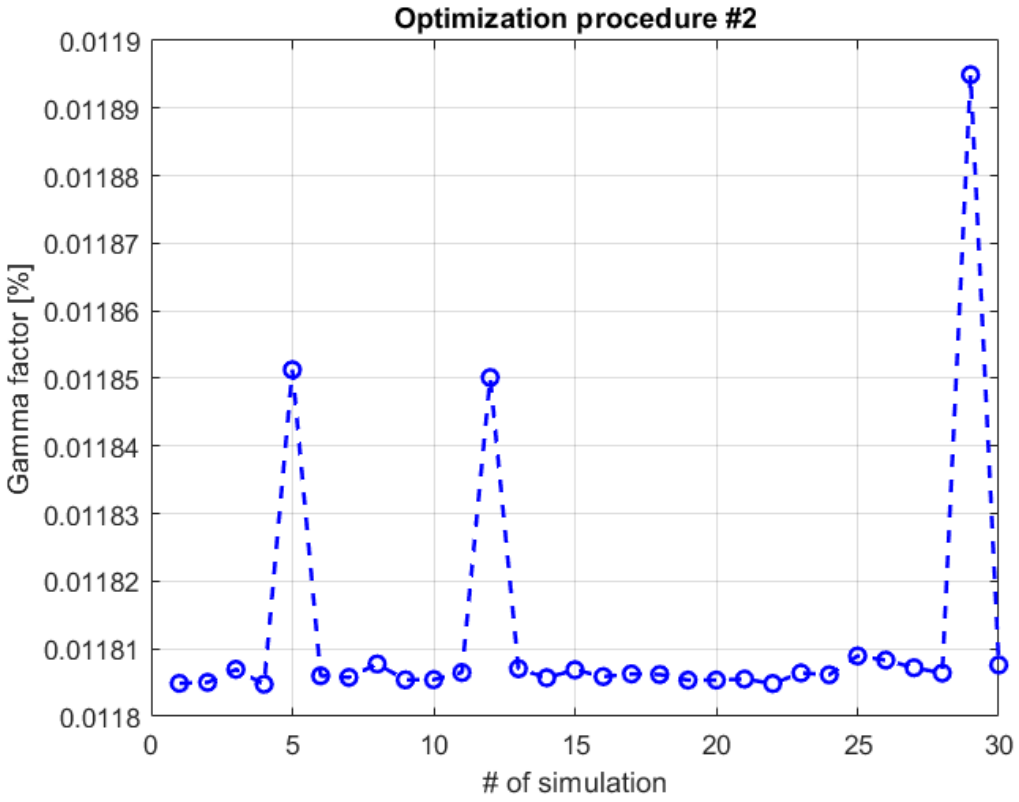

Figure 4.17: Graphical evaluation of the optimization regarding the energy management factor

Unlike the first optimization case, the procedure remains quite stable already in the first simulation attempts. The γ factor which can be extracted from Figure 4.17 is significantly lower than the one found considering the first configuration of the system, which is reported in Table 4.2. It means the optimization procedure has been effective and the parameters involved have a significant impact on the amount of wasted energy related to the system.

Economic optimization

The last optimization procedure performed in this work concerns the financial part of the project. As already outlined in section 4.1, the economic assessment is somehow influenced by the possibility of performing economy of scale, where the upfront costs are spread over a larger infrastructure, thus the investment has better probability to be returned.

Also in this case, the most cost-effective configuration of the system was looked for by keeping fixed the achievable peak power of renewable energy systems, in order to figure out which is the best trade-off regarding the electro-chemical machines to maximize the economic benefit gained through the project.

To accomplish that, it has been selected as indicator the following ratio:

$$\frac{E_{MSD}}{C_{inv}} \left[\frac{\text{kWh}}{€}\right] \tag{47}$$

The algorithm aims at minimizing the parameter, since it would mean to extract the highest revenue stream paying for a system as small as possible.

The constraints imposed to the problem are summarized in Table 4.7.

Table 4.7: Main constraint imposed to the Economic optimization

Component	**Lower bound**	**Upper bound**
Fuel Cell	50 kW	400 kW
Electrolyzer	50 kW	400 kW
Hydrogen tank	75 kg	1500 kg
Component	**Constraint**	
PV field	600 kW	
Wind turbine	330 kW	

The optimal configuration of the system is presented in Table 4.8.

Table 4.8: Results of the optimization regarding the economic assessment of the system

Component	**Optimal size**
PV field	600.0 kW
Wind turbine	330.0 kW
Fuel Cell	94.2 kW
Electrolyzer	319.8 kW
Hydrogen tank	562.8 kg

The last optimization procedure has led to expectable outcomes regarding the sizing of the P2G system: the nameplate power of the electrolyzer is deeply oversized with respect to the fuel cell, since there is a higher and more frequent need of storing energy under the form of hydrogen rather than to use hydrogen to produce electric power, given that the contribution from Renewable Energy Sources is still consistent. As it is possible to notice from Table 4.8, the size of the hydrogen tank increases with the nameplate power of the electrolyzer, in order to perform a twofold mansion: both daily and seasonal storage.

5. Conclusions and future works

The work carried out in this Master Thesis has involved the detailed study of Power-to-Power systems, a recent and innovate concept aiming at integrating renewable energy systems with storage assets to perform a wide variety of activities.

The research regarding P2P systems is started REMOTE project and it has furtherly developed in this work by investigated the behaviour of such system where they are connected to the national electricity grid and are enabled to perform ancillary services.

First, the general context was introduced by providing accurate definitions of novel concepts such as the pilot projects promoted by Terna and UVAM aggregate units.

The most substantial part of the activity has involved the development of a comprehensive MATLAB model able to incorporate input data regarding the context in which P2P systems would be inserted – for instance geographical information, data related to natural resources and anthropomorphic needs and so on.

Then the model performs a truthful simulation over a yearly timescale, which describes in detail how the system behaves in terms of covering the internal load, management of the hydrogen tank available capacity and – more importantly – compliance with dispatch orders imposed by the Italian regulator.

From the core part of the algorithm, a further branching has been developed to assess also the economic feasibility of the system.

After having evaluated the amount of energy exchanged with the grid while respecting the requisites compel by the official regulation, it was estimated the potential profit the system would be able to generate in case of actual commissioning. The assessment was made accounting for the real price oscillation proper of the MSD and MB Italian energy markets.

The final part was devoted to the presentation of the most relevant findings. It has been proven the P2P systems can operate the major part of the time in island mode. The

coordination between the electro-chemical machines and renewable energy source makes feasible the contemporaneous fulfilment of the internal load duties, as well as guaranteeing a good and reliable source of income from the participation to the ancillary services market.

The simulation model was completed with a section fully dedicated to the optimization procedure of such systems. First, it was performed a sensitivity analysis in order to figure out which are the most influencing parameter, preparing the ground for the optimization algorithm developed successively.

The Genetic Algorithm was chosen as best fit for the scope and it were carried out three different optimization processes, settling with various requirements which would occur during the system's design phase.

The added value of this work is the elaboration of an end-to-end simulation model which is agnostic to the input data and is capable to carry out the complete energy simulation, economic assessment and sizing optimization of a P2P system.

The work carried out in this Master Thesis can have further developments which would make the relative findings even more interesting, both concerning the REMOTE project and more in general for the research brought forward by the STEPS group at Politecnico of Torino.

The successive steps are briefly summarized below:

1. The Simulation Model can integrate a wider number and typologies of technologies. In this work the P2P system has been analysed considering as unique storage asset the hydrogen-based element composed by Fuel Cell, Electrolyzer and hydrogen tank. Among the many possibilities available, surely the most interesting to furtherly deepen is the adding of a Battery Energy Storage System (BESS) as short-term option to accumulate the surplus energy contribution coming from renewables. The reason why this possibility has been discarded among the objectives of the work was already outlined. Nevertheless a

simulation model where the two storage assets are coordinated would have an impact on the carried-out research, even though it would make really complex the optimization of the system's size.

2. Regarding the optimization methods, useful insights to guide the sizing of such system were produced by means of a detailed sensitivity analysis over the main parameters characterizing the plant and a basic optimization algorithm. More sophisticated heuristic methods for optimization can be employed. The Genetic Algorithm was particularly suitable for the purpose, even though other algorithm as Particle Swarm Optimization could be equally effective to reach the target.
3. Regarding the core of the Model, which aims at evaluating the hourly power exchanged at the electric node over the whole year, it can be furtherly refined by indicating in-depth information related to the components efficiency, describing how the system behaves according to different input coming from the national electricity grid. A further study could be performed regarding the availability the system is able to provide. Therefore, it would be necessary to estimate off-duty time dedicated to the predictive maintenance, whereas a random variable could represent the failure probability of the system, from which it would be reasonable to calculate the associated loss of profit. Nonetheless, the study would highly project-specific and it could vary in a consistent way according to the site location.
4. The developed model is referred to a "standard year", which is repeated as it is for the entire duration of the project. It can be evaluated the possibility of performing multi-year analysis which take into account the expected decrease of the cost of technologies or the eventual additional remuneration mechanisms that the system can adopt to capture further value.
5. For sure the most relevant breakthrough can be achieved by further analysing the interaction between P2P system and the Italian ancillary services market.

This work has set the starting point, but there are numerous topic to be discussed, Terna has launched a set of pilot projects aside from that analysed in this work. There are many other type of services a P2P system can perform, which can be stacked over the service described in this work.

6. As far the economic part of the Model is concerned, in this work has been selected the set of Key Performance Indicators considered as effective for the purpose and representative as possible. However, they are strongly related to the typology and the configuration of the specific analysed plant and it would be surely attractive to consider more comprehensive parameters to assess the performance of the system.

References

[1] Ministero dello Sviluppo Economico, "Piano Nazionale Integrato per l'Energia e il Clima," 2019.

[2] STEPS Polito, "https://www.remote-euproject.eu/," 2018. .

[3] STEPS Polito, "https://www.remote-euproject.eu/partners/," 2018. .

[4] STEPS Polito, "https://www.remote-euproject.eu/remote-project/," 2018. .

[5] STEPS Polito, "https://www.remote-euproject.eu/2020/04/17/enel-green-power-on-demo-1/," 2019. .

[6] W. P. Number *et al.*, "Deliverable number D2.2 - Technical specification of the technological demonstrators," 2018.

[7] IRENA, "Innovative Ancillary Services," p. 24, 2019.

[8] L. Marchisio and F. Genoese, "L'apertura delle risorse distribuite al mercato dei servizi: quale bilancio?," pp. 1–13, 2018.

[9] Gestore dei Mercati Energetici, "Mercato elettrico a pronti (MPE)." https://www.mercatoelettrico.org/it/Mercati/MercatoElettrico/MPE.aspx.

[10] Terna, "Progetto pilota UVAM e altri Progetti pilota ai sensi della delibera 300/2017/R/eel."

[11] TERNA, "Progetto pilota UVAM e altri Progetti pilota ai sensi della delibera 300/2017/R/eel." pp. 1–31, 2018, [Online]. Available: https://www.terna.it/it/sistema-elettrico/progetti-pilota-delibera-arera-300-2017-reel/progetto-pilota-uvam.

[12] Terna, *Regolamento recante le modalità per la creazione, qualificazione e gestione di Unità Virtuali Abilitate Miste (UVAM) al Mercato dei Servizi di Dispacciamento.* .

[13] ARERA, "Orientamenti relativi alla partecipazione dei veicoli elettrici al mercato per il servizio di dispacciamento, per il tramite delle infrastrutture di ricarica dotate di tecnologia vehicle-to-grid," 2013.

[14] ARERA, "Orientamenti relativi alla partecipazione dei veicoli elettrici al mercato per il servizio di dispacciamento, per il tramite delle infrastrutture di ricarica dotate di tecnologia vehicle-to-grid. Documento per la consultazione Mercato di incidenza: energi," 2020.

[15] J. Hamelin, K. Agbossou, A. Laperrière, F. Laurencelle, and T. K. Bose, "Dynamic behavior of a PEM fuel cell stack for stationary applications," *Int. J. Hydrogen Energy*, vol. 26, no. 6, pp. 625–629, 2001, doi: 10.1016/S0360-3199(00)00121-X.

[16] D. Guilbert and G. Vitale, "Dynamic emulation of a PEM electrolyzer by time constant based exponential model," *Energies*, vol. 12, no. 4, 2019, doi: 10.3390/en12040750.

[17] P. Marocco, D. Ferrero, and M. Gandiglio, "Remote area Energy supply with Multiple Options for integrated hydrogen-based Technologies -Design, engineering, plan for operation & maintenance and permitting process," no. 2, pp. 1–45, 2018.

[18] Gestore dei Mercati Energetici, "Rapporto di monitoraggio dei target nazionali e regionali - Energie rinnovabili in Italy 2012-2018."

[19] C. J. Smith, J. M. Bright, and R. Crook, "Cloud cover effect of clear-sky index distributions and differences between human and automatic cloud observations," *Sol. Energy*, vol. 144, pp. 10–21, 2017, doi: 10.1016/j.solener.2016.12.055.

[20] J. M. Bright, C. J. Smith, P. G. Taylor, and R. Crook, "Stochastic generation of synthetic minutely irradiance time series derived from mean hourly weather observation data," *Sol. Energy*, vol. 115, pp. 229–242, 2015, doi: 10.1016/j.solener.2015.02.032.

[21] "Google Earth." https://earth.google.com/web/@43.32959184,12.61411969,488.6914295a,1406.16455687d,35y,52.48527382h,59.9938889t,360r.

[22] M. Nfaoui and K. El-Hami, "Optimal tilt angle and orientation for solar photovoltaic arrays: case of Settat city in Morocco," *Int. J. Ambient Energy*, pp. 1–18, 2018, doi: 10.1080/01430750.2018.1451375.

[23] "Fotovoltaico Norditalia." https://www.fotovoltaiconorditalia.it/idee/orientamento-inclinazione-pannelli-fotovoltaici-rendimenti.

[24] A. M. E. Bompard, S. Bensaid, G. Chicco, "Innovative large-scale energy storage technologies and Power-to-Gas concepts after optimisation. D6.3–Report on the costs involved with PtG technologies and their potentials across the EU," 2020.

[25] Climate-data.org, "Weather data of Gubbio." https://it.climate-data.org/europa/italia/umbria/gubbio-51926/#climate-table.

[26] A. Hossam-Eldin, C. F. Gabra, and A. H. H. Ali Prof. Dr. Eng, "Effect of Ambient Temperature on The Performance of Different Types of PV Cells at Different Locations in Egypt," 2014.

[27] BloombergNEF, "Vestas Still Rules Turbine Market, But Challengers Are Closing

In."

[28] "Enercon E33 datasheet - www.thewindpower.net." https://www.thewindpower.net/turbine_en_1_enercon_e33-330.php.

[29] A. Ulazia, J. Sáenz, G. Ibarra-Berastegi, S. J. González-Rojí, and S. Carreno-Madinabeitia, "Global estimations of wind energy potential considering seasonal air density changes," *Energy*, vol. 187, 2019, doi: 10.1016/j.energy.2019.115938.

[30] T. Negash, E. Möllerström, and F. Ottermo, "An assessment of wind energy potential for the three topographic regions of Eritrea," *Energies*, vol. 13, no. 7, 2020, doi: 10.3390/en13071846.

[31] E. Hunters, "Helmann coefficient." https://www.energyhunters.it/misurare-il-vento-le-variazioni-del-vento-con-laltezza-dal-suolo/.

[32] E. Ozelkan, G. Chen, and B. Üstündağ, "Spatial estimation of wind speed: A new integrative model using inverse distance weighting and power law," *Int. J. Digit. Earth*, 2016, doi: 10.1080/17538947.2015.1127437.

[33] ABB, *Quaderni di applicazione tecnica N.13 - Impianti eolici*. 2011.

[34] F. UAV, "Hydrogen Tanks." https://www.fortressuav.com/doosan/hydrogen-tank.

[35] D. Zhu, D. Chabane, Y. Ait-Amirat, A. N'diaye, and A. Djerdir, "Estimation of the State of Charge of a Hydride Hydrogen Tank for Vehicle Applications," 2017, pp. 1–6, doi: 10.1109/VPPC.2017.8330976.

[36] Gestore dei Mercati Energetici, "Società trasparente." https://www.mercatoelettrico.org/it/GME/Info/trasparenza.aspx.

[37] U. States, D. Feldman, and P. Schwabe, "PV Project Finance in the," 2017.

[38] E. Vartiainen, G. Masson, and C. Breyer, "PV LCOE in Europe 2014-30 - Final Report, 23 June 2015," *Eur. PV Technolgoy Platf. Steer. Comm. PV LCOE Work. Gr.*, 2015, [Online]. Available: http://www.etip-pv.eu/fileadmin/Documents/FactSheets/English2015/PV_LCOE_Report_July_2015.pdf.

[39] IRENA, "The power to change: solar and wind cos treduction potential to 2025."

[40] P. Marocco *et al.*, "A study of the techno-economic feasibility of H2-based energy storage systems in remote areas," *Energy Convers. Manag.*, vol. 211, no. December 2019, p. 112768, 2020, doi: 10.1016/j.enconman.2020.112768.

[41] B. M. Institute, "Manufacturing Cost Analysis of 100 and 250 kW Fuel Cell Systems for Primary Power and Combined Heat and Power Applications."

[42] A. Christensen, "Assessment of Hydrogen Production Costs from Electrolysis: United

States and Europe," *Int. Counc. Clean Transp.*, pp. 1–73, 2020, [Online]. Available: https://theicct.org/sites/default/files/publications/final_icct2020_assessment_of_hydrogen_production_costs v2.pdf.

[43] W. A. Amos, "Costs of Storing and Transporting Hydrogen," *Other Inf. PBD 27 Jan 1999; PBD 27 Jan 1999; PBD 27 Jan 1999*, no. November, p. Medium: ED; Size: vp., 1999, [Online]. Available: http://www.osti.gov/bridge/servlets/purl/6574-OBMlES/webviewable/.

[44] MathWorks, "How the Genetic Algorithm works." https://it.mathworks.com/help/gads/how-the-genetic-algorithm-works.html.

[45] Towardsdatascience.org, "Description of Genetic Algorithm." https://towardsdatascience.com/introduction-to-genetic-algorithms-including-example-code-e396e98d8bf3.

[46] U. M. Office, "Observations: National Meteorological Library and Archive Fact Sheet 17 – Weather Observations Over land. Tech. Rep.," 2010.

[47] S. Larsen, "The atmospheric Boundary Layer over land and sea: Focus on the offshore Southern Baltic and Southern North Sea region," *http://www.southbaltic-offshore.eu/reports-studies.html*. pp. 1–36, 2013.